

Verification of mathematical models describing soft charged hydrated tissue behaviour

Citation for published version (APA):

Heus, de, H. J. (1994). *Verification of mathematical models describing soft charged hydrated tissue behaviour*. [Phd Thesis 1 (Research TU/e / Graduation TU/e), Mechanical Engineering]. Technische Universiteit Eindhoven. <https://doi.org/10.6100/IR427180>

DOI:

[10.6100/IR427180](https://doi.org/10.6100/IR427180)

Document status and date:

Published: 01/01/1994

Document Version:

Publisher's PDF, also known as Version of Record (includes final page, issue and volume numbers)

Please check the document version of this publication:

- A submitted manuscript is the version of the article upon submission and before peer-review. There can be important differences between the submitted version and the official published version of record. People interested in the research are advised to contact the author for the final version of the publication, or visit the DOI to the publisher's website.
- The final author version and the galley proof are versions of the publication after peer review.
- The final published version features the final layout of the paper including the volume, issue and page numbers.

[Link to publication](#)

General rights

Copyright and moral rights for the publications made accessible in the public portal are retained by the authors and/or other copyright owners and it is a condition of accessing publications that users recognise and abide by the legal requirements associated with these rights.

- Users may download and print one copy of any publication from the public portal for the purpose of private study or research.
- You may not further distribute the material or use it for any profit-making activity or commercial gain
- You may freely distribute the URL identifying the publication in the public portal.

If the publication is distributed under the terms of Article 25fa of the Dutch Copyright Act, indicated by the "Taverne" license above, please follow below link for the End User Agreement:

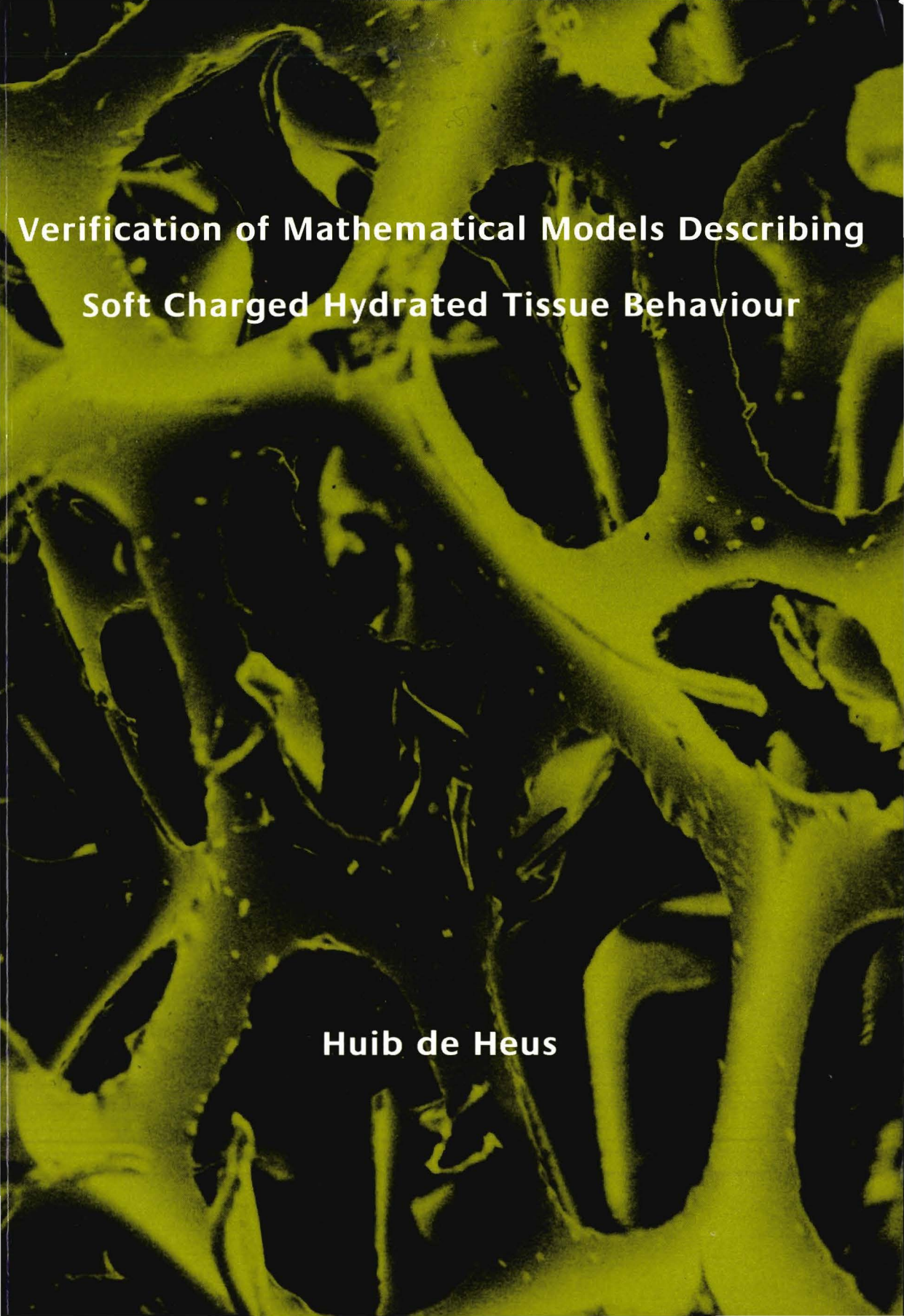
www.tue.nl/taverne

Take down policy

If you believe that this document breaches copyright please contact us at:

openaccess@tue.nl

providing details and we will investigate your claim.

The background of the cover is a microscopic image of biological tissue, likely cartilage or bone, showing a complex network of fibers and cells. The image is colorized with a gradient from blue to red, highlighting different structural components. The text is overlaid on this image.

**Verification of Mathematical Models Describing
Soft Charged Hydrated Tissue Behaviour**

Huib de Heus

Verification of Mathematical Models

Describing Soft Charged Hydrated Tissue Behaviour

CIP-GEGEVENS KONINKLIJKE BIBLIOTHEEK, DEN HAAG

Heus, Huibert Jan de

Verification of mathematical models

describing soft charged hydrated tissue behaviour /

Huibert Jan de Heus. - Eindhoven :

Eindhoven University of Technology

Thesis Eindhoven. - With ref. - With summary in Dutch.

ISBN 90-386-0294-4

Subject headings: Biomedical engineering / triphasic theory / polyelectrolyte gels.

Druk: CopyPrint 2000, Enschede

Verification of Mathematical Models

Describing Soft Charged Hydrated Tissue Behaviour

Proefschrift

ter verkrijging van de graad van doctor
aan de Technische Universiteit Eindhoven
op gezag van de Rector Magnificus, prof. dr. J.H. van Lint
voor een commissie aangewezen door het College van Dekanen
in het openbaar te verdedigen
op vrijdag 9 december 1994 om 14.00 uur

door

Huibert Jan de Heus

geboren te Delft

Dit proefschrift is goedgekeurd door de promotoren:

prof. dr. ir. J.D. Janssen
prof. dr. ir. H.E.H. Meijer

en de copromotor:

dr. ir. J.M.R.J. Huyghe

*Oh, quali io vidi
quei che son disfatti
per lor superbia*

Dante, par. XVI, 109-110

To Yvonne

Contents

| | |
|---------------------------------------------------------------------------|-----------|
| Notation | 11 |
| 1 Introduction | 13 |
| 1.1 Problem definition | 14 |
| 1.2 Basic composition and general behaviour of intervertebral disc tissue | 16 |
| 1.2.1 Tissue composition | 16 |
| 1.2.2 General behaviour | 18 |
| 1.3 Modeling aspects | 20 |
| 1.4 Synthetic model materials: Requirements | 22 |
| 1.5 Objectives | 23 |
| 1.6 Outline of the thesis | 24 |
| 2 Synthesis and characterization of model materials | 25 |
| 2.1 Introduction | 26 |
| 2.2 Copolymerization of acrylic acid and acrylamide | 28 |
| 2.3 Preparation of the model materials | 31 |
| 2.4 Experimental | 32 |
| 2.4.1 Characterization techniques | 32 |
| 2.4.2 Materials | 33 |
| 2.4.3 Synthesis of acrylic acid - acrylamide copolymer | 35 |
| 2.4.4 Synthesis of copolymers in the presence of PUR-foam | 36 |
| 2.4.5 Synthetic model materials used for mechanical studies | 36 |
| 2.5 Results and discussion | 37 |
| 2.5.1 Copolymers | 37 |
| 2.5.2 Copolymers in PUR-foams | 40 |
| 2.6 Conclusions | 42 |
| 3 Experimental determination of swelling pressures | 43 |
| 3.1 Introduction | 44 |
| 3.2 Contributions to the swelling pressure | 44 |
| 3.2.1 Osmotic exchange of solvent and ions: Donnan equilibria | 45 |
| 3.2.2 Fixed charge repulsion | 48 |
| 3.3 Experimental | 48 |

8 Contents

| | | |
|----------|----------------------------------------------------------------------|-----------|
| 3.3.1 | Materials | 48 |
| 3.3.2 | Experimental set-up | 50 |
| 3.3.3 | Experimental protocol | 51 |
| 3.3.4 | Swelling pressure studies | 53 |
| 3.4 | Results | 53 |
| 3.4.1 | General behaviour | 53 |
| 3.4.2 | Variation with external NaCl concentration | 54 |
| 3.4.3 | Estimation of NaCl diffusion coefficient | 56 |
| 3.5 | Discussion | 57 |
| 4 | Measurement of hydraulic permeabilities | 61 |
| 4.1 | Introduction | 62 |
| 4.2 | Experimental | 62 |
| 4.2.1 | Materials | 62 |
| 4.2.2 | Experimental set-up | 63 |
| 4.2.3 | Experimental protocol | 64 |
| 4.2.4 | Hydraulic permeability studies | 65 |
| 4.3 | Results | 66 |
| 4.3.1 | Hydraulic permeability of the various materials | 66 |
| 4.3.2 | Deformation dependence | 66 |
| 4.3.3 | Dependence on NaCl bathing solution concentration | 67 |
| 4.4 | Discussion | 67 |
| 5 | Confined swelling and compression behaviour | 71 |
| 5.1 | Introduction | 72 |
| 5.2 | Experimental | 72 |
| 5.2.1 | Materials | 72 |
| 5.2.2 | Experimental set-up | 73 |
| 5.2.3 | Experimental protocol | 75 |
| 5.3 | Results | 76 |
| 5.3.1 | General behaviour | 76 |
| 5.3.2 | Quantitative comparison of the various materials | 76 |
| 5.3.3 | Quantitative description confined swelling and compression behaviour | 80 |
| 5.4 | Discussion | 83 |
| 6 | Discussion, conclusions and recommendations | 89 |
| 6.1 | Discussion | 90 |
| 6.1.1 | Verification of triphasic theory | 90 |
| 6.1.2 | Synthetic model materials | 91 |
| 6.1.3 | Experimental characterization | 92 |
| 6.2 | Conclusions | 93 |
| 6.3 | Recommendations | 94 |

Contents 9

| | |
|-------------------------|------------|
| References | 97 |
| Summary | 103 |
| Samenvatting | 107 |
| Acknowledgements | 111 |
| Curriculum Vitae | 112 |

Notation

Symbols

| | |
|--------------|-----------------------------------------------------------------|
| a | activity |
| A | cross-section |
| c | concentration external bathing solution |
| C^i | concentration in synthetic model material per unit fluid volume |
| $d[M_{AA}]$ | acrylic acid monomer consumption |
| $d[M_{AAm}]$ | acrylamide monomer consumption |
| D | NaCl diffusion coefficient of synthetic model material |
| E | Green-Lagrange strain |
| h | thickness material specimen |
| H_A | aggregate modulus |
| I | initiator |
| J | relative volume change |
| K | hydraulic permeability of synthetic model material |
| l | fluid height |
| M | permeability parameter |
| m^i | molar mass |
| $M_{w,i}$ | mass average molar mass |
| M_{AA} | acrylic acid monomer |
| M_{AAm} | acrylamide monomer |
| n^i | volume fraction |
| n^p | porosity PUR-foam |
| p | hydrodynamic fluid pressure in bathing solution |
| P | hydrodynamic fluid pressure in synthetic model material |
| q | mean permeation rate |
| r_{AA} | reactivity ratio acrylic acid |
| r_{AAm} | reactivity ratio acrylamide |
| R | universal gas constant |
| $R\cdot$ | radical |
| S | second Piola Kirchhoff stress |
| t | time |

12 *Notation*

| | |
|-----------|----------------------------------------------------|
| T | absolute temperature |
| v^i | velocity |
| \bar{V} | partial molar volume |
| x^i | molar fraction |
| X^i | molar fraction in synthetic model material |
| y | position |
| α | stiffness parameter |
| γ | activity coefficient |
| Δ | difference |
| ν | molar chemical potential |
| ν^0 | concentration independent molar chemical potential |
| ϕ | osmotic coefficient |
| π | pressure |
| ρ | mass density per unit fluid volume |
| σ | Cauchy stress |
| ξ | diffusion parameter |

Subscripts

| | |
|------|------------------------|
| aps | air pressure source |
| cap | capillary tube |
| cop | copolymer |
| diff | diffusion |
| don | Donnan |
| eff | effective |
| el | elastic |
| ext | external |
| fcr | fixed charge repulsion |
| i | ion |
| osm | osmotic |
| p | permeation |
| spec | specimen |
| swel | swelling |
| w | water |
| 0 | reference |

Superscripts

| | |
|-----|--------------------------|
| cop | copolymer |
| ext | external |
| f | fluid |
| fcd | fixed charge density |
| pg | proteoglycan |
| s | solid |
| smm | synthetic model material |
| w | water |
| + | sodium |
| - | chloride |
| 0 | reference |
| * | salt |

Chapter 1

Introduction

In biomechanics, the validity of mathematical models describing the behaviour of biological materials is generally verified by comparing computed results with analytical solutions of the same equations (mathematical validation) and with results of experiments performed on the genuine biological material (biological validation). However, the former is only possible in limiting cases while, due to the complexity of the *in-vivo/in-vitro* experimental conditions, the latter validation is difficult or impossible to perform. Consequently, it is not always evident what the influence will be of the various assumptions, made within the development of the mathematical model, on the final computed results.

An approach to remove the difficulties associated with the biological validation is the use of well-controlled synthetic model materials that possess at least the most characteristic physical properties of the biological material under consideration.

In this thesis, the application of synthetic model materials is evaluated for the verification of mathematical models describing the behaviour of soft charged hydrated tissues. As a case study intervertebral disc tissue is chosen.

In the first section of this chapter, the problem definition is formulated. In the second section, the relevant biomechanical and structural components are presented as well as the general behaviour of intervertebral disc tissue. In the next section, the modeling of the behaviour of intervertebral disc tissue is treated and the relevant material parameters are summarized. Subsequently, the requirements set to the synthetic model materials are outlined followed by the objectives of the research. The chapter ends with an overview of the contents of the thesis.

1.1 Problem definition

In the development of a numerical model that describes the mechanical behaviour of biological materials, several stages can be distinguished starting from the biological material to be modeled up to the actual numerical model (figure 1.1). In every stage, approximations are introduced. Within the first stage from biological material to physical model, only a limited number of physical phenomena are taken into account. Within the second stage from physical model to mathematical model, a number of physical assumptions are made. Within the last stage from mathematical model to numerical model, discretization of the equations introduces numerical approximations.

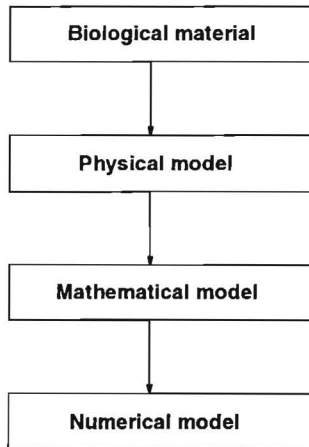


Figure 1.1: *Subsequent stages which are considered in the development of a numerical model describing the behaviour of biological materials.*

In order to verify whether the results calculated with such a numerical model are correct, generally the mathematical and physical validity of the equations is studied. The former is verified by comparing numerical results in limiting cases with results from analytical solutions of the same equations. Due to the complexity of the mathematical equations involved, mostly only analytical solutions are available that describe simple problems. Nevertheless, this comparison is usually effective to verify the validity of the approximations made within the transition from mathematical model to numerical model.

A strategy often used in biomechanics to verify the physical validity of the mathematical equations is a direct confrontation of numerical results with results from corresponding experiments performed on the genuine biological material (biological validation).

However, when performing these experiments, several difficulties are encountered:

- Short *in-vivo* measurements have a restricted duration revealing only momentary conditions. The invasiveness of these techniques often disturbs the condition of the biological system. Prolonged *in-vivo* measurements are expensive and allow a limited control over the experimental conditions.
- The properties of genuine material specimen change with time in an *in-vitro* environment. Control of the experimental conditions is therefore difficult and extension of the experiments to longer periods of time restricted (Drost *et al.* [15], Woo *et al.* [74]).
- The properties of biological material vary with region of origin and between individuals. Due to the compositional differences the reproducibility of results from similar *in-vitro* experiments is limited (Mow *et al.* [48], Best *et al.* [4], Urban *et al.* [71]).
- The preparation of material specimen with well-defined geometries for *in-vitro* measurements is cumbersome (Maroudas [44], Drost *et al.* [15]).
- Controlled variation of the composition of biological material is difficult if not impossible, although significant benefit could be obtained from such variation in order to evaluate the relative contribution of the different constituents to the overall behaviour.

Due to the complexity of the *in-vivo/in-vitro* experimental conditions, the consequences of the assumptions on the final computed results, made within the transition from biological material to mathematical model, are not easily separated. It is difficult to indicate to which extent the assumptions made within the separate stages are admissible or not.

An approach to circumvent the difficulties associated with the biological validation is the use of synthetic model materials. These materials are widely used in biomedical research *e.g.* as implants or tissue replacement, disposable medical devices and carriers of drugs in drug delivery systems (see *e.g.* Park *et al.* [51], Ikada [30]). Surprisingly, the materials have drawn little or no attention in biomechanics as alternative material for the verification of mathematical models. However, by performing first experiments on well-controlled synthetic model materials possessing the most characteristic properties of the biological material, an improvement of the verification is expected. By using these materials, the assumptions made within the transition from physical model to mathematical model can be verified separately (physical validation) (figure 1.2). At this point synthetic model materials serve as an intermediate step towards the complete verification of the mathematical model.

The major advantage of the model materials is the possibility to vary parameters that are characteristic for the material behaviour. Parameter studies can be performed which increase the insight in the relative contribution of the different constituents on the overall material behaviour. Due to the negligible variation in the composition of material specimen originating from the same reference model material, the reproducibility of the experimental

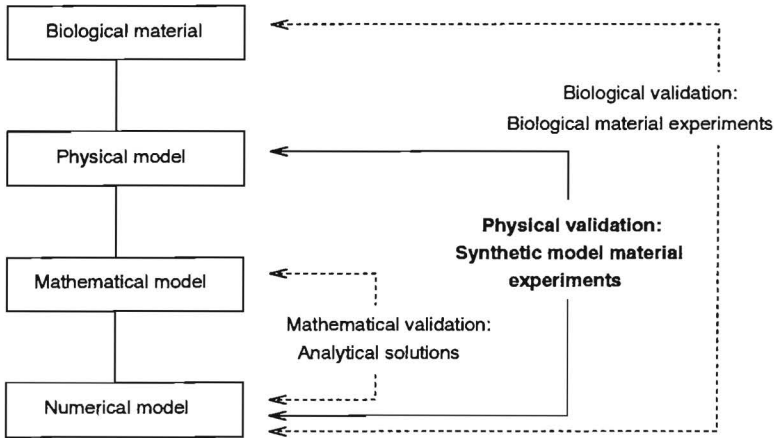


Figure 1.2: *The justification of mathematical models describing the behaviour of biological realities. Three stages of verification: mathematical, physical and biological*

results is increased. In principle, synthetic model materials do not deteriorate as easily as the biological equivalent. The experimental conditions are therefore controlled more easily and the experiments can be extended to longer periods of time. Furthermore, synthetic model materials can also be used to develop experimental techniques in well-controlled laboratory environments for possible future use in a biological environment.

The investigation presented in this thesis aims at the application of synthetic model materials for the verification of mathematical models describing the behaviour of soft charged hydrated tissues. As a case-study intervertebral disc tissue is chosen. In order to be able to specify the objective of the thesis in more detail, both the basic composition and behaviour of intervertebral disc tissue as well as its modeling are outlined in the subsequent sections.

1.2 Basic composition and general behaviour of intervertebral disc tissue

1.2.1 Tissue composition

Intervertebral discs are located between the vertebrae of the spinal column (figure 1.3, left). The discs consist of a gelatinous centre, the nucleus pulposus, surrounded by several concentrically arranged lamellae of fibrocartilage, the anulus fibrosus (figure 1.3, right). Due to the presence of both randomly orientated and aligned fiber networks, the structure of intervertebral disc tissue is anisotropic. It mainly consists of a collagen network embedded in a hydrated proteoglycan gel (figure 1.4) (Eyre *et al.* [16], Happey *et al.* [25], Humzah *et*

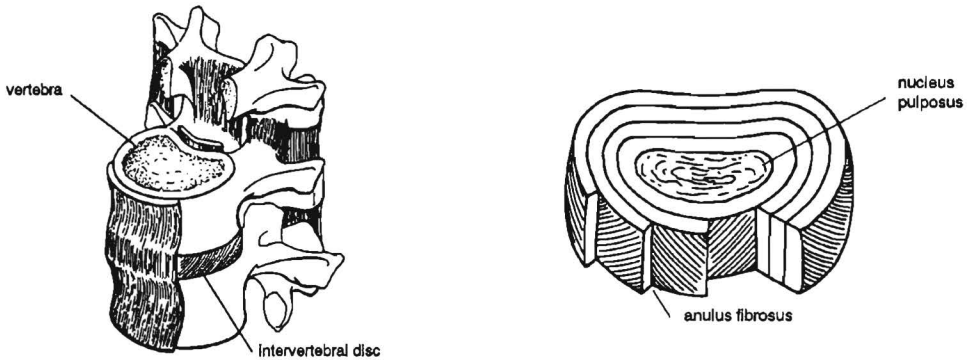


Figure 1.3: Intervertebral disc: orientation (left) and schematic view (right).

al. [29]).

Collagen is a rodlike protein molecule built of long polypeptide chains. Each polypeptide chain consists of repeating units of 18 different amino acid residuals. The basic structural units of collagen are tropocollagen macromolecules consisting of three polypeptide chains folded in a helical confirmation by hydrogen bonds (Buckwalter *et al.* [11]). The tropocollagen molecules are approximately 3000 Å long and approximately 15 Å in diameter and possess a mass average molar mass of approximately $3 \cdot 10^5$ (Happley *et al.* [25]). Collagen molecules are synthesized within cells and driven in the extracellular space where they polymerize into fibrils and fibers. During the synthesis and the aggregation, covalent intra- and intermolecular crosslinks are formed that stabilize the fiber structure (Happley *et al.* [25]). Collagen constitutes about 15 - 60% of the dry weight of the tissue (Eyre *et al.* [16], Beard *et al.* [3]).

Proteoglycans (PG) are large molecules consisting of many glycosaminoglycans (GAG) linked to core proteins. GAG are made up of long chains of polysaccharides, each chain consisting of approximately 20 disaccharide repeating units (Bogduk *et al.* [7]). The dimeric units of the GAG are usually chondroitin sulfate and keratan sulfate. Both molecules contain carboxyl and sulfate groups. PG usually aggregate into supra-molecular structures by noncovalent attachment to chains of hyaluronic acid via a link protein (Bogduk *et al.* [7]) (figure 1.5). A single hyaluronic chain may bind 20-100 proteoglycan chains forming a macromolecule of approximately 10^8 Da. The PG-aggregates entangle and form three dimensional macromolecular networks. Within the interstitial fluid, at physiological pH and ionic strength, the carboxyl and sulfate groups of the disaccharide repeating units are ionized. The density of these charges is called the fixed charge density (fcd). Due to the ionization of the carboxyl and sulfate groups the PG-macromolecules are capable of

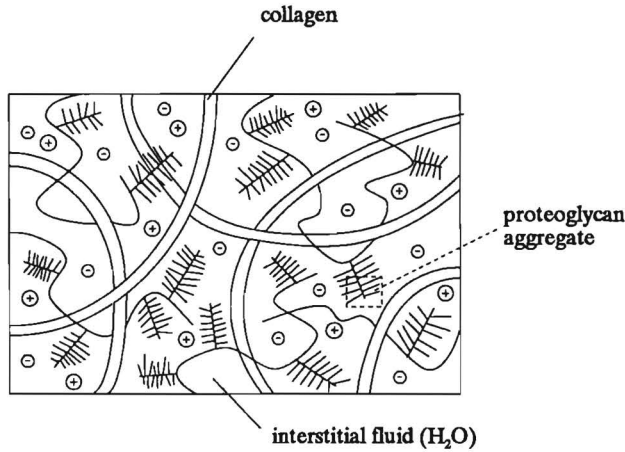


Figure 1.4: Schematic diagram of the structure of intervertebral disc tissue. The matrix of the tissue is predominantly formed by a fine network of collagen fibers embedded in a high concentration of proteoglycan macromolecules in water. At physiological conditions the proteoglycan macromolecules contain negatively charged groups. Within the fluid small nutrients and ions are dissolved.

retaining water in their domains up to a 50-fold their own weight. The water-retaining capacity of the proteoglycans is largely dependent on their fixed charge density. PG form the groundsubstance of the tissue and constitute about 15-65% of its dry weight (Urban *et al.* [68], Sedowofia *et al.* [60]).

Water constitutes approximately 80% of the wet weight of the tissue (Urban *et al.* [67, 70]). The water is found between the collagen fibers (intra-fibrillar water) and within the domains of the proteoglycans (extra-fibrillar water).

The collagen fibers and PG-aggregates are bound together by electrostatic and covalent bonds which strengthens the total macromolecular structure of the tissue. Due to the entanglements between collagen and PG network, only the interstitial fluid and the small ions are able to flow.

1.2.2 General behaviour

Deformation of intervertebral disc tissue can be generated by changes in mechanical and chemical loading conditions (Urban *et al.* [68, 69], Snijders [62]). The external load is counterbalanced by the tissue by adjustment of its internal ionic environment and the tension in the collagen-proteoglycan network via exchange of fluid and ions. The fluid flow and ion transport through the charged porous solid matrix and the subsequent solid-

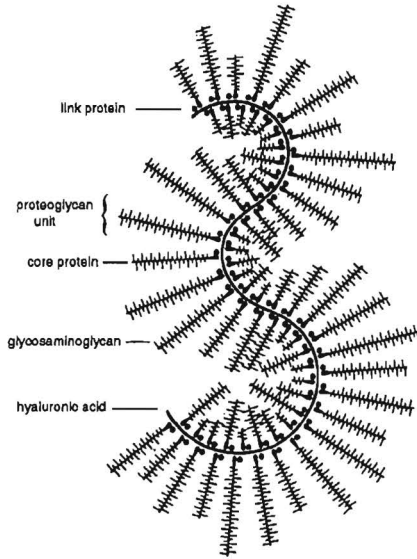


Figure 1.5: Schematic view of the proteoglycan aggregates.

fluid interaction play significant roles in the load carrying capacity of the tissue (Urban *et al.* [67, 70], Maroudas [43], Kraemer *et al.* [37]). As a result of the changes in fluid and ion content, the tissue swells or shrinks depending on the nature of the load applied.

The mobile counter- and co-ion concentrations inside the tissue are different from the external ion concentrations due to the presence of the fixed charges on the collagen-proteoglycan complex. This imbalance of ions gives rise to an additional pressure in the interstitial fluid. The resulting pressure difference is known as the Donnan osmotic pressure. When the tissue is in equilibrium with its environment, this osmotic pressure is balanced by the tension in the collagen-proteoglycan network.

When a load is applied to the tissue, the equilibrium is disturbed. In case of a compressive load, fluid is expelled from the tissue. Due to the loss of fluid, the concentration of fixed charges, and hence the osmotic pressure, increases while the tension in the collagen-proteoglycan network decreases. The fluid flow continues until the external load is balanced. Removal of the external load results in an uptake of fluid by the tissue, leading to a decrease in the osmotic pressure and an increase in tension of the network. Eventually, the original equilibrium configuration is resumed.

1.3 Modeling aspects

The most recent theories describing the mechanical and physico-chemical events in soft charged hydrated materials, such as intervertebral disc tissue, consider it to consist of a mixture of three major phases: (1) the collagen network and the proteoglycan ground matrix are modeled as a charged, porous, permeable, intrinsically incompressible solid phase, (2) the interstitial fluid is modeled as an intrinsically incompressible fluid phase and (3) the small nutrients and ions dissolved within the fluid are treated as an ion phase (Lai *et al.* [40], Snijders [63]). The latter phase is treated as a phase consisting of the monovalent salt NaCl which is miscible with the fluid. The solid phase is assumed to be immiscible with the fluid phase. Both theories are derived from the theory of mixtures which assumes that the tissue may be viewed upon as a superposition of distinct phases. Each phase is treated as a continuum following its own motion. The theories take into account the biochemical and structural composition of the tissue and describe its behaviour on the basis of finite deformation of the solid phase, fluid flow relative to the solid phase, osmotic effects, and diffusion of small ions.

The uni-axial response of soft charged hydrated materials to a mechanical or chemical load is described by three coupled differential equations governing:

(i) Large deformation of the fiber network and ground substance, complying with the momentum balance of the mixture,

$$\frac{d\sigma_{eff}}{dy} - \frac{dp}{dy} = 0 \quad (1.1)$$

where y is the uni-axial position, σ_{eff} the effective Cauchy stress of the mixture and p the hydrodynamic fluid pressure.

(ii) The fluid flow relative to the solid phase which is driven by a pressure gradient and a concentration gradient of the mobile ions and the fixed charged groups. The fluid flow is governed by

$$\frac{dv^s}{dy} + \frac{d}{dy} [n^f(v^f - v^s)] = 0 \quad (1.2)$$

$$n^f(v^f - v^s) = -K \frac{d}{dy} (p - \pi) \quad (1.3)$$

where v^s is the velocity of the solid, n^f the volume fraction of the fluid, v^f the velocity of the fluid, K the hydraulic permeability of the material and π the osmotic pressure. The latter is given by (chapter 3)

$$\pi = \phi RT(2C^- + C^{fcd}) - 2\phi^* RTc \quad (1.4)$$

where ϕ is the osmotic coefficient of the material, ϕ^* the osmotic coefficient of the external NaCl solution, R the universal gas constant, T the temperature, C^- the Cl^- concentration

in the material, C^{fcd} the fixed charge density of the material and c the external NaCl concentration. The initial C^- concentration is given by

$$2C^- = -C^{fcd} + \sqrt{(C^{fcd})^2 + 4c^2} \quad (1.5)$$

(iii) The convection-diffusion of Na^+ - and Cl^- -ions, due to fluid flow relative to the solid phase and due to differences in mobile ion concentration, governed by

$$(\dot{\rho}_i)_s + \frac{d\rho_i}{dy}(v^f - v^s) = \frac{1}{n^f} \frac{d}{dy} \left[D \left(\frac{d\rho_i}{dy} + \xi \frac{dC^{fcd}}{dy} \right) \right] \quad (1.6)$$

where $(\dot{\cdot})_s$ is the material time derivative following the solid motion, ρ_i the ion mass density per unit fluid volume, D the diffusion coefficient and ξ a diffusion parameter. The latter is given by (Snijders *et al.* [64])

$$\xi = \frac{m^- C^- - m^+ C^+}{C^- + C^+} \quad (1.7)$$

where (C^+, C^-) and (m^+, m^-) are the concentration per unit fluid volume and molar mass of the Na^+ and Cl^- -ions respectively.

Both the fixed charge density C^{fcd} and the fluid volume fraction n^f are deformation dependent according to

$$C^{fcd} = \frac{C_0^{fcd}}{1 - \frac{(1-J)}{n_0^f}} \quad (1.8)$$

$$n^f = 1 - \frac{1 - n_0^f}{J} \quad (1.9)$$

where J is the relative volume change and C_0^{fcd} and n_0^f the fixed charge density and fluid volume fraction respectively in the reference state.

The equations 1.1 to 1.9 form the set of equations describing the triphasic behaviour of soft charged hydrated tissues. In order to complete this set, additional constitutive relations are needed to describe the stress-strain behaviour of the solid phase and the permeability and diffusion behaviour.

The effective Cauchy stress σ_{eff} , the hydraulic permeability K , and the diffusion coefficient D are in principle dependent on the deformation of the material and the local salt concentration. In soft tissue mechanics, the contribution of the salt concentration is generally assumed to be negligible compared to the deformation contribution.

For the deformation dependent stress-strain relation generally an exponential function is chosen (Fung [18]), relating the second Piola Kirchhoff stress S_{eff} to the Green-Lagrange strain E according to

$$S_{eff} = H_A e^{\alpha E^2} E \quad (1.10)$$

where H_A is the reference aggregate modulus in the axial direction of the material and α a stiffness parameter. An expression commonly used for the deformation dependent permeability is (Oomens [50]),

$$K = K_0 e^{M(J-1)} \quad (1.11)$$

where K_0 is the hydraulic permeability of the material in the reference state and M a permeability parameter. In [63], Snijders uses a linear relation to describe the deformation dependence of the diffusion coefficient,

$$D = \frac{n^J}{n_0^J} J D_0 \quad (1.12)$$

where D_0 is the diffusion coefficient of the material in the reference state.

The mathematical models presented by Lai *et al.* [40] and Snijders [63] are validated via comparison of calculated results with experimental data of one dimensional confined swelling and compression experiments. In [40], the verification is limited to the quantitative comparison of equilibrium conditions using infinitesimal strain theory. In [63], a quantitative fit of the transient finite deformation behaviour of the tissue is given. However, the values determined for the diffusion coefficient of the ions and the osmotic coefficient of the tissue deviate largely from the values encountered in the biological tissue.

In the theories the swelling pressure is modeled differently: where in [63] it is modeled as an osmotic pressure which is totally accounted for by the presence of the small diffusible ions and the ionized PG, in [40] an electrical repulsive force between the charged PG molecules is added, the so-called chemical expansion stress.

It is evident from the above that even one-dimensionally the behaviour of intervertebral disc tissue is not understood completely. The verification of the models is hampered by the limited control of the experimental conditions and hence by the difficult determination of the material parameters essential for the triphasic equations. By using well-controlled synthetic model materials, these difficulties can be removed which creates possibilities to improve the fundamental understanding of the physical processes involved.

1.4 Synthetic model materials: Requirements

The design of the synthetic model materials is focused on the following criteria: (i) the materials should possess a charged permeable solid phase, an interstitial fluid phase and a monovalent ion phase. The relative amount of each constituent should reflect the genuine tissue composition, (ii) the materials should comprise characteristic physical properties of the tissue such that the macroscopic model material behaviour is similar to the behaviour of the biological tissue, (iii) the process used to obtain the materials should allow for a variation of the composition of the materials. This creates the possibility to study the separate aspects of the physical phenomena contributing to the overall behaviour.

Anisotropy of the tissue, the specific microstructure of the biopolymers and their mutual interaction are not taken into account. The above criteria result in the following requirements for the synthetic model materials:

- The materials should be sensitive to changes in external mechanical and chemical loading conditions which is expressed in swelling and shrinking behaviour.
- The materials should possess a water retaining capacity.
- The solid phase should be negatively charged similar to the proteoglycans of the tissue. The negative charges should be counterbalanced by relatively small monovalent counterions *e.g.* Na^+ -ions.
- The solid-fluid ratio of the materials should be in accordance with the 20:80 ratio encountered in the tissue.
- Specific physical properties such as fixed charge density, elasticity, permeability and diffusivity should be similar to those of the genuine tissue (table 1.1).

| parameter | value | unit | author |
|-------------|-----------------------------|------------------------|---------------------------------------------------|
| C_0^{fcd} | $0.3 \cdot 10^3$ | [mole/m ³] | Urban <i>et al.</i> [67] |
| H_A | 0.38 - 0.47 | [MPa] | Best <i>et al.</i> [4], Snijders [63] |
| D | $5 \cdot 10^{-10}$ | [m ² /s] | Maroudas <i>et al.</i> [44] |
| K | $0.22 - 0.4 \cdot 10^{-15}$ | [m ⁴ /Ns] | Best <i>et al.</i> [4], Guilak <i>et al.</i> [23] |

Table 1.1: Material parameters of intervertebral disc tissue as determined by various authors.

1.5 Objectives

Based on the problem definition as given in section 1.1, the objectives of the research are:

- Development of synthetic model materials for intervertebral disc tissue taking into account its characteristic physical properties.
- Characterization of the obtained materials.
- Determination of the behaviour of the various materials via a variation of mechanical and chemical loading conditions.
- Determination of the influence of the various constituents on the material behaviour observed.
- Application of the materials for a verification of the triphasic theory.

1.6 Outline of the thesis

In chapter 2, the synthesis and characterization of the model materials for intervertebral disc tissue are described. The structural components which are used within the material design and the polymerization mechanism are outlined.

Several experiments are performed in order to determine the material parameters that are essential for the triphasic formulation and for the later study of their behaviour.

In chapter 3, their ability to swell is studied by measurement of the swelling pressure of disc shaped specimen. For this purpose an experimental set-up is developed that is capable of measuring the pressure responses generated due to variations in external ionic environment. The measured equilibrium responses are used to estimate the initial fixed charge density and the osmotic coefficient. The characteristic time constant of the transient pressure curves is used to estimate the diffusion coefficient.

In chapter 4, the results are given of hydraulic permeability studies. The permeability is determined from fluid permeation rate measurements via application of a constant fluid pressure difference across material specimen. The dependence of the permeability on the deformation of the materials and on the ionic strength of external NaCl solutions is shown. Results are given of the permeability of the various materials measured under equal strain and external salt conditions.

In order to study their behaviour in a combination of mechanical and chemical loading conditions, one-dimensional confined swelling and compression experiments are performed. The results of these studies are presented in chapter 5. Data of a typical confined swelling and compression experiment are compared with corresponding computed results using the triphasic theory combined with the material parameters previously determined for the fluid volume fraction (chapter 2), the fixed charge density, osmotic coefficient and diffusion coefficient (chapter 3) and the hydraulic permeability (chapter 4).

The thesis concludes with a general discussion on the synthetic model materials developed, on the experiments performed and on the potential application of the materials.

Chapter 2

Synthesis and characterization of model materials

In chapter 1, the general requirements of the synthetic model materials were formulated based on the mechanical and physical properties of intervertebral disc tissue and the physical assumptions made within the triphasic mathematical modeling of its mechanical behaviour. Based on these requirements, in this chapter the synthesis and characterization of the materials is presented and discussed.

In the introduction (section 2.1), the composition of the materials and the choice of the various constituents are outlined. The synthesis of the copolymers and the preparation of the model materials is given in the sections 2.2 and 2.3 respectively. In the experimental section (section 2.4), the characterization techniques and materials used are described and the recipes of the copolymerizations given. Subsequently, the materials obtained are discussed in section 2.5 resulting in the conclusions given in section 2.6.

2.1 Introduction

The considerations presented in section 1.4 have resulted in the development of a model material with a structure that consists of a soft open cell microporous polyurethane (PUR) foam embedded in a water phase containing atactic hydrophilic synthetic copolymers. As monomer units of the copolymers, sequences of acrylic acid and acrylamide are chosen (figure 2.1). The copolymer gel belongs to a class of hydrogels which are able to absorb huge volumes of water or aqueous solutions and have proven to be a valuable tool for improving the water retention of soils and the water supply of plants (Kazanskii *et al.* [33]). Other applications include *e.g.* superabsorbent diapers, detergents and oil well drilling (Buchholz [8]).

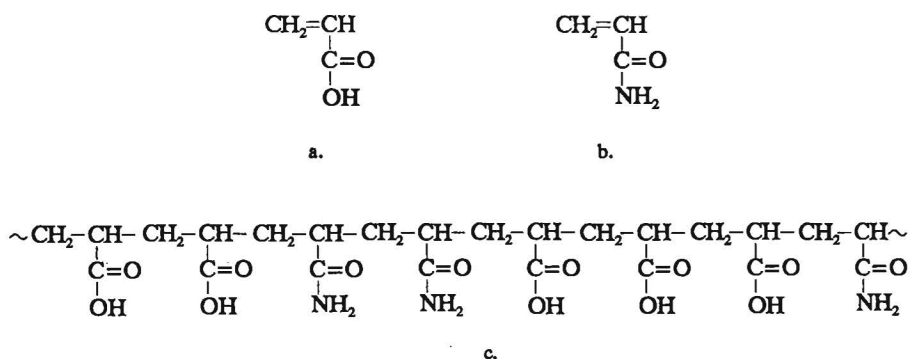


Figure 2.1: Chemical structure of the monomers used and the resulting copolymer: a. acrylic acid (AA), b. acrylamide (AAm), c. atactic poly(acrylamide-co-acrylic acid).

The reasons for the choice of the acrylic acid - acrylamide copolymers are the following:

- Poly(acrylic acid) and polyacrylamide provide ideal models for the behaviour of complex materials such as biopolymers due to the relative simple structure of the monomer units and the large number of polar and hydrogen-bonding groups per repeating unit which facilitate water solubility (Molyneaux [46]).
- The ionizability of the carboxylic group of the acrylic acid monomer can be used to obtain materials with polyelectrolyte properties. Since acrylic acid occurs in solution in non-ionized, partly ionized, and fully ionized form, depending on the pH of the environment, the number of fixed carboxylate $-\text{C}(\text{O})\text{O}^-$ -groups and hence the polyelectrolyte properties of the materials can be varied by adjustment of the pH as in nature.

- Polyacrylamide is distinguished by its highly hydrophilic character which is greater than that of most other non-ionic water-soluble polymers [73]. The application of acrylamide monomers thus ensures a high water retaining capacity of the materials.
- By composing the macromolecular chains of two synthetic components instead of one, their composition and hence their properties can be changed by adjustment of the relative amount of each component present. The application of acrylic acid - acrylamide copolymers thus provides an additional instrument to influence the overall behaviour of the materials.

To create sodium-carboxylate groups in the final materials, the acrylic acid is neutralized with sodium hydroxide (figure 2.2).

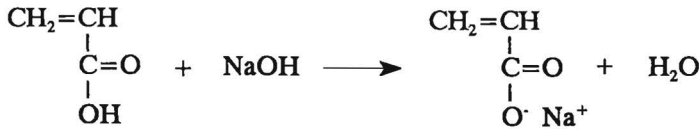


Figure 2.2: Sodium-acrylate formation

Furthermore, the copolymer chains are weakly crosslinked to enhance their mechanical properties and to decrease their solution solubility. This also ensures the retainment of the copolymers in the PUR-foam. The crosslinking is performed by using low concentrations of the difunctional monomer *N,N'*-methylenebisacrylamide (figure 2.3).

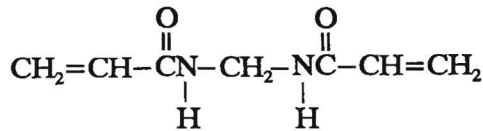


Figure 2.3: The chemical structure of the crosslinking agent *N,N'*-methylenebisacrylamide.

The synthetic model materials are prepared via *in-situ* copolymerization of acrylic acid and acrylamide in the pores of PUR-foams. The use of these foams not only increases the mechanical stability of the final materials but also creates the possibility to adjust the overall material behaviour via variation of the foam properties.

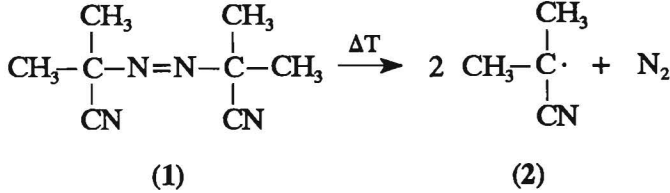


Figure 2.4: The thermal dissociation of the initiator 2,2'-azobis(isobutyronitrile) (AIBN) (1), yielding two identical cyanoisopropyl radicals (2).

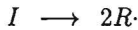
Commonly, acrylic acid and acrylamide monomers are polymerized via free radical polymerization in an aqueous solution (Buchholz [8]). As initiator of the copolymerizations, 2,2'-azobis(isobutyronitrile) (AIBN) is used (figure 2.4).

The composition of the model materials is adjusted via variation of the structure of the copolymer network and/or the properties of the PUR-foam. The former is varied via adjustment of the initial acrylic acid - acrylamide monomer ratio, the neutralization degree of the acrylic acid and the amount of crosslinking agent. PUR-foams of different pore density and stiffness are applied.

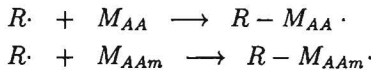
Acrylic acid - acrylamide copolymerizations are also performed in the absence of the crosslinking agent and the PUR-foams in order to characterize the copolymers obtained and to determine the possible differences between the copolymerizations performed in the presence of or without the PUR-foams.

2.2 Copolymerization of acrylic acid and acrylamide

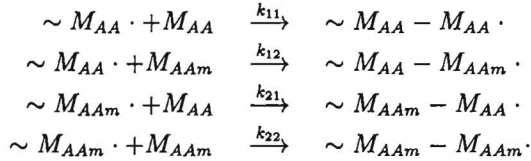
The copolymer gels required for the synthetic model materials can be obtained via free radical copolymerization of the acrylic acid and acrylamide monomers in aqueous solution. Free radical polymerization is a chain reaction initiated by the thermal dissociation of the initiator AIBN to yield a pair of identical radicals R· (Odián [49]),



The resulting primary cyanoisopropyl radicals add to either an acrylic acid (AA) or an acrylamide (AAm) monomer to produce chain initiating species $M_{AA}\cdot$ and $M_{AAm}\cdot$,



These species propagate by successive addition of monomer molecules. As the propagating radicals may react with either an acrylic acid or an acrylamide monomer, four different propagation steps are distinguished. The reactivity of the propagating radicals is assumed not to be dependent on the length of the polymer chain to which the monomer is attached (Flory's principle of equal reactivity). The successive additions can then be presented as follows (Odian [49]):



where k_{ij} is the rate constant for the propagation step ij . The preference of the chain radicals $\sim M_{AA} \cdot$ and $\sim M_{AAm} \cdot$ to react with a monomer of its own kind rather than with the other monomer is given by the reactivity ratios

$$\begin{aligned} r_{AA} &= \frac{k_{11}}{k_{12}} \\ r_{AAm} &= \frac{k_{22}}{k_{21}} \end{aligned}$$

where r_{AA} and r_{AAm} are respectively the reactivity ratios of acrylic acid and acrylamide. Both the overall acrylic acid - acrylamide monomer feed ratio $[M_{AA}]/[M_{AAm}]$ and the reactivity ratios of the monomers determine the instantaneous monomer consumption ratio $d[M_{AA}]/d[M_{AAm}]$ (Odian [49]),

$$\frac{d[M_{AA}]}{d[M_{AAm}]} = \frac{r_{AA}[M_{AA}]/[M_{AAm}] + 1}{r_{AAm}[M_{AA}]/[M_{AAm}] + 1} \quad (2.1)$$

Only when the instantaneous monomer consumption is equal to the overall monomer feed ratio, acrylic acid - acrylamide copolymers are obtained of homogeneous composition (azeotropic copolymerization). In all other cases, the monomer feed ratio constantly changes during polymerization resulting in a heterogeneity in the acrylic acid - acrylamide copolymer composition (composition drift). Generally, the greater the deviation from azeotropic copolymerization conditions, the larger the heterogeneity observed.

The growth of the copolymer chains is terminated by the destruction of propagating radicals. This termination can occur via combination or disproportionation.

The copolymerization of acrylic acid and acrylamide has been studied intensively since 1955. The reactivity ratios of the acrylic acid r_{AA} and acrylamide r_{AAm} monomers are dependent on pH (Bourdais *et al.* [9], Cabaness *et al.* [12], Potnatram *et al.* [53]), the ionic strength (Potnatram *et al.* [53]), the nature of the counterion (Shawski *et al.* [61]) and the nature of the solvent (Gromov *et al.* [21]). In figure 2.5 the experimental variation of r_{AA}

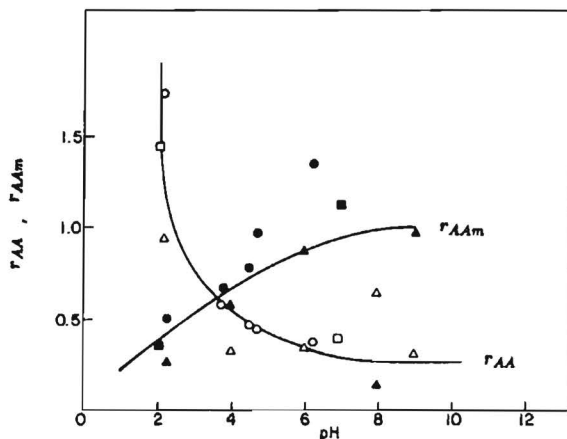


Figure 2.5: Variation of reactivity ratios of acrylic acid r_{AA} (open symbols) and acrylamide r_{AA_m} (full symbols) versus pH as determined by Bourdais *et al.* [9] (■, □), Cabaness *et al.* [12] (●, ○) and Potnatram *et al.* [53] (▲, △). The two lines represent the most probable r_{AA} and r_{AA_m} curves versus pH as determined by Truong *et al.* [66].

and r_{AA_m} versus pH is given. In principle, a decrease in r_{AA} and an increase in r_{AA_m} is observed with increasing pH. The pH-dependence is attributed to the increasing dissociation of acrylic acid with increasing pH (Blauer [6], Cabaness *et al.* [12], Kabanov [31]). Acrylic acid exists in its undissociated form at pH-values lower than two. For higher pH-values it transforms more and more in the ionized form as carboxylate anion (figure 2.6).

The scatter in the experimental data in figure 2.5 can be explained by differences in accuracy of the experimental methods used and by differences in monomer feed concentration, neutralizing agent, initiator type, reaction temperature or degree of conversion as applied by the various authors (Potnatram *et al.* [53]). The reduction in reactivity of dissociated acrylic acid compared to the reactivity of the non-ionized monomer is explained by the electrostatic charge repulsions between ionized monomers on one hand, and ionized monomer and ionized macroradicals on the other (Potnatram *et al.* [53]). Therefore, the tendency of the acrylamide monomer to react with its own radical increases with increasing pH. Based on the data given in the above studies, Truong *et al.* [66] determined a most probable r_{AA} and r_{AA_m} curve (figure 2.5). According to these curves, the r_{AA} -values decrease from 1.5 at pH = 2 to 0.35 at pH = 10 whereas the r_{AA_m} -values increase from 0.38 at pH = 2 to 0.95 at pH = 10. The most uniform copolymers are synthesized at pH = 4 ($r_{AA} \approx r_{AA_m} \approx 0.56$).

The total monomer content used in the studies given above varied between 1-7 wt % based on the aqueous solution content. The acrylic acid - acrylamide monomer feed ratios varied

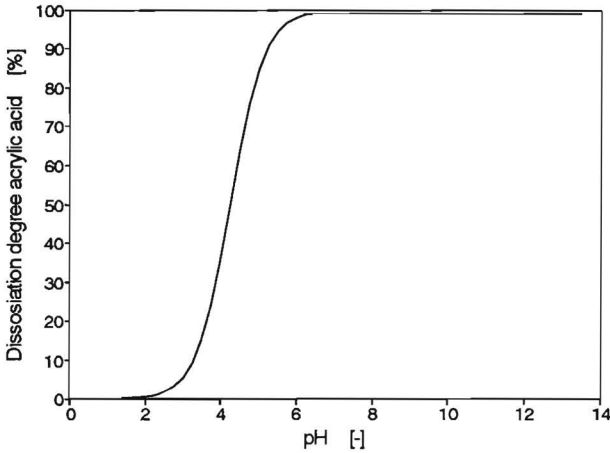


Figure 2.6: The dissociation degree of acrylic acid versus pH. The pK_a of acrylic acid is approximately 4.25 (Kabanov et al. [32]).

between 9:1 - 1:12. In case of pH adjustment, aqueous solutions of barium hydroxide or sodium hydroxide were used. In most studies the copolymerizations were initiated by potassium persulfate ($K_2S_2O_8$), but also the redox system potassium persulfate-sodium thiosulfate ($K_2S_2O_8 / Na_2S_2O_3$) and 2,2'-azobis(isobutyronitrile) (AIBN) were used. The amount of initiator varied between 0.1 and 5 wt % of the total monomer content. The copolymerizations were performed at 30° - 60°C.

2.3 Preparation of the model materials

The copolymerization conditions as given in section 2.2 have been adapted to obtain synthetic model materials with similar characteristic properties as intervertebral disc tissue. The main adaptations concern an increase of the total monomer content and the use of the PUR-foams. For reasons of clarity, a general outline of the preparation of the materials is given here. The detailed recipes are given in the experimental section 2.4.4.

The synthetic model materials are prepared via *in-situ* free radical copolymerization of acrylic acid and acrylamide in the pores of the PUR-foams in water of Millipore-Q quality. The PUR-foams used are rectangular shaped of thickness 10 and 20 mm and are deoxygenated before use. Due to the low density ($\rho_{foam} \approx 30 \text{ kg/m}^3$) and the high porosity of the foams ($0.95 < n^p < 0.98$)(section 2.4.2), monomer solutions are prepared containing a

typical total monomer content of 20 wt % in order to obtain materials with a solid-fluid ratio comparable to the 20:80 ratio encountered in intervertebral disc tissue. The acrylic acid is neutralized using sodium hydroxide in a standard amount of 70 mole % NaOH per mole acrylic acid [5]. The copolymer gels are crosslinked using *N,N'*-methylenebisacrylamide in a standard amount of one mole per 100 moles of mixed monomers. The copolymerization is initiated by addition of 2,2'-azobis(isobutyronitrile) in a typical amount of one mole per 1000 moles of mixed monomers [5]. The copolymerizations are performed under argon atmosphere at 60°C for 48 hours.

After synthesis, the raw materials are isolated from the surrounding copolymer gel and stored in sealed glass bottles.

According to the procedure given above, materials are prepared using initial acrylic acid - acrylamide monomer feed ratios of 1:0, 4:1, 1:1 and 1:4. Also materials are prepared starting with a standard acrylic acid - acrylamide monomer feed ratio of 4:1 and applying single changes in neutralization degree (0.35 mole NaOH instead of 0.7 mole NaOH per mole acrylic acid) or the amount of crosslinking agent (3 instead of 1 mole *N,N'*-methylenebisacrylamide per 100 moles of mixed monomers).

2.4 Experimental

2.4.1 Characterization techniques

FT-IR, Infrared Spectroscopy, was used to collect infrared spectra of poly(acrylic acid) (PAA), polyacrylamide (PAAm) and poly(acrylic acid-co-acrylamide) samples. The spectra were recorded with a Mattson-Polaris FT-IR spectrometer equipped with a standard DTGS detector and He/Ne laser. The spectra were obtained after accumulation of 32 scans at a resolution of 4 cm^{-1} between 4000 cm^{-1} and 400 cm^{-1} . The sample compartment was held under nitrogen atmosphere at room temperature. (Co)polymer gel samples were either mixed with KBr powder or placed as a thin film (solution-cast) on KBr plates.

SEM, Scanning Electron Microscopy, was performed to study the morphology of the PUR-foams using a Cambridge Stereoscan 200 microscope operating at 15 kV. Micrographs were made of PUR-samples fractured in liquid nitrogen and subsequently coated with a thin Au-film.

HPLC, High Performance Liquid Chromatography, was performed to determine the conversion during polymerization using Waters apparatus composed of: pump model 510, automatic injector WISP model 710b (injection volume 1 μl) and UV-detector model 490 adjusted at 250 nm. The apparatus was equipped with μ -Bondapak NH_2 (35°C) columns (dimensions 300 x 3.9 mm, flow 1ml/min), calibrated with 3 wt % acrylic acid and acrylamide monomer solutions. As eluent 0.1 M sodium dihydrogen phosphate buffer was used. The water was of HPLC grade.

TGA, Thermogravimetric Analysis (Perkin Elmer, TGA-7), was used to determine the amount of rest solvent in the hydrophilic copolymers. Copolymer gel samples were dried in vacuum for 48 hours at 150°. The resulting copolymers were heated from 50° to 700°C using a standard heating rate of 10K/min in atmosphere of air.

Solid content analysis was used to estimate the polymerization conversion and the solid-fluid ratio of the synthetic model materials. Material samples of known mass were heated in vacuum for 24 hours at 150°C. The polymerization conversion and solid-fluid ratio were calculated using the rest mass of the dried samples.

2.4.2 Materials

AA, acrylic acid (melting point 13°C, received from Merck, Schuchardt, Germany), was distilled from inhibitor hydroquinon under vacuum (pressure 3-4 kPa at 65°-75°C). The distillation was done over red-copper windings to prevent the vapor from early polymerization. The distilled monomer was received in a recipient cooled with melting ice. After distillation, the monomer was stored at 4°C.

AAM, acrylamide (melting point 84°C, purity > 99%, received from Merck, Schuchardt, Germany), and **N,N'-methylenebisacrylamide** (melting point 300°C, purity > 96%, received from Janssen Chimica, Tilburg, The Netherlands) were used as received.

NaOH, sodium hydroxide, was first grade and used as received from Merck, Darmstadt, Germany.

AIBN, 2,2'-azobis(isobutyronitrile) (melting point 102°C, purity > 96%), was used as received from Merck, Schuchardt, Germany.

H₂O, water, was purified from extraneous minerals by a Millipore-Q water system. Before use, the water was boiled for 15 minutes and deoxygenated by argon during 30 minutes.

PUR, open cell microporous polyurethane foams, were used as received from UXEM B.V., Valkenburg Z.H., The Netherlands. Three different types of foam were applied with variations in pore density and stiffness. The foams were either reticulated and based on polyester with 30 and 60 pores per inch respectively (type PPI30 and PPI60) or based on polyether (type 38HH). The properties of the foams are given in table 2.1. In figure 2.7 the structure of the foams is shown.

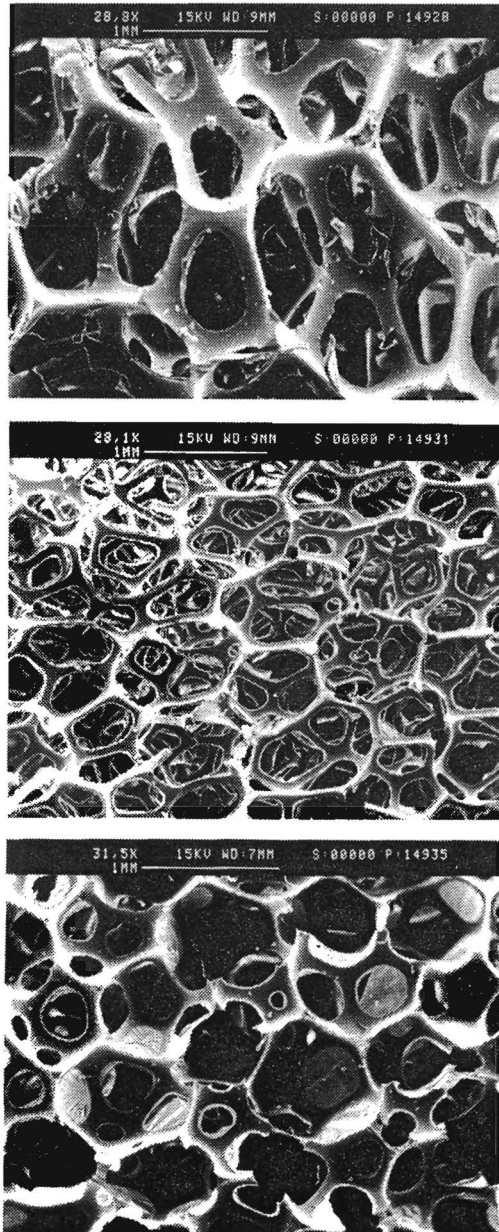


Figure 2.7: SEM micrographs of the PUR-foams used: top: polyester reticulated, 30 pores per inch, middle: polyester reticulated, 60 pores per inch, bottom: polyether 38HH.

| type foam | density ^a [kg/m ³] | density ^b [kg/m ³] | porosity ^b [-] | stiffness ^a [kPa] | elongation to break ^a [%] |
|-----------|----------------------------------------------|----------------------------------------------|------------------------------|---------------------------------|-----------------------------------------|
| PPI30 | 30 | 30.9 ± 0.1 | 0.98 ± 0.01 | 80 | > 200 |
| PPI60 | 30 | 31.6 ± 0.1 | 0.95 ± 0.01 | 80 | > 200 |
| 38HH | 38 | 38.5 ± 0.1 | 0.98 ± 0.01 | 110 | 140 |

Table 2.1: Properties of the PUR-foams. ^a: specifications of UXEM B.V., ^b: as determined by mass measurements.

2.4.3 Synthesis of acrylic acid - acrylamide copolymer

At room temperature, 30 ml acrylic acid was dissolved in 300 ml deoxygenated water. Hereafter, 11.66 g sodium hydroxide based on the acrylic acid content was added to the solution. A homogeneous solution was obtained by stirring at room temperature for five minutes. Subsequently, 30 g acrylamide was added. After stirring for another five minutes the temperature was increased to 62°C and 2,2'-azobis(isobutyronitrile) (AIBN) was added in an amount of 136 mg based on the total monomer content. Polymerization was performed under argon atmosphere for 48 h. After approximately 2 hours the solution became viscous. After copolymerization for 48 hours, a transparent highly viscous gel was obtained. Finally, the temperature of the reaction mixture was decreased to room temperature and the copolymer gel isolated and stored in a sealed glass bottle.

IR: $\nu = 1660-1670, 1565-1575$ (C=O) cm⁻¹

HPLC: acrylic acid : rt = 5.32 min, peak-area 87%
acrylamide : rt = 3.73 min, peak-area 13%

By using the same procedure as above also copolymerizations were performed using:

- 48 ml acrylic acid, 18.66 g sodium hydroxide and 12 g acrylamide
- 12 ml acrylic acid, 4.66 g sodium hydroxide and 48 g acrylamide

In both cases, transparent highly viscous gels were obtained. An increase in the viscosity of the gels was observed with increasing initial acrylamide content.

IR: $\nu = 1660-1670, 1565-1575$ (C=O) cm⁻¹

HPLC: AA:AAm = 1:1 : acrylic acid : rt = 5.32 min, peak-area 64%
acrylamide : rt = 3.73 min, peak-area 36%
AA:AAm = 1:4 : acrylic acid : rt = 5.32 min, peak-area 36%
acrylamide : rt = 3.73 min, peak-area 64%

2.4.4 Synthesis of copolymers in the presence of PUR-foam

At room temperature, 30 ml acrylic acid was dissolved in 300 ml deoxygenated water. Hereafter, 11.66 g sodium hydroxide based on the acrylic acid content was added to the solution. A homogeneous solution was obtained by stirring at room temperature for five minutes. Subsequently, 30 g acrylamide and 1.28 g N,N'-methylenebisacrylamide, based on the comonomer content, was added. The solution was stirred for another five minutes to obtain homogeneity. Hereafter, rectangular shaped PUR-foams of thickness 10 and 20 mm were placed in the solution and deoxygenated. Subsequently, the temperature was increased to 62°C and 2,2'-azobis(isobutyronitrile) was added in an amount of 136 mg based on the total monomer content. Polymerization was performed under argon atmosphere for 48 h. After approximately 2 hours the solution became viscous. After polymerization for 48 hours, transparent crosslinked gels were obtained comprising the PUR-foams. Finally, the temperature of the reaction mixture was decreased to room temperature. The model materials were isolated from the surrounding copolymer gel and stored in sealed glass bottles.

By using the same procedure as above also copolymerizations were performed in the presence of the PUR-foams using relative amounts of the constituents as given in table 2.2.

In all cases, transparent crosslinked gels were obtained comprising the PUR-foams. No visual differences were observed between the copolymer gels *in-situ* or outside the PUR-foams.

IR: $\nu = 1660-1670, 1565-1575$ (C=O) cm^{-1} .

| AA [ml] | NaOH [g] | AAm [g] | crossl. agent [g] | AIBN [mg] |
|---------|----------|---------|-------------------|-----------|
| 48 | 18.66 | 12 | 1.28 | 136 |
| 12 | 4.66 | 48 | 1.28 | 136 |
| 60 | 23.3 | - | 1.28 | 136 |
| 48 | 9.33 | 12 | 1.28 | 136 |
| 48 | 18.66 | 12 | 3.84 | 136 |

Table 2.2: Overview of the relative amounts of the constituents used for the preparation of various model materials. In all cases, PUR-foams of type PPI30, PPI60 and 38HH were used.

2.4.5 Synthetic model materials used for mechanical studies

From the model materials prepared, the materials listed in table 2.3 were selected to study the mechanical behaviour of the materials in general and the influence of the various constituents on this behaviour in particular. The influence of the type of PUR-foam, the

initial acrylic acid - acrylamide monomer ratio, the crosslink degree and the initial degree of neutralization on the mechanical behaviour is studied with this set of materials. Each material is given a code reflecting its composition. The material types having a four-digit code were prepared using standard degree of neutralization (70 mole % sodium hydroxide per mole acrylic acid) and standard amount of crosslinking agent (1 mole % N,N' -methylenebisacrylamide per mole of mixed monomers). The first two digits of the material code refer to the initial acrylic acid - acrylamide ratio, the second to the PUR-foam used. For example: the 4130 material was prepared with an initial acrylic acid - acrylamide monomer ratio of 4:1 and a PUR-foam of type PPI30. For the materials 6 and 7 the last digits refer to the deviations in the concentration of the crosslinking agent (3 mole %) and the degree of neutralization (35 mole %) respectively.

| code | ratio AA/AAm | PUR-foam | degree neutralization ^a | conc. crosslinking agent ^b |
|--------|--------------|----------|------------------------------------|---------------------------------------|
| 4130 | 4:1 | PPI30 | 70 | 1 |
| 4160 | 4:1 | PPI60 | 70 | 1 |
| 4138 | 4:1 | 38HH | 70 | 1 |
| 1160 | 1:1 | PPI60 | 70 | 1 |
| 1460 | 1:4 | PPI60 | 70 | 1 |
| 41303 | 4:1 | PPI30 | 70 | 3 |
| 413035 | 4:1 | PPI30 | 35 | 1 |
| 1030 | 1:0 | PPI30 | 70 | 1 |

Table 2.3: Overview of the composition of the synthetic model materials used to study their mechanical behaviour. ^a: mole % NaOH per mole acrylic acid, ^b: mole % per mole mixed monomers.

2.5 Results and discussion

2.5.1 Copolymers

Acrylic acid (AA) - acrylamide (AAm) copolymerizations were performed in an aqueous solution in the absence of crosslinking agent and PUR-foams using a total monomer content of 20 wt % based on the water content and initial AA:AAm monomer feed ratios of 4:1, 1:1 and 1:4. Temperature and pH were automatically registered during synthesis. Data were collected every 30 minutes. The polymerizations were performed at $62 \pm 2^\circ\text{C}$.

For the HPLC experiments, samples of approximately 10 ml were taken every 10 minutes from the solution during the first three hours of the copolymerizations in order to determine the monomer consumption. Hereafter, the gels became too viscous to collect another sample. After polymerization, a final sample was taken, dissolved in a 20-fold amount of water, and analyzed by HPLC to determine the polymerization conversion.

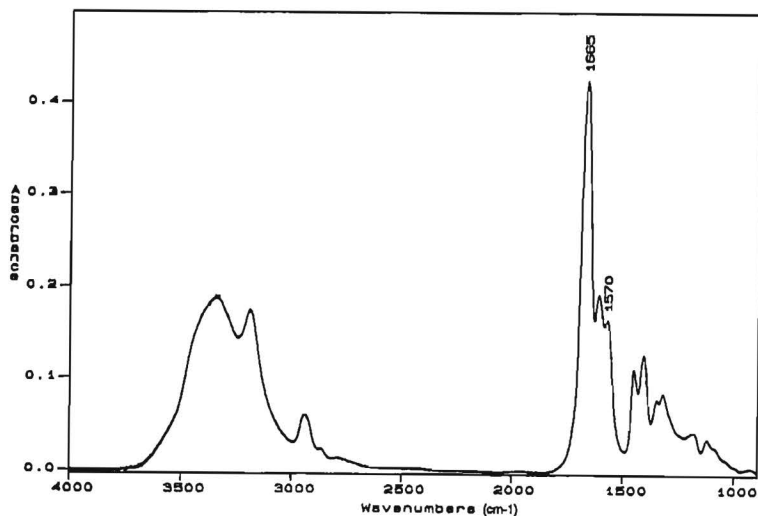


Figure 2.8: IR absorption spectrum of acrylic acid (AA) - acrylamide (AAm) copolymer synthesized with an initial AA:AAm monomer feed ratio of 1:4.

The HPLC measurements showed that for all three copolymerizations the monomer consumption remains equal to the initial monomer feed ratio during the first three hours of polymerization, indicating that in this period copolymers of homogeneous composition are obtained. Approximately 15 - 20% of the monomers are converted in 3 hours. Klein *et al.* [36] reported conversions of about 20% after 45 minutes using 0.1-1% $K_2S_2O_8$ as initiator and 1-3 wt% monomer content in aqueous solution at 60°C. The HPLC data of the final samples showed that all samples contained less than 1% monomer.

IR experiments were performed to study the composition of the acrylic acid - acrylamide copolymers. For comparison also the IR-spectra of the homopolymers of acrylic acid and acrylamide were recorded. The main difference observed between the IR-spectra of poly(acrylic acid) and poly(sodium acrylate) is a shift of the carbonyl-group absorption $\nu_{C=O}$ with increasing ionization from 1710 cm^{-1} towards 1565-1575 cm^{-1} . The latter peak is characteristic for the vibration of the ionized $-C(O)O^-$ -group (Bardet *et al.* [2]). The presence of the carbonyl band at 1570 cm^{-1} in all copolymer IR-spectra confirmed the presence of carboxylate groups. The vibration of the carbonyl-group of polyacrylamide was found at 1660-1670 cm^{-1} in accordance with literature (Kulicic *et al.* [39]). An example of the recorded spectra is given in figure 2.8.

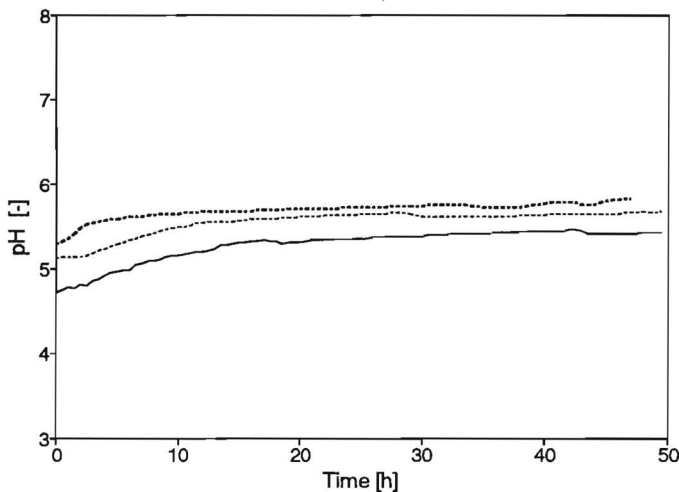


Figure 2.9: Experimental pH-data versus time of the acrylic acid (AA) - acrylamide (AAm) copolymerizations performed with initial AA:AAm monomer feed ratios of 4:1 (—), 1:1 (···) and 1:4 (-·-·).

The TGA experiments showed that the copolymers contained approximately 5 wt% water, even after prolonged vacuum drying at 150°C for 48 h. This amount of water is absorbed by the hydrophilic side groups of the copolymer chains. At low temperatures, a mass loss occurred, associated with the loss of water, which gradually increased with temperature. A first increase in the rate of mass loss was observed near 245°-255°C, which is likely to be due to the facilitated loss of retained water resulting from the heating of the samples above the glass transition temperature. In literature, a T_g of sodium polyacrylate is reported of approximately 251°C [24, 73].

Initial pH-values were measured of 4.75, 5.10 and 5.30 for the solutions containing an initial AA:AAm monomer feed ratio of 4:1, 1:1 and 1:4 respectively (figure 2.9). As the acrylic acid content was neutralized standardly with 70 mole % sodium hydroxide, a slight increase in pH occurred with decreasing acrylic acid content. At these pH-values the acrylic acid content is dissociated 74%, 88%, and 92% respectively (figure 2.6). For all copolymerizations, the pH slightly increases during polymerization by approximately 0.5 unit which is attributed to the conversion of acrylic acid ($pK_a \approx 4.25$) to poly(acrylic acid) ($pK_a \approx 6.4$, Kabanov *et al.* [32]). Truong *et al.* [66] also reported an increase in the pH of approximately 0.5 unit. For all syntheses the pH reaches a more or less steady value after 20 hours.

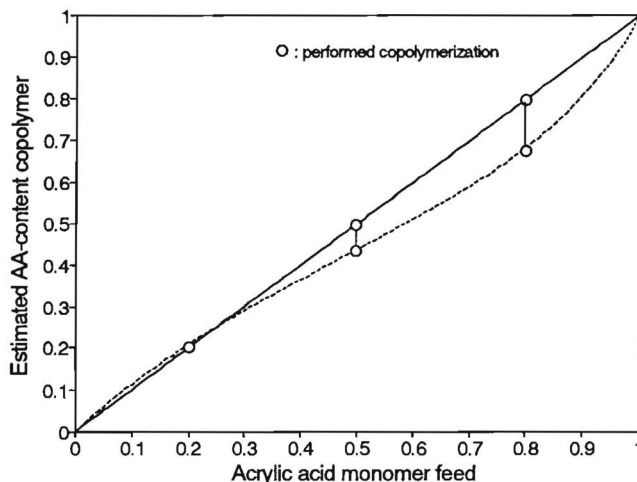


Figure 2.10: Acrylic acid monomer feed versus estimated acrylic acid content of the copolymers: Comparison of azeotropic (—) and estimated actual copolymerization conditions (···) using values for the reactivity ratios of acrylic acid and acrylamide of 0.4 and 0.8 respectively.

By comparing the pH-data measured with the data given in figure 2.5, the reactivity ratios of acrylic acid r_{AA} and acrylamide r_{AAm} during the copolymerizations were estimated as 0.4 and 0.8 respectively. For these estimates the most probable r_{AA} and r_{AAm} curves were used. For these values, the estimated deviation from azeotropic copolymerization conditions is given in figure 2.10. Based on these curves, the copolymers prepared with an initial AA:AAm monomer feed ratio of 1:4 are polymerized under nearly azeotropic conditions, hence the resulting copolymers are likely to be of homogeneous composition. With increasing initial acrylic acid monomer feed, the copolymerization conditions become more and more non-azeotropic. As a result, an increase in the heterogeneity of the copolymer composition is expected for the copolymers polymerized with initial AA:AAm monomer feed ratios of 1:1 and 4:1.

2.5.2 Copolymers in PUR-foams

IR experiments were performed to characterize the copolymers present in the various materials. For the measurements only crosslinked copolymer gel samples were taken. All IR-spectra, except those of the copolymers present in the 1030 and 413035 materials, showed characteristics similar to the spectra of the copolymers synthesized in the absence of the PUR-foams and the crosslinking agent. In the spectra the carbonyl band of acrylamide as well as the carbonyl band of the ionized acrylic acid were present at $1660\text{--}1670\text{ cm}^{-1}$ and

1565-1575 cm^{-1} respectively.

For the polymers present in the 1030 material, which are purely based on acrylic acid, two main peaks were recorded at 1570 and 1640 cm^{-1} respectively. The former peak is related to the carbonyl vibration of the carboxylate $-\text{C}(\text{O})\text{O}^-$ -group, while the latter is probably associated with unreacted monomer. The vibration of the unsaturated $\text{C}=\text{C}$ bond of the monomers is typically found at 1640 cm^{-1} .

This peak was also observed in the IR-spectrum of the copolymers present in the 413035 material which was prepared with a NaOH neutralization degree of 35 mole %. Due to the reduced neutralization of the acrylic acid, the preparation of the material is performed at lower pH. For these pH-conditions the reactivity ratio of acrylic acid is increased while the reactivity ratio of acrylamide is decreased (figure 2.5). This results in different reaction products and possibly to the presence of rest monomer. Unfortunately, a quantitative analysis was not possible. However, based on the HPLC results obtained for the copolymer samples synthesized in the absence of crosslinking agent and PUR-foams, it is likely that the copolymerizations are performed to almost full conversion.

Polymerization conversion data could not be obtained via solid content analysis of material samples as the measurements are influenced by the presence of the water absorbed by the hydrophilic side groups of the copolymer chains (section 2.5.1). However, by assuming that this amount of water is not able to participate in fluid processes, the results of the measurements can be used for an estimation of the solid-fluid fraction of the materials (table 2.4). The solid content of the materials varies between 22-27 wt %.

| code | initial mass [mg] | rest mass [mg] | solid fraction | fluid fraction |
|--------|-------------------|----------------|----------------|----------------|
| 4130 | 152 | 39 | 0.257 | 0.743 |
| 4160 | 118 | 30 | 0.254 | 0.746 |
| 4138 | 118 | 31 | 0.263 | 0.737 |
| 1160 | 84 | 19 | 0.226 | 0.774 |
| 1460 | 90 | 23 | 0.256 | 0.744 |
| 41303 | 125 | 28 | 0.224 | 0.776 |
| 413035 | 142 | 37 | 0.261 | 0.739 |
| 1030 | 141 | 39 | 0.277 | 0.723 |

Table 2.4: Solid - fluid fractions of the materials.

2.6 Conclusions

Model materials were synthesized consisting of an open cell microporous PUR-foam embedded in a hydrophilic copolymer gel. The copolymer gel consists of a water phase containing atactic acrylic acid - acrylamide copolymers.

The materials were successfully prepared in an aqueous solution via free-radical *in-situ* copolymerization of acrylic acid and acrylamide in the pores of the PUR-foams. Via addition of sodium hydroxide and N,N'-methylenebisacrylamide, charged crosslinked copolymer gels were obtained.

The synthesis of the acrylic acid - acrylamide copolymers proceeded in the presence of the PUR-foams. Unfortunately, no accurate conversion data could be determined from the resulting copolymers. However, in the absence of the PUR-foams and the crosslinking agent, the copolymerizations resulted in almost full conversion after 48 hours.

Materials of different composition were prepared by adjustment of the structure of the copolymer network and the properties of the PUR-foams. The structure was adjusted by variation of the initial acrylic acid - acrylamide monomer feed ratio, the neutralization degree of the acrylic acid and the amount of crosslinking agent. The properties of the PUR-foams varied in pore-density and stiffness.

Chapter 3

Experimental determination of swelling pressures

In this chapter, the ability of the materials to swell is studied by analysis of swelling pressure experiments. The experiments are performed on disc shaped material samples, kept at fixed initial height and subjected to NaCl bathing solutions of varying ionic strength.

After the introduction (section 3.1), the phenomena contributing to the swelling pressure of the materials are outlined in section 3.2. Subsequently, the materials and methods are described in section 3.3. Detailed information is given of the experimental set-up, the experimental protocol and the swelling pressure studies performed. The results of the measurements are given in section 3.4, showing the general pressure behaviour of the materials and its variation with NaCl concentration. The transient pressure behaviour is used to estimate the diffusion coefficient of the materials. The chapter concludes in section 3.5 with a discussion of the results obtained.

3.1 Introduction

Since the synthetic model materials contain highly hydrophilic copolymer gels, composed of water-swollen weakly crosslinked poly(acrylamide-co-sodium acrylate) chains, the exposure of the materials to aqueous solutions will give rise to swelling processes (Sakohara *et al.* [59]). The swelling is associated with the following phenomena (Helfferich [26]): (i) the osmotic exchange of water and mobile ions due to the presence of the hydrophilic copolymer chains and the difference in ionic strength between the material and the external solution, (ii) the electrostatic repulsion of neighboring fixed carboxylate $-C(O)O^-$ -groups. The coiled and packed chains of the copolymer network unfold and make room for solvent molecules, but only to a limited degree as they are interconnected by crosslinks. As a result, the materials swell but do not dissolve.

As the swelling progresses, all the expanding forces decrease. With increasing dilution, the initial difference in ionic strength between the material and external solution is reduced, the solvation tendency of the copolymer chains is decreased with approaching completion of the solvation shells and the electrostatic repulsion between the fixed carboxylate $-C(O)O^-$ -groups is diminished with increasing distance between the groups. Finally, a situation is attained in which the dissolution tendency of the material is balanced by the increased tension in the PUR-copolymer network.

The tendency of the materials to swell depends on the total amount of ionic groups present, their ionization state, the degree of crosslinking of the copolymer network, and the ionic strength of the external solution (Helfferich [26]). For poly(acrylamide-co-sodium acrylate) gels, an increase in swelling is observed with increasing fixed charge density and decreasing degree of crosslinking of the copolymer network and with decreasing ionic strength of the external solution (Ricka *et al.* [57], Vasheghani *et al.* [72], Yoshio *et al.* [75]).

In order to quantify the ability of the materials to swell, experiments are performed to determine the pressure developed by the materials during swelling. In the experiments sodium chloride solutions are used as bathing solutions.

3.2 Contributions to the swelling pressure

When immersed in a sodium chloride (NaCl) solution, the swelling equilibrium of the model material is given by (Flory [17]),

$$\pi_{swel} = \pi_{el} + \pi_{fcr} + \pi_{osm} = p_{ext} \quad (3.1)$$

where π_{swel} is the swelling pressure which equals any applied external pressure p_{ext} and consists of an elastic contribution π_{el} from the deformation of the PUR-copolymer network, a contribution π_{fcr} from the repulsion of the fixed charged carboxylate groups and an osmotic contribution π_{osm} from the mixing of the copolymer network and the ions with

the solvent. According to mixture theory, the first two contributions embody the effective Cauchy stress σ_{eff} of the material (section 1.3). The corresponding equilibrium condition is given by Eq. 1.1,

$$\sigma_{eff} - p = p_{ext}$$

where p is the hydrodynamic fluid pressure which equals in equilibrium the osmotic pressure π_{osm} . The elastic contribution is accounted for by relation 1.10. In the subsequent sections the contributions π_{osm} and π_{fcr} are outlined.

3.2.1 Osmotic exchange of solvent and ions: Donnan equilibria

When two NaCl solutions of different concentration are separated by a membrane which is permeable to both Na^+ and Cl^- -ions as well as the common solvent, the equilibrium concentrations of NaCl will be equal on both sides of the membrane. However, if on one side the NaCl solution also contains charged macromolecules, which are too large to move through the membrane to the other side, the equilibrium concentrations of both the Na^+ and Cl^- -ions on the two sides will be different.

This situation occurs also if a model material sample is brought into contact with a NaCl solution. Because of the presence of the carboxylate groups immobilized within the material, the equilibrium concentrations of the Na^+ and Cl^- -ions inside the material are different from the corresponding external bath concentrations. The unequal distribution of mobile ions produces a pressure difference between the material and the external solution which is known as the osmotic pressure. Expressions for the ion-distribution in the material and the osmotic pressure are derived from the electro-neutrality conditions and the equality of the chemical potentials of the ions and solvent in the material and the external solution.

Electro-neutrality within the external solution is given by

$$c^+ = c^- = c \quad (3.2)$$

where c^+ and c^- are the external Na^+ and Cl^- -ion concentration respectively. Within the material, the equilibrium concentration of Na^+ -ions (C^+) equals the concentration of Na^+ -ions required to balance the negative fixed charges on the copolymer network (C^{fd}) and the concentration Na^+ -ions equivalent to the concentration of Cl^- -ions (C^-),

$$C^+ = C^{fd} + C^- \quad (3.3)$$

The chemical potential per mole of a constituent i is given by (Katchalsky [34])

$$\nu_i = \nu_i^0(T) + \bar{V}_i P + RT \ln(a_i) \quad (3.4)$$

where $\nu_i^0(T)$ is the concentration independent molar chemical potential, \bar{V}_i the partial molar volume, P the fluid pressure, R the universal gas constant, T the absolute temperature

and a_i the activity of the constituent i . The latter is related to the molar fraction X_i and the activity-coefficient γ_i of the constituent according to

$$a_i = \gamma_i X_i \quad (3.5)$$

For the chemical potential of the ions, the second term in the right hand side of Eq. 3.4 can be neglected compared to the activity term. By considering the chemical potential of the ions as a whole

$$\nu_{NaCl} = \nu_{Na^+} + \nu_{Cl^-} \quad (3.6)$$

and assuming ideal behaviour ($\gamma_i = 1$), the chemical potential in the external bath and material is given by

$$\nu_{NaCl}^{ext} = \nu_0(T) + RT \ln(x^- x^+) \quad (3.7)$$

$$\nu_{NaCl}^{smm} = \nu_0(T) + RT \ln(X^- X^+) \quad (3.8)$$

where (x^-, x^+) and (X^-, X^+) are the molar fractions of the Cl^- -ions and Na^+ -ions in external bath and material respectively. The molar fractions are written as

$$x^- = \frac{c^-}{c^- + c^+ + c^w} \approx \frac{c^-}{c^w} \quad \text{and} \quad x^+ \approx \frac{c^+}{c^w} \quad (3.9)$$

$$X^- = \frac{C^-}{C^- + C^+ + C^w} \approx \frac{C^-}{C^w} \quad \text{and} \quad X^+ \approx \frac{C^+}{C^w} \quad (3.10)$$

where c^w and C^w are the molar water concentrations in the external solution and in the material. Assuming $c_w \approx C_w$, the equality of the chemical potential of the ions yields

$$c^+ c^- = C^+ C^- \quad (3.11)$$

By substituting the electro-neutrality conditions (3.2) and (3.3) in Eq. 3.11, the equilibrium ion-distribution in the synthetic model material is given by

$$2C^+ = C^{fcd} + \sqrt{(C^{fcd})^2 + 4c^2} \quad (3.12)$$

$$2C^- = -C^{fcd} + \sqrt{(C^{fcd})^2 + 4c^2} \quad (3.13)$$

The unequal distribution of counter and co-ions, due to the presence of the fixed charges on the copolymer network, is called the Donnan effect (Donnan [14]). This effect is only completely eliminated for high external NaCl concentrations.

The chemical potential of the solvent in the external solution and the material is given by (Katchalsky [34])

$$\nu_w^{ext} = \nu_0(T) + \bar{V}_w^{ext} p + RT \ln(x^w) \quad (3.14)$$

$$\nu_w^{smm} = \nu_0(T) + \bar{V}_w^{smm} P + RT \ln(X^w) \quad (3.15)$$

where $(\bar{V}_w^{ext}, \bar{V}_w^{smm})$ are the partial molar fluid volumes, (p, P) the fluid pressures and (x^w, X^w) the fluid molar fractions of the external solution and material respectively. Assuming $\bar{V}_w^{ext} \approx \bar{V}_w^{smm}$, the equality of the chemical potentials yields the pressure difference between external solution and material, i.e. the osmotic pressure π_{osm} ,

$$\pi_{osm} = P - p = \frac{RT}{\bar{V}_w} \ln \left(\frac{x^w}{X^w} \right) \quad (3.16)$$

The logarithmic term can be elaborated (Lakshminarayanaiah [41]) according to

$$\begin{aligned} \ln \left(\frac{x^w}{X^w} \right) &= \ln \left(\frac{1 - x^+ - x^-}{1 - X^+ - X^- - X^{cop}} \right) \\ &\approx X^+ + X^- - 2x + X^{cop} \end{aligned} \quad (3.17)$$

where X^{cop} is the molar fraction of the copolymer network. Eq. 3.16 is then written as

$$\begin{aligned} \pi_{osm} &= \frac{RT}{\bar{V}_w} (X^+ + X^- - 2x + X^{cop}) \\ &\approx RT(C^+ + C^- - 2c + C^{cop}) \end{aligned} \quad (3.18)$$

The latter contribution to the osmotic pressure arises from the mixing of the copolymer network with the solvent. This contribution can be written as (Richards [56])

$$\pi_{cop} = RT \frac{c_{cop}}{M_{cop}} + \mathcal{O} \left(\frac{c_{cop}^2}{M_{w,cop}^2} \right) \quad (3.19)$$

where c_{cop} is the copolymer concentration in unit mass per unit fluid volume and $M_{w,cop}$ the mass average molar mass of the copolymer network. The contribution π_{cop} to the osmotic pressure is neglected compared to the electrolyte contribution, due to the high molar mass of the network. The osmotic pressure is then only dependent on the Donnan effect, i.e. the imbalance of the mobile ions,

$$\pi_{don} = RT(C^+ + C^- - 2c) \quad (3.20)$$

Using Eqs. 3.12 and 3.13 the Donnan osmotic pressure is written as

$$\pi_{don} = RT(\sqrt{(C^{fcd})^2 + 4c^2} - 2c) \quad (3.21)$$

Eq. 3.21 describes the pressure difference between external bath and material assuming ideal behaviour. To account for possible non-ideal behaviour, osmotic coefficients for the synthetic model material ϕ^{smm} and the external NaCl solution ϕ^* are introduced accounting for the ion-copolymer and ion-ion interactions respectively (Richards [56])

$$\pi_{don} = \phi^{smm} RT \sqrt{(C^{fcd})^2 + 4c^2} - 2\phi^* RTc \quad (3.22)$$

3.2.2 Fixed charge repulsion

In principle, the electrostatic repulsion between the fixed charged carboxylate - C(O)O⁻ groups contributes to the swelling pressure (Helfferich [26]). This charge repulsion is known in mixture theory as the chemical expansion stress (Lai *et al.* [40]), i.e. the stress exerted on the solid phase of the material by actions other than the osmotic pressure or the elastic stresses due to deformation of the material. Whether this contribution is relevant depends on the number of fixed charges present and their relative spacing. The fixed charge repulsion is expected to be manifest when the materials are either strongly charged (figure 3.1 A), or only moderately charged but subjected to large compressive loads (figure 3.1 B). In the latter case the fixed negative charges are brought into closer proximity which increases the electrostatic forces. The effect of charge repulsion is also influenced by the amount of mobile Na⁺ and Cl⁻ ions present. When the external solution consists of a dilute NaCl solution, only a small number of mobile ions is present in the poly(acrylamide-co-sodium acrylate) gel which promotes the charge repulsion. With increasing NaCl concentration, the repulsion tends to reduce in strength due to an increased charge shielding by the mobile ions (figure 3.1 C).

The swelling pressure experiments should prove whether the above contribution is significant or not. In the experiments, the pressure is measured without deformation of the material, hence the elastic contribution to the pressure has not to be taken into account. By comparing the swelling pressure responses with Donnan theory, an indication can be obtained of the relative contribution of the fixed charge repulsion and the osmotic pressure.

3.3 Experimental

3.3.1 Materials

Synthetic model materials were prepared according to the procedure given in chapter 2. From the raw materials, cylindrical bars 10 mm in diameter were cut using a slowly rotating cork borer. From these bars, discs with heights between 1 - 2 mm were prepared with a scalpel. The samples were stored in sealed glass bottles until use.

In table 2.3 of chapter 2 the composition is given of the materials which were used in the swelling pressure experiments. For the properties of the PUR-foams the reader is referred to the experimental section of chapter 2.

The sodium chloride for the bathing solutions was first grade and used as received from Merck (Darmstadt, Germany). Ultra purified water was used for the preparation of the solutions.

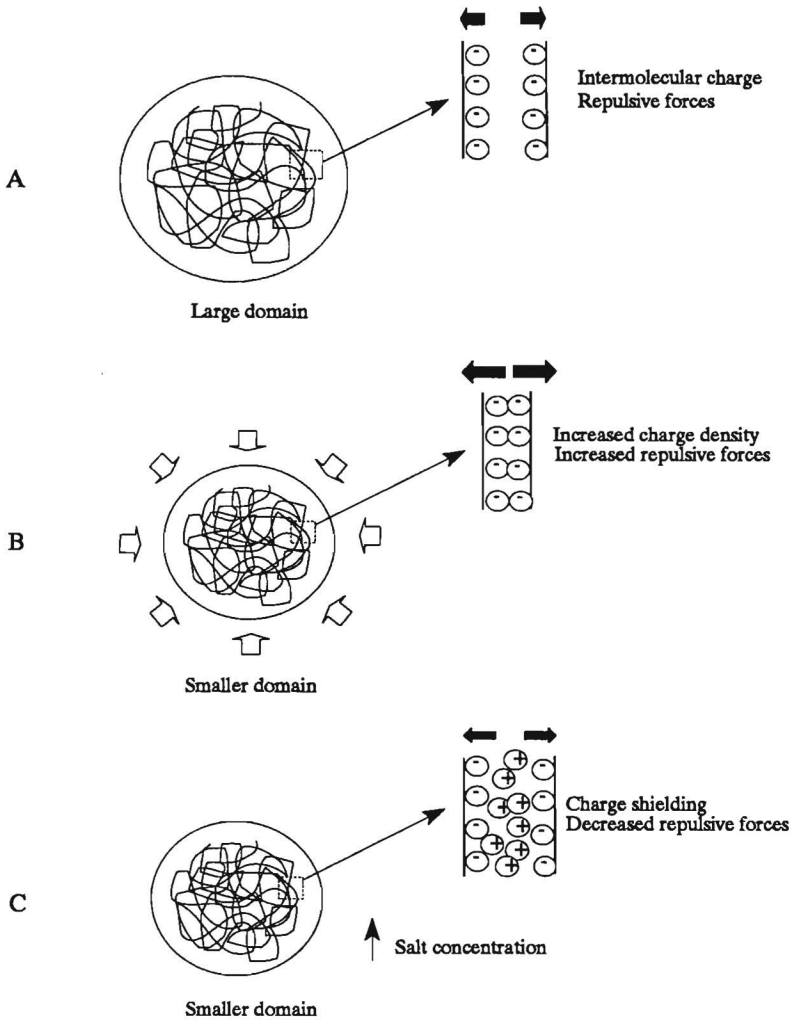


Figure 3.1: The poly(acrylamide-co-sodium acrylate) gel of the materials contains charged carboxylate $-C(O)O^-$ groups which are firmly attached to the copolymer network. High densities of these groups give rise to electrostatic charge repulsive forces which contribute to the swelling pressure of the materials (A). Compression of the materials brings the charged groups closer together thereby increasing the charge repulsive forces (B). A decrease in fixed charge repulsion is caused by charge shielding due to an increase in mobile ion concentration (C).

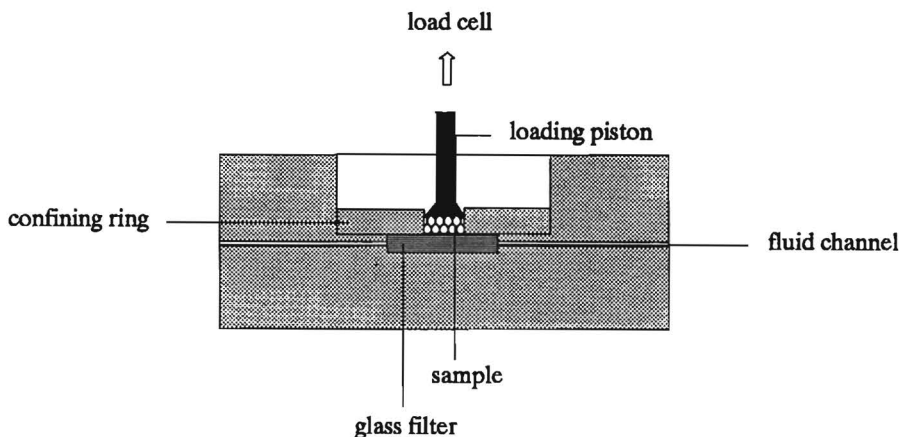


Figure 3.2: Schematic representation of the testing chamber developed for the swelling pressure measurements.

3.3.2 Experimental set-up

The experiments were performed in a PMMA testing chamber (figure 3.2). The cylindrically shaped sample was kept in a PMMA confining ring which rested on a sintered glass filter. The pore size of the filter varied between 100-160 μm . Through the filter the material was in contact with the NaCl bathing solution. By altering the ionic strength of the solution the material was loaded chemically. The solution was recirculated through the filter via a fluid channel, minimizing the influence of stagnant films on the transport of the ionic solutes into the material. The sample was kept at fixed initial height by a 10 mm diameter polyester loading piston, connected to a DC operated load cell (model TD010, nominal load 100 N, Peekel, Rotterdam, The Netherlands). The load cell was capable of detecting load changes as small as 0.005 N.

The testing chamber, being part of a larger test apparatus (figure 3.3), rested along two guide-posts on a fixed block comprising two micrometers. The latter were positioned at equal distance from the center-line of the test apparatus. With the micrometers the testing chamber could be positioned precisely with respect to the piston of the load cell. The load cell rested on a circular plate on top of the guide-posts and was connected to the measurement amplifier, equipped with an analogue low-pass measurement filter (Krohn-Hite, model 3750), and interfaced by a Labmaster AD converter to an IBM-AT. During the experiments the load change was automatically recorded. The sample frequency was 0.016 Hz.

The test apparatus was connected to the NaCl solution circulation via the fluid channel of the testing chamber. The solution was circulated by a fluid pump (Samson, Zoetermeer, The Netherlands) from a storage reservoir into an overflow reservoir which was placed in

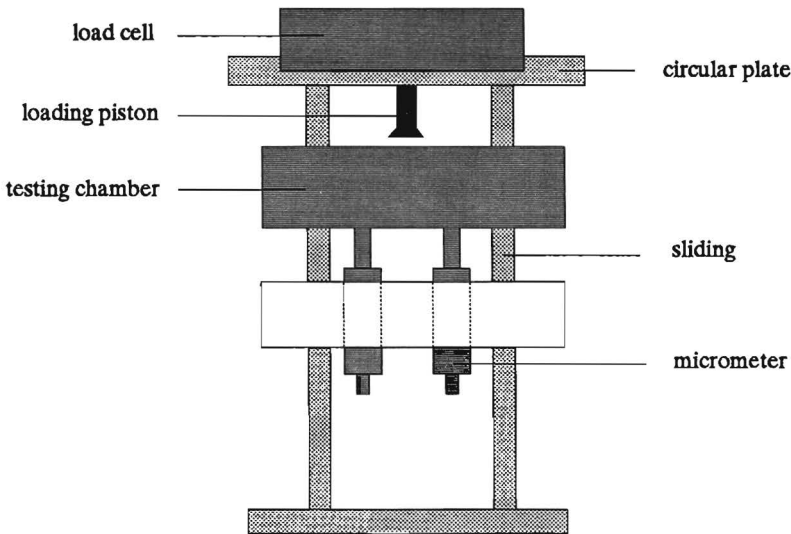


Figure 3.3: Schematic representation of the complete test apparatus.

elevation with respect to the test apparatus (figure 3.4). Circulation between the overflow reservoir - test apparatus - storage reservoir was established using flexible tubes equipped with tap connections. The fluid flow was controlled manually with the tap connections. The solution was driven into the fluid channel of the testing chamber by the hydrostatic pressure caused by the elevation of the overflow reservoir. The elevation and position of the tap connection were chosen such that no upward load was applied to the material due to the fluid pressure. After passing through the glass filter, the NaCl bathing solution flowed back into the storage reservoir.

3.3.3 Experimental protocol

The thickness of the material specimen was measured using a separate measurement device equipped with a linear variable displacement transducer (LVDT, Schaevitz, accuracy 0.02 mm, chapter 5.) The material specimen was placed in the confining ring on top of the glass filter of the testing chamber which was subsequently placed along the two guide-posts of the test apparatus. The load cell with the polyester loading piston was secured on top of the circular plate connected to the guide-posts. With the micrometers the testing chamber was moved towards the loading piston. Parallel displacement of the testing chamber was ensured by alternative equal turning of the micrometers. The upward motion of the testing chamber was interrupted as soon as the the material specimen made contact with the loading piston and a load was measured by the load cell. This initial load was always less than

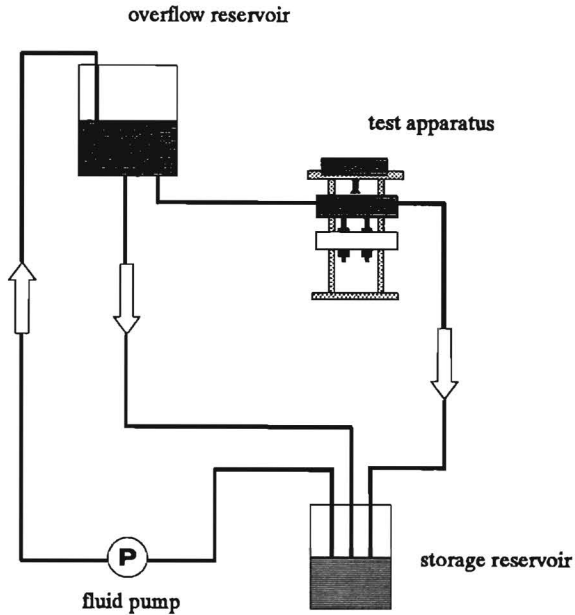


Figure 3.4: Overview of the circulation of the NaCl bathing solution.

0.01 N. The testing chamber was fastened along the guide-posts by screw-fittings, thereby ensuring no displacement of the testing chamber during the experiment. The initial load indication was taken as zero-load.

The circulation of the NaCl solution was established between storage and overflow reservoir. The flexible tube, used as intermediate between the overflow reservoir and test apparatus, was connected to the overflow reservoir and filled with solution until the end tap connection was soaked with solution. The tap connection was closed and placed into the fluid channel of the testing chamber. Subsequently, the tap connection of the second flexible tube was connected to the end of the fluid channel. The solution circulation through the fluid channel and the glass filter was established by opening the tap connection at the beginning of the fluid channel. By this procedure the air present in the fluid channel and the glass filter was removed. Immediately hereafter, the load measured by the load cell increased rapidly. Equilibrium loads were attained within 5-20 hours, depending on the thickness of the material specimen under consideration.

The NaCl solution was changed according to the following procedure: (1) The fluid pump was disconnected to allow the previous used solution to flow back into the storage reservoir, (2) the flexible tubes were disconnected from the testing chamber and emptied, (3) the fluid pump was replaced by a second pump for the circulation of the new NaCl solution, (4) a new storage reservoir containing the fresh NaCl bathing solution was placed in the

fluid circuit and the fluid circulation was resumed between storage reservoir and overflow reservoir, (5) the flexible tubes were replaced into position and the circulation resumed according to the procedure described earlier.

Mixed solutions, due to remnants of the previous used NaCl solution in the fluid channel and glass filter, were separately collected during the first minutes after recirculation. Hereafter, a homogeneous solution was assumed. The total time needed to change the solutions was less than five minutes. After a period of approximately 2 minutes, a change was observed in the load measured. In the experiments, several cycles of NaCl solutions were applied. The swelling pressure data were obtained from the load - cross section characteristics. After each experiment the material specimen was removed from the testing chamber. The testing chamber and loading piston were cleaned and the glass filter dehydrated.

3.3.4 Swelling pressure studies

The following experiments were performed according to the protocol given in section 3.3.3.:

- The swelling pressure characteristics of the materials were studied by subjecting material specimen to the following NaCl salt concentration protocol: 0.2 M - 0.6 M - 0.2 M - 0.6 M. The total experimental time per material was approximately 40-80 hours. Average pressures were calculated from the equilibrium responses of the first and second series. By comparing the equilibrium responses of the various materials against the 0.2 and 0.6 M NaCl solutions, an indication was obtained of the swelling pressure range and the influence of the material composition.
- The dependence of the swelling pressure of the materials on the external salt concentration was determined by subjecting a 41303 material specimen to NaCl solutions with concentrations ranging from 0.05 M to 1.2 M. The material was tested during a successive measurement time of approximately 240 hours. The course of the equilibrium pressures versus concentration of the NaCl bathing solution was used to estimate to which extent the osmotic pressure and fixed charge repulsion contributed to the observed swelling pressure response.

3.4 Results

3.4.1 General behaviour

A typical result of the swelling pressure measurements is given in figure 3.5 showing the response of the materials versus time due to the application to 0.2 M and 0.6 M NaCl solutions. An increase in swelling pressure occurs when the material specimen is equilibrated against 0.2 M NaCl, followed by a decrease in pressure when the specimen is subjected to 0.6 M NaCl. The equilibrium responses are reached within 5-20 h and seem to be reached faster during the application of the downward step change in ionic strength of the bathing solution. In all cases, the application of the second series of 0.2 M and 0.6 M NaCl solutions

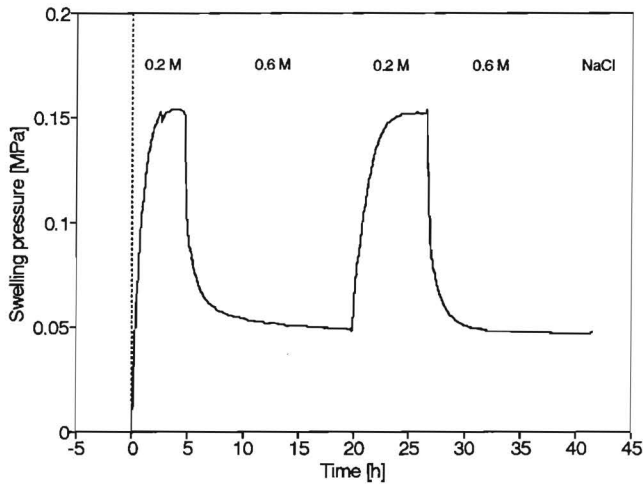


Figure 3.5: *Experimental swelling pressure data of a typical experiment.*

resulted in the recording of reproducible pressure curves.

The average equilibrium swelling pressures of the various materials are given in table 3.1. The pressure responses vary between 0.05 - 0.16 MPa for the 0.6 M NaCl solutions and 0.15 - 0.3 MPa for the 0.2 M NaCl solutions. The 41303 material exhibits the smallest swelling pressure whereas the largest is found for the 413035 material.

3.4.2 Variation with external NaCl concentration

In figure 3.6 the equilibrium swelling pressure versus the external NaCl concentration is given. Within the concentration range 0.05 M - 1.2 M, pressure responses are determined between 0.34 and 0.04 MPa. One can observe that the equilibrium swelling pressure of the material decreases monotonically with increasing ionic strength of the NaCl solution. After the testing period of approximately 240 hours, no deterioration of the material was observed when removed from the experimental set-up.

To estimate the contributions of the osmotic pressure and fixed charge repulsion to the swelling pressure response, the experimental data were curvefitted using Eq. 3.22,

$$\pi_{don} = \phi^{smm} RT \sqrt{(C_0^{fcd})^2 + 4c^2} - 2\phi^* RTc$$

Unknowns in this equation are the osmotic coefficient of the material ϕ^{smm} and its fixed charge density C_0^{fcd} . The values of the osmotic coefficient ϕ^* of the NaCl solutions are well

| code | $\pi_{0.2M}$ [MPa] | $\pi_{0.6M}$ [MPa] |
|--------|--------------------|--------------------|
| 4130 | 0.242 ± 0.019 | 0.099 ± 0.010 |
| 4160 | 0.280 ± 0.03 | 0.160 ± 0.010 |
| 4138 | 0.282 ± 0.02 | 0.150 ± 0.006 |
| 1160 | 0.280 ± 0.014 | 0.119 ± 0.005 |
| 1460 | 0.260 ± 0.010 | 0.150 ± 0.012 |
| 41303 | 0.154 ± 0.002 | 0.050 ± 0.003 |
| 413035 | 0.300 ± 0.018 | 0.115 ± 0.012 |
| 1030 | 0.200 ± 0.015 | 0.094 ± 0.002 |

Table 3.1: Average swelling pressures of the various materials as determined from the equilibrium responses against the 0.2 M and 0.6 M NaCl bathing solutions. For the interpretation of the material codes the reader is referred to table 2.3 of chapter 2.

known and tabulated (Robinson *et al.* [58]). Within the concentration range studied the value of ϕ^* is taken 0.93.

Using a least square fit the course of the experimental data is predicted by the Donnan effect with an average inaccuracy of 6% (figure 3.6). Due to the good agreement, it is possible to estimate the fixed charge density and the osmotic coefficient of the materials via substitution of the pressure data given in table 3.1 in Eq. 3.22. The results are given in table 3.2. The given inaccuracy is based on the maximum measurement error of the equilibrium swelling pressures. The osmotic coefficients of the materials are found to be nearly equivalent to the osmotic coefficient of the external NaCl solutions ($\phi^* \approx 0.93$). The fixed charge densities of the materials vary from $0.24 \cdot 10^3$ to $0.35 \cdot 10^3$ mole/m³.

| code | ϕ^{smm} [-] | C_0^{fcd} [10^3 mole / m ³] |
|--------|-------------------|----------------------------------------------|
| 4130 | 0.934 ± 0.007 | 0.306 ± 0.042 |
| 4160 | 0.951 ± 0.009 | 0.318 ± 0.046 |
| 4138 | 0.947 ± 0.003 | 0.324 ± 0.027 |
| 1160 | 0.935 ± 0.005 | 0.333 ± 0.017 |
| 1460 | 0.950 ± 0.005 | 0.308 ± 0.037 |
| 41303 | 0.928 ± 0.002 | 0.244 ± 0.008 |
| 413035 | 0.930 ± 0.004 | 0.351 ± 0.031 |
| 1030 | 0.938 ± 0.003 | 0.272 ± 0.032 |

Table 3.2: Osmotic coefficients ϕ^{smm} and fixed charge densities C_0^{fcd} of the various materials as estimated from the average pressure data given in table 3.2 using Donnan equilibrium theory. For the interpretation of the material codes the reader is referred to table 2.3 of chapter 2.

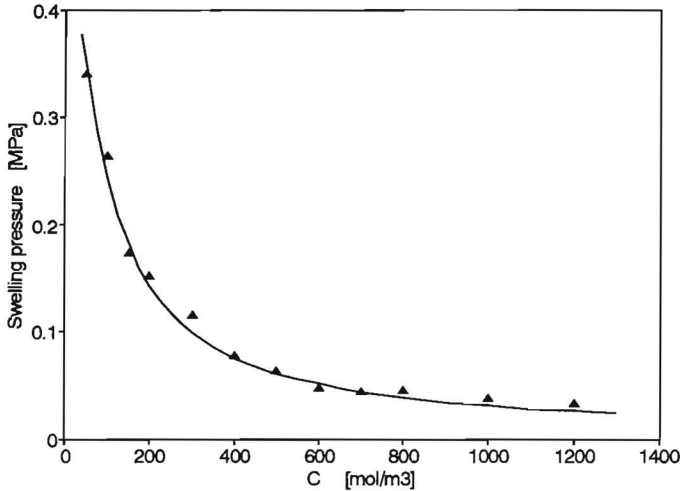


Figure 3.6: Experimental swelling pressure data (\blacktriangle) and curvefit pressure response (—), as predicted by the Donnan effect, versus concentration of the NaCl bathing solution. Data obtained for a 41303 material.

3.4.3 Estimation of NaCl diffusion coefficient

Due to the tri-axial confinement of the material samples during the experiments, only mobile counter- and co-ions are exchanged between the materials and the external NaCl solutions in order to reach equilibrium. Consequently, the course of the transient pressure response can be used for an estimate of the diffusivity of the mobile ions in the materials. Assuming that the diffusion of the mobile ions is independent of the salt concentration in the material, the average diffusion coefficient \bar{D}_{NaCl} may be estimated from (Grodzinsky *et al.* [20]),

$$\bar{D}_{NaCl} = \frac{h^2}{\tau_{diff}} \quad (3.23)$$

where h is the height of the material and τ_{diff} the characteristic time of the diffusion process. The average characteristic time constant of the pressure responses was approximately 3.4 h. By substituting this value in Eq. 3.23, together with the average material height of 1.8 mm, an average NaCl diffusion coefficient of the materials is estimated of approximately $3 \cdot 10^{-10} \text{ m}^2/\text{s}$.

3.5 Discussion

The study presented in this chapter demonstrates that the swelling pressure responses of the model materials, due to step-changes in ionic strength of the external NaCl bathing solutions, are in good agreement with Donnan theory. Although no experimental technique capable of separating the effects of Donnan osmotic pressure and fixed charge repulsion was available, it is likely that the repulsion between the charges of the fixed carboxylate - C(O)O⁻-groups of the copolymer network does not contribute significantly to the swelling pressure of the materials. As a result, the swelling pressure change is accounted for by the presence of the small diffusible Na⁺ and Cl⁻-ions and the ionized copolymer network. These findings support the results of Snijders [63], who concluded that the swelling behaviour of intervertebral disc tissue of similar fixed charge density is caused by Donnan osmosis only. Therefore, incorporation in triphasic theory of a chemical expansion stress, as has been done by Lai *et al.* [40], seems not necessary in order to describe the swelling behaviour of moderately charged soft hydrated materials (C^{cd} in the order of $0.3 \cdot 10^3$ mole/m³).

The course of the swelling pressure versus NaCl concentration (figure 3.6) is consistent with the swelling behaviour observed for poly(acrylamide co-sodium acrylate) gels in general (Yoshio *et al.* [75], Vasheghani *et al.* [72]). For these gels, Ricka *et al.* [57] were also able to predict the experimentally observed swelling versus the ionic composition of the swelling agent by using Donnan theory. The remark made by Brannon-Peppas *et al.* [10] and Baker *et al.* [1], that the Donnan theory would be only applicable to highly-swollen, lightly-charged hydrogels, is not supported and is probably related to differences in gel-composition.

Reproducible pressure responses are measured with the experimental set-up. In the experiments, the materials are tested in a completely confined environment and hence are not able to undergo volume changes when subjected to the NaCl bathing solutions. Due to this the concentration of the fixed charges in the material remains constant during the experiments. By using Donnan equilibrium theory, the fixed charge density and osmotic coefficient of the materials are estimated from equilibrium swelling pressure responses. The values determined may be subject to the following additional measurement errors:

- In positioning the material specimen with respect to the loading piston of the load cell, the specimen may be deformed at the initial contact. Due to the initial deformation, the material is pre-stressed resulting in the measurement of higher equilibrium pressures and hence in the determination of higher fixed charge densities. Since the initial load indication, due to the contact between material and loading piston, was always less than 0.01 N, a maximum initial stress of approximately 120 Pa is induced on the specimen. Considering linear elastic behaviour and a material stiffness of $\mathcal{O}(\text{MPa})$, an initial strain of $\mathcal{O}(10^{-5})$ is applied to the specimen indicating that this deformation effect is negligible.

- Possible deviation from the ideal confinement of the material specimen due to irregularities in material diameter leads to the measurement of lower equilibrium swelling pressures and hence to an underestimation of the fixed charge density. Irregularities in material specimen diameter result in an uptake of fluid until the specimen is completely confined. The fixed charge density of the material is decreased due to the increase in material volume. Considering a maximum diameter variation of approximately 0.2 mm, a maximum volume change of 4% results, leading to a maximum underestimation of the fixed charge density of approximately 5%.
- The load cell used for the swelling pressure measurements is equipped with strain gauges. According to the specifications of the load cell, the displacement of the cell at nominal load (100 N) is less than 100 μm . In case of displacement, fluid is taken up by the specimen resulting in the measurement of lower equilibrium pressures. As the maximum load measured during the experiments never exceeded 30 N, the maximum displacement of the load cell was restricted to 30 μm . Considering a specimen thickness of 2 mm, this displacement results in a maximum volume change of 1.5% leading to a maximum underestimation of the fixed charge density of approximately 2%.

The equilibrium swelling pressures of the materials as given in table 3.1 are averaged values based on the responses against the 0.2 and 0.6 M NaCl bathing solutions. Within this concentration range, equilibrium pressures are found between 0.05 - 0.3 MPa resulting in estimated fixed charge densities ranging from 0.24 to $0.35 \cdot 10^3$ mole/ m^3 . This range is similar to the range of fixed charge densities encountered in intervertebral disc tissue. In the human intervertebral disc the fixed charge density varies between 0.08 - $0.35 \cdot 10^3$ mole/ m^3 depending on the location within the disc (Urban *et al.* [67, 69]). The osmotic coefficients of the materials are found to be nearly equivalent to the osmotic coefficient of the external NaCl bathing solutions.

The estimated value for the diffusion coefficient of the materials ($D \approx 3 \cdot 10^{-10}$ m^2/s) is approximately four times lower than the value encountered in aqueous solution (Robinson *et al.* [58]) and consistent with values found for other soft charged hydrated materials (Maroudas [44], Yoshio *et al.* [75]). In case of an upward step in ionic strength of the NaCl solution, the mobile ions diffuse from the external solution into the material specimen and associate with the fixed ionic groups on the copolymer gel network (Gehrke *et al.* [19]). This probably explains the increase in duration to reach equilibrium in case of the transition from 0.2 M to 0.6 M NaCl.

By measuring the swelling pressure of the materials in a tri-axial confined environment without deforming the specimen, the influence of the strain, due to deformation of the PUR-copolymer network, on the measured responses is eliminated. As a result, the differences observed in equilibrium pressure are related to variations in copolymer gel content and copolymer network composition of the materials. Since the differences in porosity of the PUR-foams used are small (chapter 2, table 2.1), all materials contain almost equal amounts of copolymer gel. Consequently, the observed differences in equilibrium

swelling pressures are almost entirely due to differences in copolymer network composition. This composition varies with respect to the acrylic acid - acrylamide ratio, the degree of crosslinking and the number of sodium-acrylate groups present. The latter is not only determined by the acrylic acid content but also by the current pH-conditions. During preparation of the materials the observed pH-conditions indicate that not all the carboxylic groups present are converted to the sodium-acrylate salt-form (chapter 2). The total amount of non-converted carboxylic groups increases with decreasing pH, hence with increasing initial acrylic acid content. However, when immersed in neutral NaCl solutions (pH = 7), it is likely that remnant carboxylic groups are converted to the sodium-acrylate salt form due to exchange of H⁺-ions for Na⁺-cations (Helfferich [26]). It is not clear whether all carboxylic groups are converted. It is therefore difficult to relate the observed differences in pressure response to the variation of the acrylic acid - acrylamide content of the materials (table 3.1).

An exception to this are the 4130, 4160 and 4138 materials and the 41303 material. The former three materials are synthesized in the same chemical batch, hence comprise a copolymer network of similar structure. As a result, the equilibrium pressures should be of similar order which is confirmed by the experimental pressure data. The latter material is synthesized using an increased amount of crosslinking agent. The comparison of the results for the 4130 and 41303 materials shows that by increasing the crosslinking agent concentration, the equilibrium pressure response is reduced.

Chapter 4

Measurement of hydraulic permeabilities

In this chapter, fluid permeation rate experiments are performed on synthetic model materials. The purpose of these experiments is to determine the hydraulic permeability of the materials and its dependence on the deformation state of the material and on the salt concentration of the surrounding solution.

After the introduction (section 4.1), the materials and methods are outlined in the experimental section (section 4.2). Detailed information is given of the experimental set-up and the experimental protocol. The results of the hydraulic permeability studies are given in section 4.3. The chapter ends with a discussion on the results obtained (section 4.4).

4.1 Introduction

In chapter 1, the triphasic equations describing the mechanical and physico-chemical behaviour of soft charged hydrated materials were outlined. One of the material parameters occurring in these equations is the hydraulic permeability of the material which is a macroscopic measure of the ease with which a fluid can flow through the solid matrix of the material. The permeability of soft charged hydrated connective tissues and gels typically has low values, ranging from 10^{-14} - 10^{-16} m⁴/Ns (Maroudas [44], Oomens *et al.* [50], Snijders [63], Quinn *et al.* [54]). The pore-sizes in the macromolecular network of these materials are of the order 60 - 250 Å (Holmes *et al.* [28], Kremer *et al.* [38]). Since the compressibility of the material components is low, the volume strain during deformation of the material is almost exclusively associated with fluid motion. Therefore, the permeability determines to a great extent the behaviour of the materials during mechanical and chemical loading and plays an important role in their load bearing capacity.

In case of changes in loading conditions, the fluid content of the materials changes which has consequences for the permeability. In case the ionic strength of the surrounding salt solution is decreased, fluid is taken up by the material to reduce the difference in ionic strength between the material and the external environment. During this process the effective pore-size is increased whereas the fixed charge density is decreased. The former results in an increased space for fluid flow, while a reduced part of the fluid is bound by the latter. Both processes result in an increase of the permeability (Gu *et al.* [22]). During squeezing of fluid, the opposite is valid.

The hydraulic permeability of soft charged hydrated materials generally depends on the deformation state of the material and the ionic concentration of the surrounding salt solution (Mansour *et al.* [42], Mow *et al.* [47], Quinn *et al.* [54]). In this chapter the dependence of the permeability of the model materials on both parameters is studied. In the experiments sodium chloride solutions are used as bathing solutions.

4.2 Experimental

4.2.1 Materials

Synthetic model materials were prepared according to the procedure given in chapter 2. From the raw materials, cylindrical bars 10 mm in diameter were cut using a slowly rotating cork borer. From these bars, discs with heights between 1 - 2 mm were prepared with a scalpel. The samples were stored in sealed glass bottles until use.

In table 2.3 of chapter 2 the composition is given of the materials which were used in the hydraulic permeability experiments. For the properties of the PUR-foams, the reader is referred to the experimental section of chapter 2.

The sodium chloride for the bathing solutions was first grade and used as received from Merck (Darmstadt, Germany). The solutions were prepared with ultra purified water.

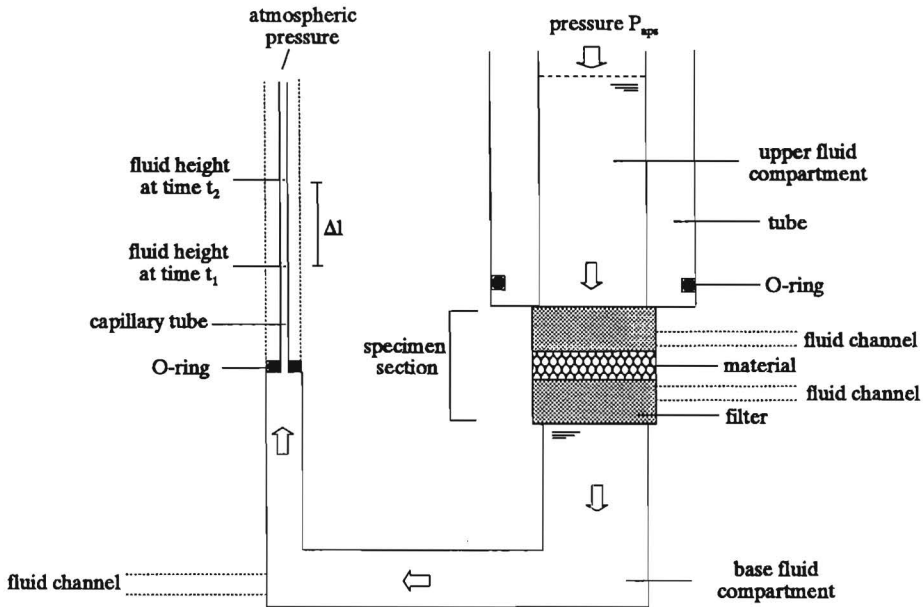


Figure 4.1: Schematic representation of the test-apparatus developed to measure the hydraulic permeability of synthetic model material specimen under various strain conditions and NaCl salt concentrations. The arrows show the fluid flow through the apparatus and the material specimen due to a fluid pressure P_{appl} . Fluid permeation rates were determined from the change in fluid height (Δl) in the capillary tube during a time interval $t_2 - t_1$.

4.2.2 Experimental set-up

The hydraulic permeability experiments were performed in a PMMA test apparatus capable of measuring the permeability of the materials as function of the deformation state of the material and the ionic strength of the surrounding NaCl bathing solution. A schematic representation of the test apparatus is given in figure 4.1. The cylindrically shaped material specimen of known initial height was kept at a fixed confined deformed state between two porous glass filters in the specimen section. Through these filters the material was in contact with the surrounding NaCl bathing solution. The pore-size of the filters varied between 100 - 160 μm . During the experiment, confinement of the material and filters to the specimen section was ensured by a PMMA-tube. The tube contained a rubber O-ring at the bottom which prevented fluid leakage along the tube during the permeation experiments.

The NaCl solution was forced through the material via application of a direct fluid pressure difference across the specimen, the flow being from top to bottom. The actual pressure was

generated by an air pressure source. Fluid permeation rates were determined by measuring the change in fluid height in the capillary tube as a function of time. The inner diameter of this tube was 0.38 ± 0.01 mm. It was surrounded at the bottom by a rubber O-ring to prevent fluid leakage along the tube.

The fluid flow through the material and test apparatus is shown schematically in figure 4.1. Due to the pressure difference across the material, the fluid rose in the capillary tube. At the top of the tube the pressure was of atmospheric level.

Fluid channels were present at the end of the base fluid compartment and on the level of the glass filters allowing separate filling and emptying of the fluid compartments. Chemical loading of the material was performed by changing the ionic strength of the surrounding NaCl solution.

4.2.3 Experimental protocol

The thickness of the material specimen in the undeformed state and the thicknesses of the glass filters were measured using a separate measurement device equipped with a linear variable displacement transducer (LVDT, Schaevitz, accuracy 0.02 mm, chapter 5). Hereafter, the lower glass filter was placed at the bottom of the specimen section, followed by the material specimen and the upper glass filter. By placing the PMMA-tube into position, the material and filters were confined to the specimen section. The height of the filters was chosen such that the desired strain was achieved after placing the tube into position. The axial strain was defined as the ratio of the change in thickness to the initial thickness of the material specimen. The tube was secured to the test apparatus to ensure fixed confinement of the material during the experiment.

The base fluid compartment was filled with the desired solution via the lower fluid channel until the lower filter was soaked with fluid and the air present was removed via the fluid channel connected to the lower glass filter. After placing the capillary tube into position, the upper fluid compartment was filled with the desired solution via the fluid channel connected to the upper glass filter. By filling the compartment from below the air present escaped easily. Finally, the air pressure source was connected. Subsequently, a period of approximately 20 hours was maintained to allow the material specimen to reach equilibrium.

After this period, an additional pressure of 0.2 MPa was applied to the upper side of the material specimen by means of air pressure with an accuracy of approximately 1 kPa. The actual pressure difference was corrected for the influence of the counteracting pressure due to the rise of the fluid column in the capillary tube. This counteracting pressure never exceeded 3 kPa. Fluid heights were read from the millimeter scale attached to the capillary tube with an accuracy of 0.5 mm. During the experiment, changes in fluid height Δl in the capillary tube were measured as a function of the time elapsed. For every time interval the corresponding permeation rate was calculated. The final permeation rate was obtained by determining its mean value and standard deviation. At least fifteen separate measurements were used for this purpose.

The permeability values were calculated using Darcy's law,

$$K = \frac{A_{cap}}{A_{spec}} \frac{h}{\Delta P} \frac{\Delta l}{\Delta t} = \frac{A_{cap}}{A_{spec}} \frac{h}{\Delta P} q_p \quad (4.1)$$

where A_{cap} and A_{spec} are the cross-sections of capillary tube and material specimen, h the thickness of the specimen, ΔP the pressure difference applied and q_p the mean permeation rate. The measurement error was estimated on the basis of the errors made in the measurement of the height of the specimen and the glass filters, the measurement of the diameter of the capillary tube and material specimen, the error made in the applied pressure difference, and the standard deviation of the mean permeation rate.

The NaCl solution was changed according to the following procedure: (1) the air pressure source was disconnected, (2) the upper fluid compartment was emptied via the fluid channel connected to the upper glass filter, (3) the base fluid compartment was emptied via the lower fluid channel, (4) the capillary tube was disconnected, (5) the capillary tube, both the fluid compartments and the glass filters were blown dry with low air pressure, (6) the fluid compartments were refilled with the new NaCl solution, the capillary tube replaced and the air pressure reconnected according to the procedure described earlier. During this procedure the material specimen was kept confined in the specimen section.

The total time needed to change the solution was less than five minutes. Hereafter, another period of approximately 20 hours was maintained to allow the material specimen to reach equilibrium. After each test the fluid compartments were emptied, the material specimen and glass filters removed and the test apparatus cleaned.

4.2.4 Hydraulic permeability studies

The following experiments were performed according to the protocol given in section 4.2.3:

- The hydraulic permeability of the various materials was measured by subjecting material samples to equal compressive strains of 20% applying a salt concentration protocol of 0.6 M - 0.2 M - 0.6 M NaCl. The total experimental time per material specimen was approximately 90 hours. Fresh samples, filters and NaCl solutions were used for each separate test.
- The dependence of the hydraulic permeability of the materials on the applied strain was studied by subjecting 4130 material samples to various strain conditions using 0.6 M NaCl solutions for all tests. The total experimental time per material was approximately 40 - 50 hours. Fresh samples, filters and NaCl solutions were used for each separate test.
- The dependence of the hydraulic permeability of the materials on the ionic strength of the surrounding NaCl solution was studied by subjecting one 4130 material sample to a constant compressive strain of 9% using NaCl solutions with concentrations ranging from 0.05 M to 1.5 M. The material was tested during a successive measurement time of approximately 240 hours.

4.3 Results

4.3.1 Hydraulic permeability of the various materials

In table 4.1 the hydraulic permeability data of the various materials are given. Permeability values in the order of 10^{-16} m⁴/Ns are determined. A decrease in permeability is observed when the concentration of the solution is lowered from 0.6 M to 0.2 M NaCl. The subsequent step-change to 0.6 M yielded for all cases permeability values consistent with the values found during the first subjection to 0.6 M NaCl.

Only small differences are found between the permeability values of the various materials. The permeability varies between $1.03 \cdot 10^{-16}$ m⁴/Ns and $2.12 \cdot 10^{-16}$ m⁴/Ns when the materials are bathed in 0.6 M NaCl. When equilibrated against 0.2 M NaCl, permeabilities are found between $0.88 \cdot 10^{-16}$ m⁴/Ns and $1.65 \cdot 10^{-16}$ m⁴/Ns. The permeability of the 4160, 1160 and 1460 materials is observed to decrease with increasing acrylamide content of the materials.

| code | $K_{0.6M}$ [10^{-16} m ⁴ /Ns] | $K_{0.2M}$ [10^{-16} m ⁴ /Ns] |
|--------|---------------------------------------------|---------------------------------------------|
| 4130 | 1.40 ± 0.10 | 1.20 ± 0.12 |
| 4160 | 1.43 ± 0.36 | 1.09 ± 0.24 |
| 4138 | 2.12 ± 0.20 | 1.65 ± 0.18 |
| 1160 | 1.33 ± 0.18 | 1.07 ± 0.19 |
| 1460 | 1.03 ± 0.15 | 0.88 ± 0.10 |
| 41303 | 1.48 ± 0.18 | 1.28 ± 0.14 |
| 413035 | 1.12 ± 0.12 | 0.88 ± 0.08 |
| 1030 | 1.54 ± 0.15 | 1.38 ± 0.13 |

Table 4.1: Experimental permeability data of the various materials subjected to 20% compressive strain and equilibrated against 0.6 M and 0.2 M NaCl bathing solutions. For the interpretation of the material codes the reader is referred to table 2.3 of chapter 2.

4.3.2 Deformation dependence

The 4130 material samples were subjected to axial strains ranging from -0.7 to 0.1. In figure 4.2 the hydraulic permeability data are plotted versus the uniaxial deformation. The permeability values range from $0.25 \cdot 10^{-16}$ m⁴/Ns to $2.14 \cdot 10^{-16}$ m⁴/Ns. Within the deformation range studied, the permeability is observed to increase almost linearly with decreasing compressive strain. Using a least square fit, the permeability data were linearly fitted with a regression coefficient of 0.98. The slope of the linear fit was $2.18 \cdot 10^{-16}$ m⁴/Ns, the permeability at zero axial strain $1.76 \cdot 10^{-16}$ m⁴/Ns.

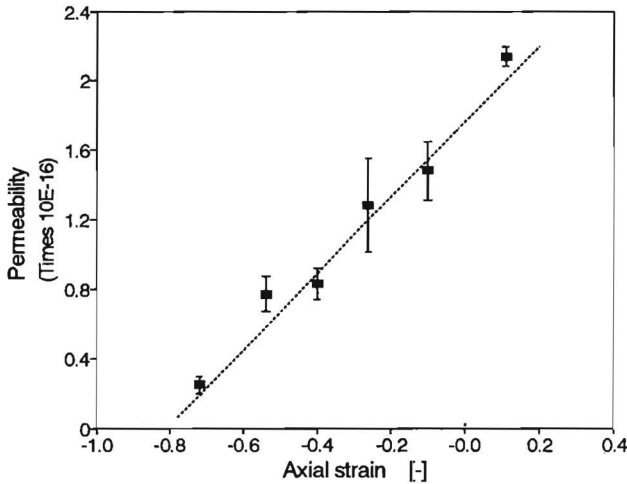


Figure 4.2: Experimental permeability data (■) with corresponding measurement errors versus axial strain. The data were obtained for 4130 materials equilibrated against 0.6 M NaCl. The dashed line shows the best linear fit through the experimental data.

4.3.3 Dependence on NaCl bathing solution concentration

In figure 4.3 the hydraulic permeability data are plotted as function of the molarity of the NaCl solutions. Within the concentration range studied the permeability is observed to increase approximately linearly with increasing NaCl concentration. An initial maximum in permeability is observed for 0.05 M NaCl. Permeability values are determined between $1.1 \cdot 10^{-16} \text{ m}^4/\text{Ns}$ and $2.31 \cdot 10^{-16} \text{ m}^4/\text{Ns}$.

4.4 Discussion

In this chapter the permeability of the various synthetic model materials has been studied by analysis of permeation rate measurements of NaCl solutions through disc shaped material specimen. The materials were either kept at a fixed deformed state and subjected to NaCl solutions of varying ionic strength, or subjected to various strain conditions and bathed in NaCl solutions of equal molarity. The study demonstrates that the hydraulic permeability of the materials is both dependent on the deformation state of the material and the ionic strength of the surrounding NaCl solution. Permeability values of $O(10^{-16}) \text{ m}^4/\text{Ns}$ are found.

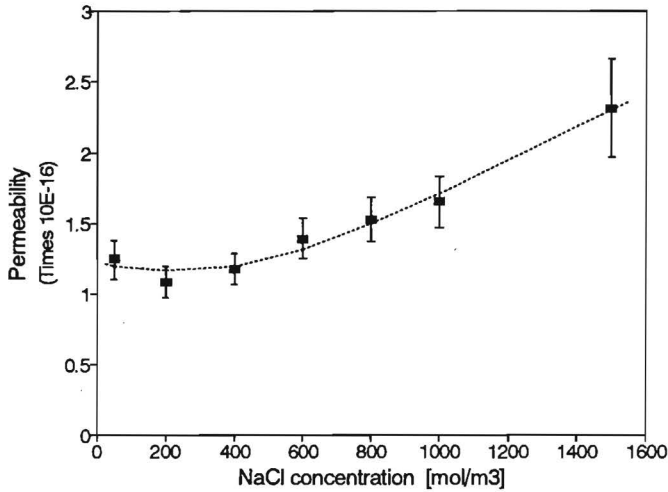


Figure 4.3: Experimental permeability data (■) with corresponding measurement errors versus concentration of the external NaCl solution. The data were obtained for a 4180 material subjected to a compressive strain of 9%.

Within the deformation range studied, the permeability increases almost linearly with increasing elongation. Both the increase of the pore-size and the decrease of the fixed charge density of the material with increasing elongation contribute to the observed increase in permeability. In the experiments, the deformation of the material specimen is varied from 70% compressive strain to 10% swelling strain. For higher swelling strains the permeability values determined are expected to become inaccurate due to fluid flow along the material specimen. In this deformation range the permeability of the materials is expected to increase in a non-linear manner with increasing deformation (Holmes *et al.* [28], Quinn *et al.* [54]).

For NaCl concentrations ranging from 0.05 M to 1.5 M, the permeability generally increases with increasing NaCl concentration. The observed dependence of the permeability on the salt concentration may be due to the presence of electrical potentials. As the materials contain fixed negative groups and hence more counterions than co-ions, the fluid tends to convect more positive than negative charges through the material during the experiment, due to the excess hydrostatic pressure exerted on the upper solution. However, the displacement of the net electric charge builds up an electrical potential difference or streaming potential (Helfferich [26]) which accelerates the co-ions and slows down the counterions so that both species, despite their different concentrations, transfer equivalent amounts of

electric charge. As the streaming potential acts on the electrically charged pore liquid as a whole, the effect of the pressure difference may be partly balanced resulting in a reduced fluid flow across the material specimen. According to Helfferich, the effect of streaming potentials decreases with increasing concentration of the external solution. This may explain the observed increase in permeability with increasing NaCl concentration. No explanation is found for the small increase in permeability observed when the material specimen was subjected to the 0.05 M NaCl solution.

Only small differences in permeability are found between the various materials (table 4.1). The differences observed are probably related to differences in pore-size distribution of the materials. According to Kremer *et al.* [38], the pore-size distribution of polyelectrolyte hydrogels is affected by the solid content, the crosslink density and the fixed charge density of the material under consideration. As all three parameters work in concert, it is difficult to relate the differences in permeability to the differences in material composition.

The permeability of the materials lies within the range of permeabilities found for intervertebral disc tissue and other gels. Best *et al.* [4] determined permeability data of intervertebral disc tissue from experimental swelling creep data of specimen kept at their initial thickness and equilibrated against 0.15 M NaCl bathing solutions. For non-degenerated intervertebral discs, average permeability data were found of $2.2 \cdot 10^{-16} \text{ m}^4/\text{Ns}$.

Quinn *et al.* [54] determined the hydraulic permeability of poly(methacrylic acid) gels using a similar procedure. Gel specimen were equilibrated under free swelling conditions against KCl bathing solutions and then uni-axially compressed. Hydraulic permeability data were computed from transient stress relaxation data using the stress relaxation time-constant and the 'tangent' modulus from the equilibrium stress-strain curves. Permeability data were determined ranging from 2 to $8 \cdot 10^{-16} \text{ m}^4/\text{Ns}$.

Chapter 5

Confined swelling and compression behaviour

In this chapter, uni-axial confined swelling and compression experiments are performed in order to study the transient deformation behaviour of the materials and to verify whether the triphasic theory is able to describe their mechanical and physico-chemical behaviour. The loading protocol consists of a combination of mechanical and chemical loading.

After the introduction (section 5.1), the materials and methods are described in the experimental section (section 5.2). Detailed information is given of the experimental set-up and the experimental protocol. In section 5.3, after discussing a typical result of the confined swelling and compression experiments, an overview is given of the behaviour observed for the various materials. The difference in material behaviour is studied by comparison of axial stretch data. The experimental displacement data obtained for a 4130 material are compared with corresponding computed results using the triphasic theory and the material parameters determined in the previous chapters for the porosity, the fixed charge density, the osmotic coefficient, the diffusion coefficient and the hydraulic permeability. The chapter concludes in section 5.4 with a discussion on the results obtained.

5.1 Introduction

In the previous chapters, the swelling pressure and hydraulic permeability were measured by keeping the material specimen in a fixed confined environment and by subjecting them to NaCl solutions of varying concentration and, in the latter experiment, also to fluid pressures. As the swelling of the materials is prohibited in these experiments, the experimental results are not affected by changes in effective stress of the material, assuming that the effect of fixed charge repulsion can be neglected (chapter 3). This changes if the material is allowed to deform. In that case, the response of the material to a mechanical or chemical load is also determined by the stiffness of both the PUR-foam and the copolymer network. The influence of network parameters on the behaviour of soft charged crosslinked materials is generally studied in free swelling experiments (Peppas [52], Vasheghani *et al.* [72]). The materials are compared by their swelling degree which is defined as the mass ratio of the swollen material to the initial (dry) material. However, when immersed in electrolyte solutions, the materials exhibit large swelling degrees up to a factor 100 (Ricka *et al.* [57], Sakohara *et al.* [59]). As the stiffness of the resulting swollen materials is almost zero, these experiments are less suitable to study the deformation behaviour of the synthetic model materials under both swelling and compression. Moreover, as the swelling progresses in three dimensions, the material parameters, as quantified in the previous chapters, can not be used for the description of the material behaviour observed, since they are determined in one-dimensional configurations.

Therefore, the behaviour of the materials during swelling and compression is studied in a confined environment under a combination of changing mechanical and chemical loading conditions. The mechanical load is always non-zero and compressive, ensuring that the swelling degrees remain within reasonable limits and thus the stiffnesses of the materials sufficiently high. The experimental data of such an experiment are suited for a one-dimensional verification of the triphasic theory including the use of the material parameters previously determined. In the experiments sodium chloride solutions are used as bathing solutions.

5.2 Experimental

5.2.1 Materials

Materials were prepared according to the procedure given in chapter 2. From the raw materials cylindrical bars 10 mm in diameter were cut using a slowly rotating cork borer. From these bars, discs with heights between 1 - 2 mm were prepared using a scalpel. The samples were stored in sealed glass bottles until use. In table 2.3 of chapter 2 the composition is given of the materials which were used in the confined swelling and compression experiments. For the properties of the PUR-foams the reader is referred to the experimental section of chapter 2. The bathing solutions were prepared with first grade sodium chloride, as received from Merck (Darmstadt, Germany), and with ultra purified water.

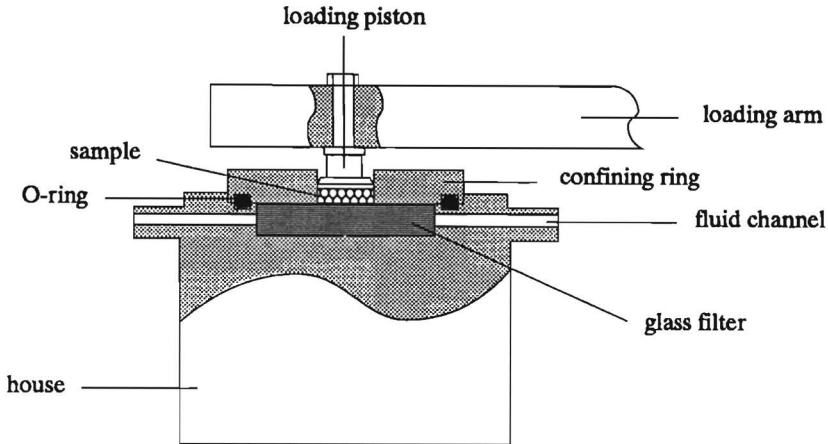


Figure 5.1: Schematic representation of the testing chamber.

5.2.2 Experimental set-up

The confined swelling and compression experiments were performed in a stainless steel testing chamber (Snijders [63], figure 5.1). The cylindrically shaped material sample was kept in a stainless steel confining ring (inner diameter 10 mm) which rested on a porous glass filter with pore-sizes varying from 100 to 160 μm . Through the filter the material was in contact with the NaCl bathing solution. A rubber O-ring between the confining ring and the house of the testing chamber prevented fluid leakage along the confining ring. The bathing solution was circulated through the filter via a fluid channel, minimizing the influence of stagnant films on the transport of the ionic solutes into the material. By altering the ionic strength of the NaCl bathing solution, the material was loaded chemically. The solutions were used at room temperature. The material was loaded mechanically by means of a conic impervious stainless steel loading piston. The maximum diameter of the piston was 9.95 mm. The opening angle of the piston was chosen such that no stick occurred during the experiment. The loading piston was connected to a loading arm, which minimized edge errors.

The complete test apparatus (Snijders [63]) is given schematically in figure 5.2. The testing chamber rested on a table. The loading arm was connected to a rotation axis with pre-stressed ball bearings which minimized the friction moment. In the unloaded situation, the

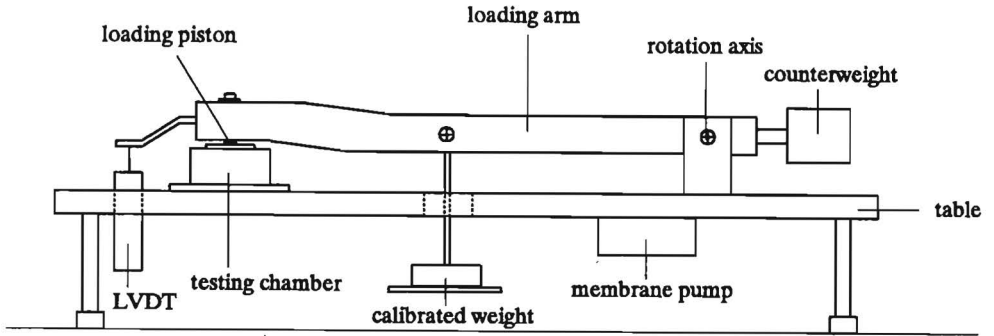


Figure 5.2: Schematic representation of the test apparatus used for the confined swelling and compression experiments.

arm was balanced by a counter weight. The actual mechanical load was achieved by placing a calibrated weight on a scale. As the scale was positioned halfway the loading piston and the rotation axis of the loading arm, only half of the weight was counterbalanced by the material: A DC operated linear variable displacement transducer (LVDT, Schaevitz), connected to the loading arm, gave its signal via an analogue low-pass measurement filter (Krohn-Hite, model 3750), interfaced by a Labmaster AD-converter, to an IBM-AT. During the experiments the displacement of the loading piston was automatically recorded. The sample frequency was 0.016 Hz. In order to avoid any stick phenomena between the material specimen and the confining ring, the test apparatus was vibrated by a membrane pump during 0.5 seconds after data-sampling.

The experimental set-up was connected to the NaCl solution circulation via the fluid channel of the testing chamber. The solution was circulated via a fluid pump (Samson, Zoetermeer, The Netherlands) from a storage reservoir into an overflow reservoir placed in elevation with respect to the test apparatus. The circulation between overflow reservoir - test apparatus - storage reservoir was established using flexible tubes equipped with tap connections. The flow was controlled manually with the tap connections. The solution was driven into the fluid channel of the testing chamber by the hydrostatic pressure caused by the elevation of the overflow reservoir. The elevation and position of the tap connection were chosen such that no upward load was applied to the material due to the fluid pressure. After permeating the filter, the solution flowed back into the storage reservoir.

Before fluid circulation, the flexible tubes and filter were deaerated by a vacuum pump in order to optimize the initial contact between material and solution. The solutions were changed via manipulation of the tap connections.

5.2.3 Experimental protocol

The loading piston was moved around the work-point in order to check for any friction or stick. The zero thickness was recorded by placing the loading piston on the glass filter of the testing chamber. Hereafter, the material specimen was placed in the confining ring on top of the filter. The actual material thickness was measured by placing the counter weight such that the loading piston was positioned just on top of the material. Subsequently, the material was mechanically loaded with a conditioning preload of 3N (0.038 MPa). Due to the application of the mechanical load, a decrease in thickness occurred. After setting of the material, the minimum thickness recorded was taken as initial thickness. Hereafter, the flexible tubes and filter were deaerated and the circulation of the NaCl bathing solution established. At first, the material was loaded chemically with a conditioning solution of 0.6 M NaCl. Immediately after the contact of the material with the solution, a rapid increase of the thickness of the material occurred. Equilibrium heights were attained within 18-24 hours depending on the initial thickness of the material.

The experimental protocol consisted of four stages including the conditioning stage in which the material was equilibrated against the mechanical and chemical load of 0.038 MPa and 0.6 M NaCl respectively (table 5.1).

| stage | A | B | C | D |
|------------------------|--------------|----------|---------------|---------|
| | conditioning | swelling | consolidation | control |
| mechanical load [MPa] | 0.038 | 0.038 | 0.086 | 0.038 |
| concentration NaCl [M] | 0.6 | 0.2 | 0.2 | 0.2 |

Table 5.1: *Experimental stages of the confined swelling and compression experiments.*

In the second stage, the swelling stage, the concentration of the NaCl solution was decreased to 0.2 M while maintaining the mechanical load at 0.038 MPa. Approximately five minutes after the transition from 0.6 M to 0.2 M, an subsequent increase of the thickness of the material occurred. Within 22-25 hours the new equilibrium heights were attained. The third stage, the consolidation stage, was initiated by a step increase of the mechanical load to 6.75 N (0.086 MPa) while the chemical load was maintained at 0.2 M NaCl. A decrease of the thickness of the material occurred. Equilibrium heights were attained within 10 hours. The fourth stage, the control stage, consisted of a stepwise mechanical unloading back to 3N (0.038 MPa), while the chemical load was still maintained at 0.2 M NaCl. The mechanical and chemical load for this stage were identical to the loads of the swelling stage. After removal of the additional mechanical load, a re-swelling of the material was observed. Within 15-20 hours the final equilibrium heights were attained. The equilibrium heights of the swelling stage and the control stage were compared to verify whether any copolymer gel material was lost during the experiment.

The total experimental time was approximately 90 hours. After each experiment the material specimen was removed from the testing chamber. The testing chamber and loading piston were cleaned and the glass filter dehydrated.

The bathing solution was changed according to the following procedure: (1) the circulation was interrupted via manipulation of the tap connections, (2) the fluid pump was disconnected to allow the 0.6 M solution to flow back from the overflow reservoir to the storage reservoir, (3) the fluid pump was replaced by a second pump for the circulation of the 0.2 M solution, (4) a new storage reservoir containing the 0.2 M solution was placed in the fluid circuit and the circulation was re-established between storage and overflow reservoir, (5) by re-opening the tap connection to the testing chamber, the fluid circulation was resumed. The outflow was separately collected during the first five minutes after recirculation. After this period a homogeneous solution was assumed. The total time needed to change the solutions was less than five minutes. During this period the material specimen was still in contact with NaCl solution.

5.3 Results

5.3.1 General behaviour

A typical result of the uni-axial confined swelling and compression behaviour of the materials is given in figure 5.3. In all stages equilibrium heights are attained. During the first two stages, a strong swelling of the material is observed. It reacts on the new environment by exchanging fluid and ions with the external NaCl solution. The application of the additional mechanical load during the third stage causes finite consolidation deformation. In the control stage, a renewed swelling of the material occurs to approximately the same height as reached during the swelling stage. The period of time needed to equilibrate the change in mechanical load is about half the period of time that is required to equilibrate the change in chemical load. The observed initial response during the swelling stage is slower than during the consolidation and control stages.

5.3.2 Quantitative comparison of the various materials

For every type of synthetic model material, a confined swelling and compression curve was recorded according to the protocol and loading program given in section 5.2.3 (figures 5.4 and 5.5). For almost all material specimen equilibrium heights are attained in all stages. Only the 1030 material specimen showed a continuing decrease in height during the consolidation stage. After the conditioning stage, the specific composition of the material under consideration determines its sensitivity to the change in chemical and mechanical load during the swelling and consolidation stage respectively. In order to compare this behaviour of the various materials, the axial stretch relative to the conditioning stage was observed (table 5.2).

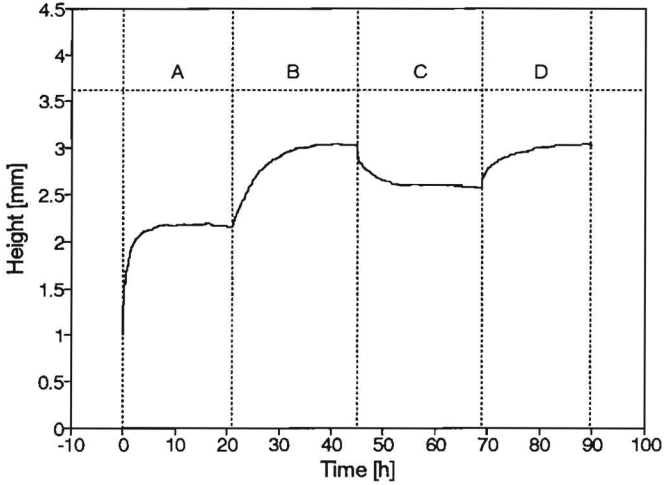


Figure 5.3: *Experimental displacement data of a typical experiment: height of the material versus time. Stage A: conditioning, stage B: swelling, stage C: consolidation, stage D: control.*

Axial stretches are found between 1.20 and 1.56. The smallest axial stretch is found for the 1460 material specimen, the largest for the 413035 material specimen. The decrease in axial stretch during consolidation varies between 0.14 and 0.28. Some of the material specimen do not reach the same height at the end of the control stage as reached at the end of the swelling stage. For these materials, the loss of height between the end of the swelling stage and the end of the control stage lies between 0.5-2% of the equilibrium height of the swelling stage.

The axial stretch of the 4160, 1160 and 1460 materials is observed to decrease with increasing acrylamide content of the materials (De Heus *et al.* [27]). The 41303 material exhibits a reduced swelling compared to the 4130 material. Only small differences in axial stretch are found for the 4130, 4160 and 4138 materials.

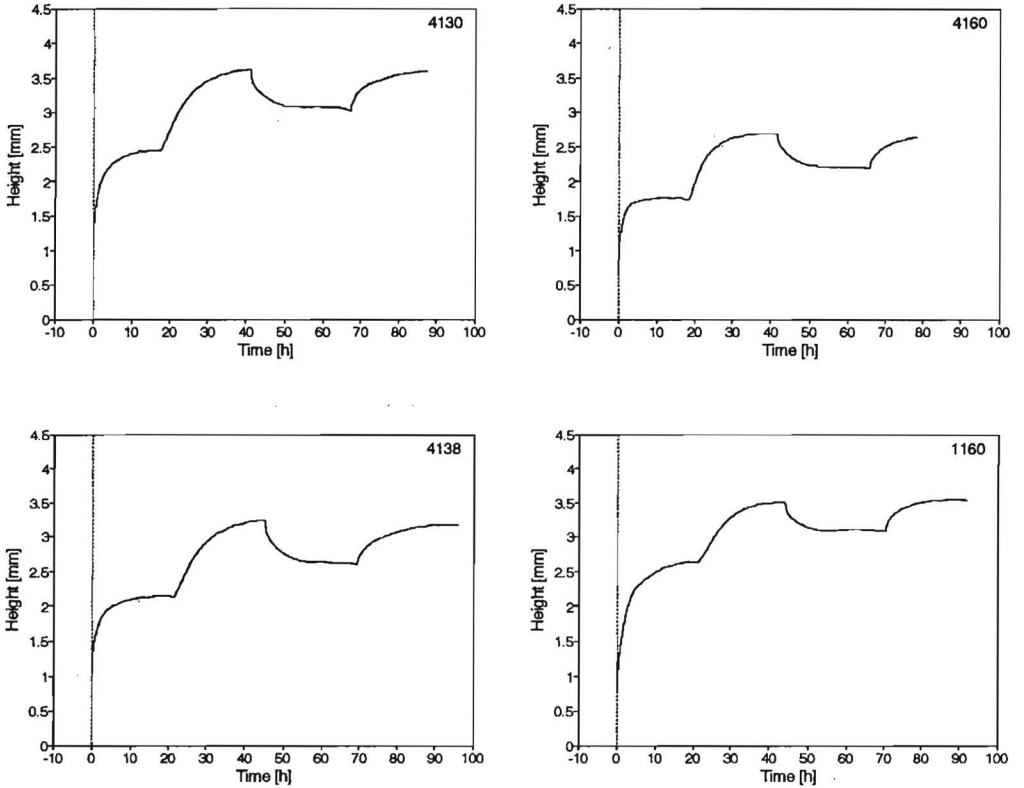


Figure 5.4: Overview of the confined swelling and compression behaviour of the various materials

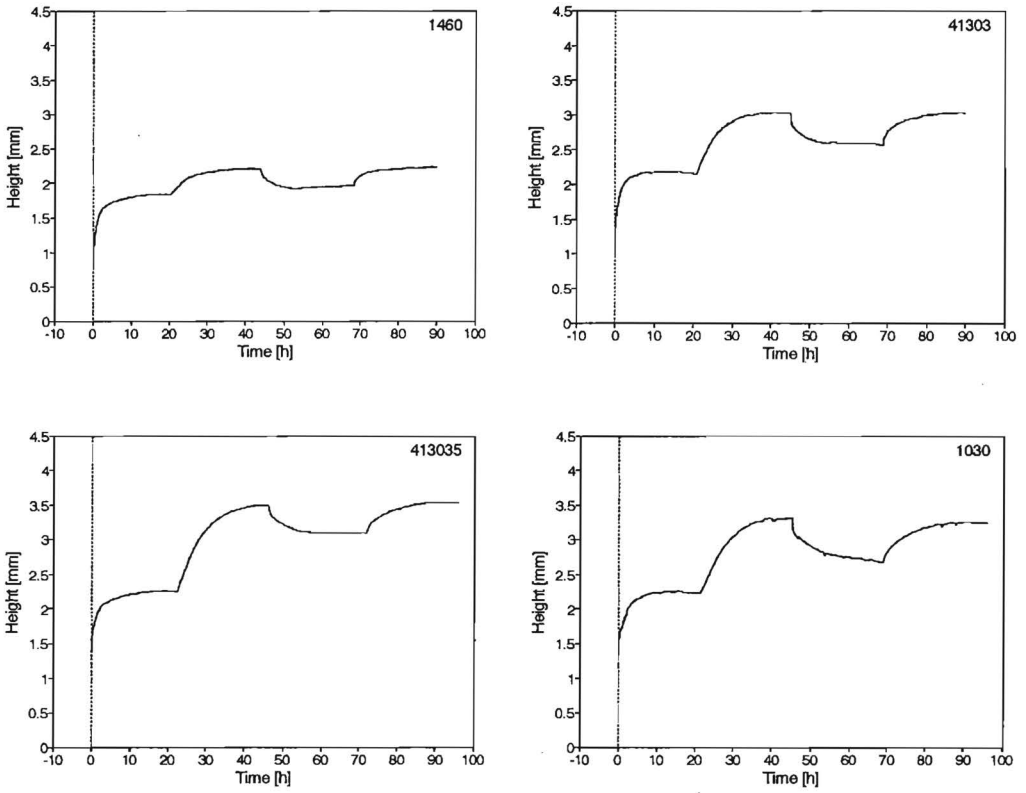


Figure 5.5: Overview of the confined swelling and compression behaviour of the various materials

| Axial stretch relative to conditioning stage | | | |
|----------------------------------------------|----------|---------------|---------|
| code | swelling | consolidation | control |
| 4130 | 1.47 | 1.26 | 1.46 |
| 4160 | 1.54 | 1.26 | 1.52 |
| 4138 | 1.52 | 1.24 | 1.49 |
| 1160 | 1.33 | 1.18 | 1.34 |
| 1460 | 1.20 | 1.06 | 1.21 |
| 41303 | 1.41 | 1.20 | 1.41 |
| 413035 | 1.56 | 1.38 | 1.57 |
| 1030 | 1.48 | ± 1.21 | 1.46 |

Table 5.2: *Experimental axial stretch data of the various materials for the swelling, consolidation and control stage. The data are determined relative to the conditioning stage. For the interpretation of the material codes the reader is referred to table 2.3 of chapter 2.*

5.3.3 Quantitative description confined swelling and compression behaviour

The experimental displacement data of the swelling and consolidation stage are used to verify whether the triphasic theory, combined with the material parameters determined in the previous chapters, is able to describe the transient behaviour of the materials. For this purpose the numerical model developed by Snijders [63] is used. The basic set of equations describing the uni-axial response of the materials to a combination of mechanical and chemical loading conditions is given by the Eqs. 1.1 - 1.9 (chapter 1, section 1.3). These set is completed by choosing additional constitutive relations for the description of the stress-strain behaviour and the permeability and diffusivity of the materials.

In principle, two phenomena contribute to the effective Cauchy stress during deformation of the materials: the elastic deformation of the PUR-copolymer network and the change in fixed charge repulsion due to changes in local salt concentration. In the swelling pressure experiments, no evidence was found for a possible contribution of the latter. Therefore, the dependence on local salt concentration is not taken into account. For the deformation dependent stress-strain relation, Eq. 1.10 is chosen.

The permeability of the materials was found dependent on the deformation state of the materials and the ionic strength of the surrounding NaCl solution (chapter 4). As a first approximation, the contribution to the change in permeability of the variation in NaCl concentration from 0.6 M to 0.2 M, as applied in the experiment, is assumed negligible compared to the deformation contribution. For the description of the deformation dependence of the permeability, Eq. 1.11 is chosen.

In order to describe the change of the diffusion coefficient, due to the change in solid-fluid ratio during deformation, Eq. 1.12 is used. An overview of the constitutive equations used is given in table 5.3.

| | |
|-----------------------------------------------------|--------|
| $\pi = \phi^{smm} RT(2C^- + C^{fcd}) - 2\phi^* RTc$ | (1.4) |
| $C^{fcd} = \frac{C_0^{fcd}}{1 - \frac{n_0^f}{J}}$ | (1.8) |
| $n^f = 1 - \frac{1 - n_0^f}{J}$ | (1.9) |
| $S_{eff} = H_A e^{\alpha E^2} E$ | (1.10) |
| $K = K_0 e^{M(J-1)}$ | (1.11) |
| $D = \frac{n^f}{n_0^f} J D_0$ | (1.12) |

Table 5.3: Overview of the constitutive equations used. For the interpretation of the symbols, the reader is referred to section 1.3.

For the triphasic calculations, the values of the material parameters occurring in the equations, have to be prescribed at the beginning of the swelling stage. From these parameters, the following were determined in the previous chapters: the fluid fraction n_0^f (chapter 2), the fixed charge density C_0^{fcd} , the osmotic coefficient ϕ^{smm} and the diffusion coefficient D_0 (chapter 3), and the permeability K_0 (chapter 4). In order to be able to use the latter parameter, the material deformation at the beginning of the swelling stage should be in the deformation range of the permeability experiments. Neither of the confined swelling and compression curves presented in section 5.2 satisfies this condition. Therefore, an additional curve was recorded for a 4130 material using a conditioning mechanical load increased to 6.25 N (0.08 MPa). In the consolidation stage the mechanical load was set to 8.75 N (0.11 MPa). The result of the experiment is given in figure 5.6. For this particular experiment the axial strain of the material at the beginning of the swelling stage was approximately 0.04 which is in the range of the permeability measurements.

The values at the beginning of the swelling stage for the fixed charge density, porosity and diffusion coefficient are calculated using the equations 1.8, 1.9 and 1.12 (table 5.3) and the reference values of the material parameters determined for the fixed charge density C_0^{fcd} ($(0.306 \pm 0.042) \cdot 10^3$ mole/m³, table 3.2), the fluid fraction n_0^f (0.743, table 2.4) and the diffusion coefficient D_0 ($3 \cdot 10^{-10}$ m²/s, section 3.4) respectively.

The value for the permeability K_0 at the beginning of the swelling stage is derived from figure 4.2 ($K_0 \approx 1.85 \cdot 10^{-16}$ m⁴/Ns). For the calculation of the osmotic pressure (table 5.3, Eq. 1.4) also the value determined for the osmotic coefficient of the material ϕ^{smm} is used (0.934 ± 0.007 , table 3.2). The osmotic coefficient ϕ^* of the external NaCl solution is taken 0.93 (Robinson *et al.* [58]). The value for the diffusion parameter ξ is calculated using the equations 1.7, 3.12 and 3.13 together with the initial value for the fixed charge density.

By using the set of known material parameters (n_0^f , C_0^{fcd} , ϕ^{smm} , K_0 , D_0 , ξ) and by adjusting the other material parameters (H_A , α , M), only the finite equilibrium conditions and the transient consolidation behaviour of the material are approximately described (figure 5.7,

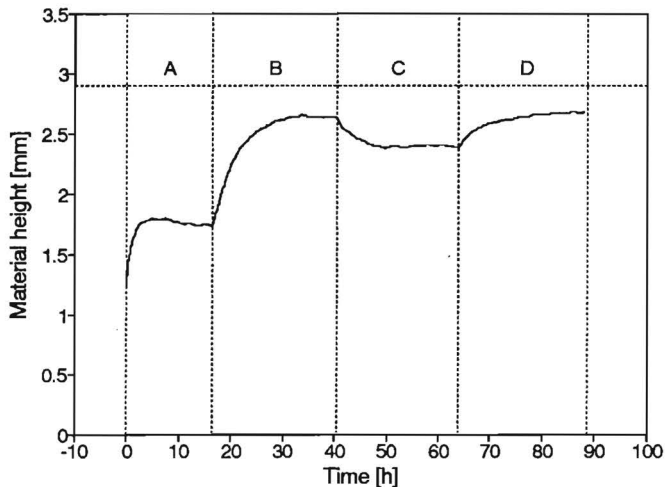


Figure 5.6: Experimental confined swelling and compression curve of a 4130 material equilibrated against a mechanical load of 0.08 and 0.11 MPa during the conditioning and consolidation stage respectively. Stage A: conditioning, stage B: swelling, stage C: consolidation, stage D: control. The displacement data of the swelling and consolidation stage are used for comparison with the triphasic calculations.

top). By changing the diffusion coefficient to an unrealistic value of $5.95 \cdot 10^{-9} \text{ m}^2/\text{s}$, which is almost four times the value encountered in aqueous solution (Robinson *et al.* [58]), the complete transient behaviour is described (figure 5.7, bottom). An overview of the material parameters used is given in table 5.4.

The equilibrium conditions of the confined swelling and compression curve are determined by the parameter set $(H_A, \alpha, \phi^{smm}, n_0^f, C_0^{fcd})$. The first two parameters are responsible for the mechanical stiffness of the material, the remainder are related to the osmotic stiffness. Variation of one of these parameters causes a horizontal shift of the equilibrium conditions. The transient response of the materials is mainly determined by the permeability parameter M and the diffusion coefficient D_0 . The influence of both parameters on the computed displacement is illustrated in figure 5.8. For these computations the other parameters were taken according to values given in table 5.4. During deformation, the value of the parameter M determines the rate of fluid flow in the material. The lower the value for M is taken, the longer the material needs to reach equilibrium (figure 5.8, top). The value for the diffusion coefficient determines the diffusion rate of the Na^+ and Cl^- ions to the external solution during the transition from 0.6 M to 0.2 M NaCl. The

| parameter | fit A | fit B | unit |
|--------------|-----------------------|----------------------|------------------------|
| H_A | 0.005 | id. | [MPa] |
| α | 0.0 | id. | [-] |
| K_0 | $1.85 \cdot 10^{-16}$ | id. | [m ⁴ /Ns] |
| M | 4.10 | id. | [-] |
| ϕ^{smm} | 0.93 | id. | [-] |
| n_0^f | 0.743 | id. | [-] |
| C_0^{fcd} | $0.315 \cdot 10^3$ | id. | [mole/m ³] |
| D_0 | $3 \cdot 10^{-10}$ | $5.95 \cdot 10^{-9}$ | [m ² /s] |
| ξ | -0.01 | id. | [kg/mole] |

Table 5.4: Overview of the material parameters which were used to describe the transient swelling and compression behaviour of the 4130 material as given in figure 5.7.

smaller the value for D_0 is taken, the longer the initial difference in ionic strength between the material and the external NaCl solution exists, thereby promoting the preservation of the osmotic pressure difference. Apparently, this results in an initial overestimation of the fluid absorption to level the difference in ionic strength and hence to an initial overestimation of the displacement (figure 5.8, bottom). For the second computation (b), a diffusion coefficient was chosen similar to the harmonic average diffusion coefficient of NaCl in water.

Examining the material parameters given in table 5.4, a rather low value is observed for the aggregate modulus which points to a dominant role of the osmotic stiffness of the material. By using the Eqs. 1.4 and 1.8 (table 5.3) together with Eq. 3.12, the change in osmotic pressure during consolidation of the material specimen is calculated as 0.023 MPa. The comparison of this value to the opposed mechanical load of 0.031 MPa indicates that approximately 76% of the load during consolidation is transferred by the osmotic pressure. The remaining 24% is counterbalanced by the deformation of the PUR-copolymer network. The value obtained for M indicates that the permeability behaviour of the materials is non-linear for large swelling strains. For the description of the stress-strain behaviour, a linear relationship between the second Piola Kirchhoff stress and Green-Lagrange strain suffices, as the stiffness parameter α was found equivalent to zero. The value used for the fixed charge density lies within measurement accuracy.

5.4 Discussion

In this chapter the transient deformation behaviour of the materials to step changes in mechanical and chemical loading conditions has been studied by performing uni-axial confined swelling and compression experiments. The analysis of the confined swelling and compression data, using the triphasic theory combined with the set of known material parameters (n_0^f , C_0^{fcd} , ϕ^{smm} , K_0 , D_0 , ξ), points to an incomplete description by the triphasic theory

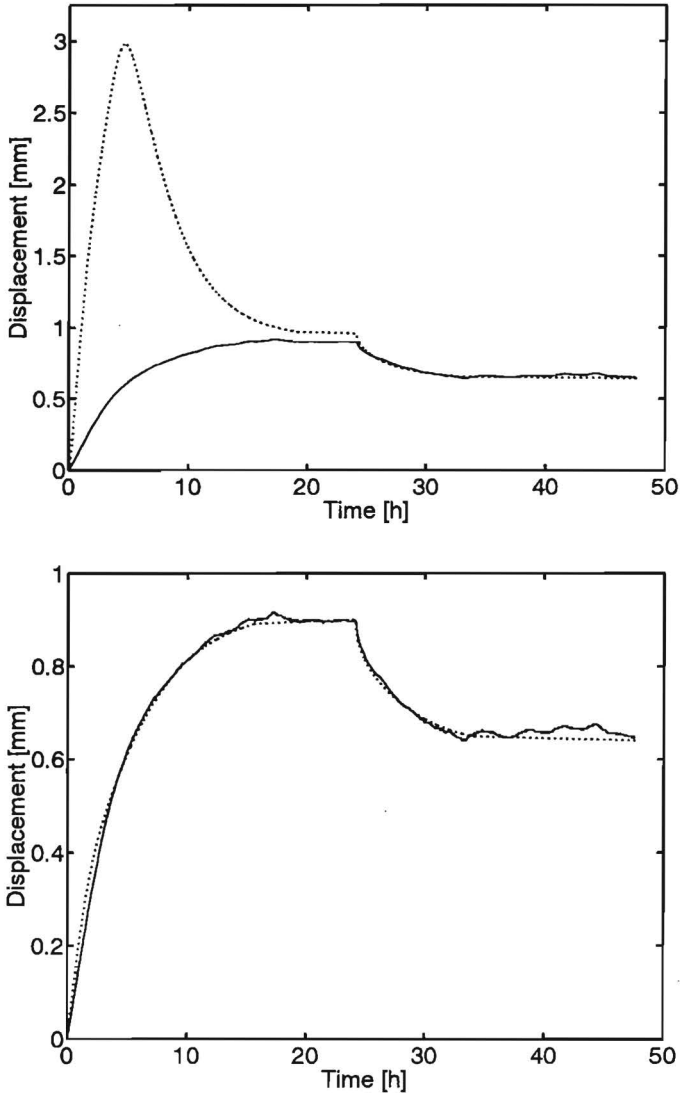


Figure 5.7: Measured (—) and calculated (· · ·) displacement.

Top: Computation performed with the known parameter set $(n_0^f, C_0^{fcd}, \phi^{smm}, K_0, D_0, \xi)$.

Bottom: Computation performed with the known parameter set $(n_0^f, C_0^{fcd}, \phi^{smm}, K_0, \xi)$ and a diffusion coefficient D_0 of $5.95 \cdot 10^{-9} \text{ m}^2/\text{s}$.

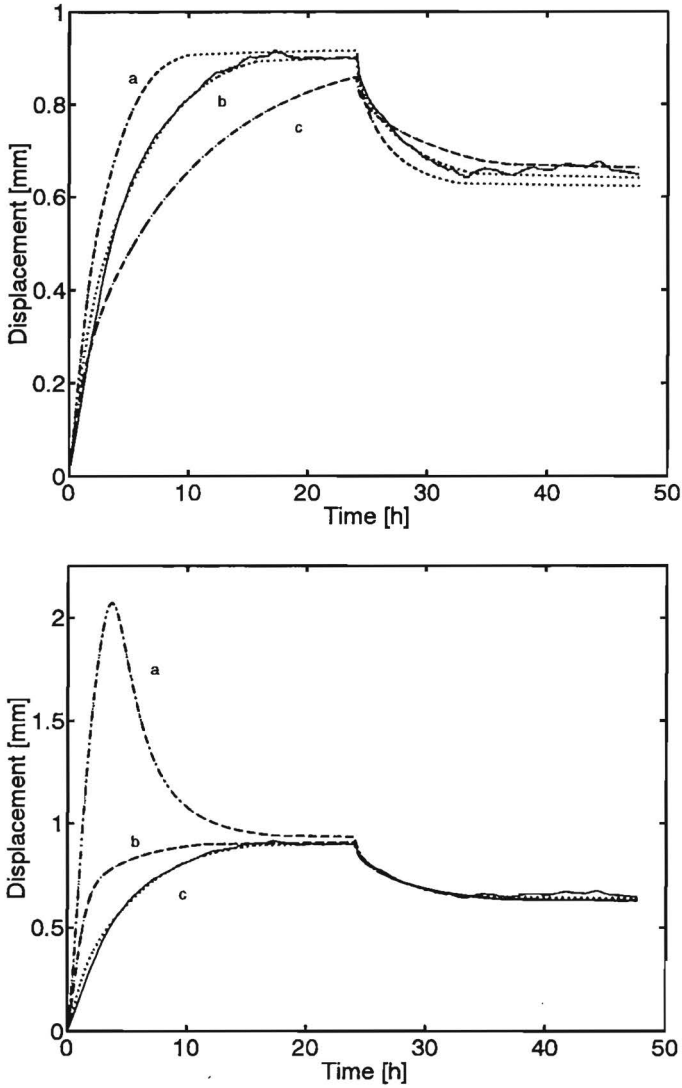


Figure 5.8: The influence of the permeability parameter M and the diffusion coefficient D_0 on the computed displacement.

Top: Variation with M ($D_0 = 5.95 \cdot 10^{-9} \text{ m}^2/\text{s}$): a. $M = 5.5$ (- - -), b. $M = 4.1$ (···), c. $M = 2.5$ (-·-·).

Bottom: Variation with D_0 ($M = 4.1$): a. $D_0 = 5.95 \cdot 10^{-10} \text{ m}^2/\text{s}$ (-·-·), b. $D_0 = D_{\text{NaCl}}$ (in water) $= 1.66 \cdot 10^{-9} \text{ m}^2/\text{s}$ (- - -), c. $D_0 = 5.95 \cdot 10^{-9} \text{ m}^2/\text{s}$ (···).

The experimental displacement curve (—) is added for comparison.

of the transport phenomena taking place in soft charged hydrated materials. By using the diffusion coefficient, as estimated from the swelling pressure experiments, the transient finite swelling behaviour is initially overestimated. However, the equilibrium conditions and transient finite consolidation behaviour of the material were described correctly. The overestimation completely disappears by choosing a diffusion coefficient which is approximately four times higher than the value encountered in water. These findings confirm the observations of Snijders [63] who used a diffusion coefficient which was approximately ten times the value found in water in order to describe the transient behaviour of intervertebral disc tissue. The discrepancy observed is probably due to the presence of electrical potentials in the material which influence both fluid flow and ion diffusion. These effects are not incorporated in triphasic theory.

The diffusivity of the Na^+ and Cl^- -ions in the material is expected to be reduced compared to their diffusivity in aqueous solution, similar to other soft hydrated charged materials (Maroudas [44], Yoshio [75]). The decrease in diffusivity is not likely to be caused by steric factors associated with the presence of solids, considering the large water content of the materials (already initially approximately 75%), and the relative small dimensions of the ions compared to the cross sectional area of the pore space through which they diffuse. On the contrary, electrical effects, associated with the presence of the fixed carboxylate groups, may very well cause the decrease in diffusivity. As the counter-ion content in the material is larger than the co-ion content, the (de)sorption of NaCl is hindered due to exclusion of the Cl^- -ions by the material (Helfferich [26]). As a result, the materials show a selective character with respect to the diffusion of the Na^+ and Cl^- -ions respectively. The overall rate of diffusion is controlled by the diffusion of the Cl^- co-ion. According to Helfferich, the rate limiting effect of co-ion diffusion intensifies with decreasing concentration of the external NaCl solution.

In addition, the fluid flow in the materials may be slowed down due to the influence of streaming potentials that are generated by the displacement of unequal amounts of counter- and co-ions (chapter 4). As this effect is not taken into account, fluid absorption may initially overrule the diffusion of the mobile ions, in case diffusion coefficients are chosen as observed in soft charged hydrated materials, in order to level the difference in ionic strength between material and external solution. This results in the observed overestimation of the displacement. As extensive changes in fluid and ion-content primarily occur in case of step changes of NaCl solution, these effects are particularly present during the swelling stage of the material.

It can be argued that the description of the transient swelling behaviour can be improved by incorporating an electrical repulsive force between the fixed charged groups as has been done by Lai *et al.* [40]. In our case, such a contribution would only increase the swelling tendency of the materials and hence intensify the inconsistency observed. Moreover, since the swelling pressure responses can be fitted satisfactorily by Donnan theory (chapter 3), such a contribution seems not necessary to describe the swelling behaviour of the materials. Furthermore, the evaluation of the triphasic material parameters confirms that the swelling

pressure of the moderately charged model materials (C^{fcd} in the order $0.3 \cdot 10^3$ mole/m³) can be modelled by Donnan osmosis.

It is noted that the fluid osmotic pressure is responsible for the transfer of the majority of the mechanical load during consolidation. Similar results are reported for intervertebral disc tissue (Urban *et al.* [70]). The permeability behaviour of the materials should be modelled non-linearly dependent on the deformation for large swelling strains. Considering that nine material parameters were used for the triphasic calculations, uniqueness of the material values can not be claimed. However, as both the finite equilibrium conditions and transient material behaviour are described correctly with the set of parameters, which includes values experimentally determined for the fluid fraction, fixed charge density, osmotic coefficient, hydraulic permeability and diffusion parameter ξ , parameter variation is restricted.

The transient confined swelling and compression behaviour of the materials, measured under a combination of mechanical and chemical loading conditions, is comparable to that of intervertebral disc tissue (Snijders [63]). All materials undergo large deformations during swelling and compression. Both the fixed charge density and the stiffness of the PUR-copolymer network determine the final deformation of the materials during these stages. The small differences in swelling and compression behaviour observed for the 4130, 4160 and 4138 materials (table 5.2) indicate that the influence of the difference in type of PUR-foam on the overall behaviour is limited. Furthermore, the deformation of the materials is restricted by increasing the acrylamide content or the crosslink density of the materials, as in both cases the mechanical stiffness of the copolymer network is increased. Similar results are reported by Yoshio *et al.* [75] for lightly crosslinked poly(acrylamide-co-acrylic acid) gels in general. Baker *et al.* [1] also report a decreasing swelling ratio with increasing acrylamide content for charged acrylamide based hydrogels of fixed crosslink density and charge concentration. The relatively large deformation during swelling and limited deformation during consolidation of the 413035 material (table 5.2) is likely to be due to its higher fixed charge density ($C_0^{fcd} \approx 0.35 \cdot 10^3$ mole/m³, table 3.2).

For some of the materials, small differences are observed between the equilibrium height reached during the swelling stage and the control stage respectively. This might point to deterioration of the materials. However, when removed from the experimental set-up, no deterioration of the materials was visible, except for the 1030 material. This probably explains also the continuing decrease in height observed during the consolidation of the material. For the other materials, the loss of copolymer gel material, which might account for the loss in equilibrium height, seems negligible. The decrease in equilibrium height may be attributed to small evaporation of the 0.2 M NaCl solution during the experiment, in spite of almost complete sealing of the fluid reservoirs. The 0.2 M solution is circulated for almost 72 hours. In case of fluid evaporation, the NaCl concentration of the external bath slightly increases which causes a reduced re-swelling of the material during the control stage.

Chapter 6

Discussion, conclusions and recommendations

The research presented in this thesis is discussed in section 6.1. In section 6.2, the conclusions are formulated as derived from the verification of the triphasic theory, the development of the synthetic model materials and the various experiments. In section 6.3, recommendations are given for a further study of the transport of fluid and ions in the materials together with suggestions for a further verification of the triphasic theory.

6.1 Discussion

The objective of the research was to evaluate the application of synthetic model materials for the verification of mathematical models describing the behaviour of soft charged hydrated tissues. For this purpose, model materials were synthesized based on characteristic properties and behaviour of intervertebral disc tissue.

The study encompassed the development and characterization of the materials, the determination of their behaviour under various mechanical and chemical loading conditions and the verification of the mathematical models. Accordingly, the same issues are addressed in the discussion.

6.1.1 Verification of triphasic theory

The synthetic model materials have proven to be a significant and feasible tool for the verification of the triphasic theory. The comparison of experimental confined swelling and compression data with numerical data, computed using the triphasic equations combined with the material parameters experimentally determined, showed that the finite equilibrium deformation conditions and transient consolidation behaviour of the material are described correctly. However, an inconsistency was observed between measured and calculated transient swelling behaviour. The only way to match the triphasic calculations with the swelling experiment was to choose an unrealistic value for the diffusivity of the NaCl-ions. This result questions the validity of the triphasic equations as presented by Snijders [63]. On the contrary, considering the variation in strain of more than 50% during the confined swelling of the material, it is evident that the numerical model is capable of describing large material deformations. Although primarily designed for the description of the behaviour of soft charged biological tissues, the calculations performed show that the applicability of the numerical model can be extended for the description of the mechanical and physico-chemical behaviour of hydrogels.

The inconsistency between calculated and measured swelling behaviour may be related to the presence of electrical potentials, due to the unequal mobile ion distribution in the material, which may cause disturbances in fluid and ion flux. The fluid flow in the material may be slowed down due to the influence of streaming potentials generated by the initial displacement of net electric charge in the material (chapter 4). Furthermore, the presence of the fixed carboxylate groups probably also influences the (de)sorption of NaCl of the materials due to exclusion of the Cl⁻-ions by the material. The rate of electrolyte diffusion is generally controlled by the species that is in the minority (Helfferich [26]). According to Helfferich, the co-ion exclusion as well as the influence of streaming potentials increases with increasing fixed charge density of the material and decreasing concentration of the external NaCl solution. Both phenomena are not incorporated in the triphasic equations and may contribute to the inconsistency observed.

No indication has been found that the swelling pressure of the materials due to step changes in ionic strength of the external NaCl bathing solution is caused by other effects than Donnan osmosis. Therefore, the incorporation of a chemical expansion stress, as has been done by Lai *et al.* [40], is questioned in order to describe the swelling behaviour of moderately charged soft hydrated materials (C^{fd} in the order of $0.3 \cdot 10^3$ mole/m³).

6.1.2 Synthetic model materials

The *in-situ* radical copolymerization in aqueous solutions of acrylic acid and acrylamide in the pores of open cell microporous polyurethane (PUR) foams, yielded synthetic model materials exhibiting hydraulic permeability, ion diffusivity and deformation characteristics quantitatively similar to intervertebral disc tissue. Unlike the genuine tissue, the composition of the materials can be tailored to the needs of the user while their shape and dimensions can be chosen within a wide range.

To our knowledge, the syntheses performed embody the first attempt to copolymerize acrylic acid and acrylamide *in-situ* in the pores of a microporous material. In all cases, the copolymerizations proceeded successfully. Unfortunately, no accurate conversion data could be obtained from the resulting copolymers. However, in the absence of PUR-foams and crosslinking agent, the copolymerizations resulted in almost full conversion as quantified by HPLC.

The variation of the composition of the materials via the adjustment of the initial acrylic acid - acrylamide monomer feed ratio, the neutralization degree of the acrylic acid, the concentration of crosslinking agent, and the properties of the PUR-foams, yielded materials of different behaviour, but only in a limited range. Notwithstanding the small variation of the material properties, the material parameters of intervertebral disc tissue lie within this range. Nevertheless, the significance of the materials for the verification of the triphasic theory can be enlarged by applying materials that exhibit larger differences in material behaviour. One could think of adjusting the total monomer content and/or applying PUR-foams of higher stiffness and reduced porosity to meet this requirement.

The stiffness of the PUR-foam, the amount of acrylamide and the concentration of crosslinking agent are important parameters for the mechanical stiffness of the materials. An increase of either one results in an increase of the mechanical stiffness. The swelling tendency of the materials, and hence their osmotic stiffness, increases with increasing number of carboxylate groups present. Adaptation of the neutralization degree of the acrylic acid primarily influences the copolymerization conditions during preparation of the materials and is therefore only of importance for the homogeneity of the copolymer composition.

In general, the analysis of the copolymers is obstructed by the tenacious retention of water absorbed by the hydrophilic side-groups of the copolymer chains. Even prolonged vacuum drying of the samples, which ought to be done preferably at temperatures exceeding their glass temperature, does not remove all the water present. Rather than drying samples

to determine the copolymer content, it might be advisable to precipitate the copolymer out of a large volume of volatile, water-miscible non-solvent such as methanol and ethanol (Potnatram *et al.* [53], Klein *et al.* [36]).

A first step has been made for the development of the synthetic model materials. In order to reduce the complexity of the resulting materials, several characteristic features of intervertebral disc tissue were not considered such as its anisotropy. Nevertheless, the resulting materials exhibited behaviour similar to the genuine tissue. On longer term however, it might be worthwhile to investigate the influence of anisotropy on the model material behaviour via *e.g.* the incorporation of fiber networks in the basic microporous material.

6.1.3 Experimental characterization

To determine the material parameters essential for the triphasic formulations and to study the behaviour of the materials under changing mechanical and/or chemical loading conditions, experiments were performed which quantified swelling pressure, hydraulic permeability and confined swelling and compression behaviour of the materials. As swelling agent NaCl solutions were used. The cylindrical confinement of the material samples in all experiments ensured that flow, diffusion and deformation phenomena were approximately one-dimensional.

In all experiments, the experimental set-up and experimental protocol yielded reproducible results. An important factor which contributed largely to the reproducibility was the mechanical stability of the materials. Even after testing periods of more than 240 hours, no deterioration of the samples was observed except for the 1030 material. Use of the latter material for extensive mechanical testing should therefore be avoided.

Fixed charge density and osmotic coefficient of the materials were determined from equilibrium swelling pressure responses using Donnan theory. However, one has to bear in mind that the determination of both parameters in this manner can not be performed for any soft charged hydrated material. Only because the materials were moderately charged, a good agreement was found between experimental results and theory which justified the approach. Deviations from this behaviour are expected for materials that are higher charged. In principle, the diffusivity of NaCl in the materials can be estimated from the transient pressure curves, as the equilibrium values are attained on the basis of the diffusion of the mobile ions only, due to the tri-axial confinement of the samples. However, it should be noted that the determined value of $3 \cdot 10^{-10} \text{ m}^2/\text{s}$ is only a rough indication of the ion-diffusivity. Moreover, determination of diffusion coefficients in this manner does not cover any dependence on salt concentration. Therefore, direct measurement of the ion-diffusivity in the materials should be performed.

An important drawback of the hydraulic permeability set-up is its limited use to determine

the permeability of the materials for swelling strains larger than 10%. For these strains, the values determined are expected to become inaccurate due to fluid flow along the material sample. However, measurement of the permeability in this deformation range could possibly confirm the non-linearity as observed during confined swelling and compression of the materials.

Although complicated to perform, the latter experiment is one of the few possibilities to study in a controlled way the transient behaviour of the materials under both changing mechanical and chemical loading conditions. An important advantage is that the design of the experiment is suited for a one-dimensional verification of the triphasic theory including the use of the material parameters determined in the various experiments.

The application of the experimental techniques, as used in this thesis to determine the material parameters, for a possible future use in a biological environment, is probably restricted mainly because of the variability of the properties of genuine biological material with time and region of origin. With respect to that, a mixed numerical experimental approach, as used by Van Ratingen [55], might produce better results.

6.2 Conclusions

- The *in-situ* radical copolymerization in an aqueous solution of acrylic acid and acrylamide in the pores of open cell microporous PUR-foams, yields soft charged hydrated materials exhibiting hydraulic permeability, ion diffusivity and swelling characteristics quantitatively similar to intervertebral disc tissue.
- The mathematical model developed by Snijders [63] is able to describe the finite equilibrium conditions and transient consolidation behaviour of the materials during one-dimensional confined swelling and compression for axial strains of more than 50%.
- The mathematical model developed by Snijders [63] is able to describe the complete finite transient deformation behaviour of the materials during one-dimensional confined swelling and compression for axial strains of more than 50%, only when unrealistically high values of the diffusion coefficient are used.
- No evidence is found that other physical effects than Donnan osmosis are needed to describe the equilibrium swelling behaviour of the moderately charged model materials (C^{fd} in the order of $0.3 \cdot 10^3$ mole/m³). The experimental results show no need for the incorporation of electrostatic forces due to repulsion of the fixed charged groups.
- The hydraulic permeability of soft charged hydrated materials is both dependent on the deformation state of the material and the concentration of the external salt solution. For axial strains > 20% and NaCl concentrations between 0.05 - 1.5 M,

the contribution of the salt concentration to the change in permeability is negligible compared to the deformation contribution.

- Unlike *in-vitro* intervertebral disc tissue specimen, the materials can be used for testing periods up to 240 hours without deterioration of the materials.

6.3 Recommendations

Considering the possible influence of electrical phenomena on the overall material behaviour, it is recommended that the transport of fluid and ions in the materials is studied in much more detail. The classical set-up to study electrokinetic processes consists of two compartments containing salt solutions which are separated by a plug of porous charged material. This concept was also used for the design of the hydraulic permeability measurement set-up. In such a system, motion of fluid and ions in the material can be generated either by gradients in pressure, salt concentration or electrical potential (Kedem *et al.* [35], Katchalsky [34], Meares [45]). Extension of the permeability set-up with electrodes on either side of the material would already enable the study of electromechanical transport of electrolyte solutions through the materials under *e.g.* zero streaming potential or electro-osmosis conditions. This would also enable the measurement of streaming potentials.

Although diffusion coefficients can be determined from transient swelling pressure responses, it is advisable to measure the ion-diffusivity directly, thereby quantifying its dependence on the deformation state of the material and the local salt concentration. Generally, two sets of methods can be used for the determination of diffusion coefficients *in vitro*, both involving radioactive tracers. The first method is a steady state method (Stokes [65], Helfferich [26]), in which a material slice is used as a membrane between two compartments of a diffusion cell and the rate of solute transfer across the membrane is measured as a function of time. Preliminary test-measurements performed in a comparable set-up, without use of radio-active tracers, showed only very small changes in molarity with time. Therefore, the accuracy of this method is questioned for the materials developed. An alternative is the unsteady state method in which a material sample is equilibrated in a solution containing the given solute tagged with radio-active tracer. The desorption of the tracer is subsequently studied as function of time. From the efflux curves thus obtained, it is possible to determine the diffusion coefficient of the solute (Crank [13]). Simultaneous measurement of diffusion potentials would also enable the determination of the difference between counterion and co-ion diffusivity. The latter method can also be used for thick material samples.

A further verification of the triphasic theory should be performed. In that respect, the above mentioned study of the electrical phenomena taking place in the materials is important. Furthermore, one could think of:

- The use of the materials in multi-axial deformation experiments or the subsection of

the materials to more complex loading conditions such as simultaneous variation of mechanical and chemical loading.

- The study of the influence of the initial monomer content and the pH of the external environment on the swelling behaviour of the materials.
- The simultaneous measurement of swelling pressure and *in-situ* hydrodynamic pressure using a micropipet pressure measurement system.
- The study of the material behaviour using other electrolyte solutions such as KCl or CaCl₂.
- The use of open cell microporous (PUR) foams of higher stiffness and reduced porosity to increase the influence of the foam on the overall material behaviour.
- The introduction of fiber networks in the materials to obtain anisotropic structures.

References

- [1] Baker J.P., Hong L.H., Blanch H.W., Prausnitz J.M.: *Effect of initial total monomer concentration on the swelling behavior of cationic acrylamide-based hydrogels*, *Macromolecules*, Vol. 27, pp. 1446-1454, 1994.
- [2] Bardet L., Cassanas-Fabre G., Alain L.: *Etude de la transition conformationnelle de l'acide polyacrylique syndiotactique en solution aqueuse par spectroscopie de vibration*, *J. Mol. Struct.*, Vol. 24, pp. 153-164, 1975.
- [3] Beard H.K., Stevens R.L.: *Biochemical changes in the intervertebral disc*, in 'The lumbar spine and backache', 2nd ed., Pitman London, pp. 407-436, 1980.
- [4] Best B.A., Guilak F., Weidenbaum M., Mow V.C.: *Compressive stiffness and permeability of intervertebral disc tissues: Variation with radial position, region and level*, *Proc. WAM-ASME*, San Francisco, pp. 73-74, 1989.
- [5] Shell Research (KSLA), Amsterdam, The Netherlands, Binsbergen F.L., personal communication.
- [6] Blauer G.: *Polymerization of methacrylic acid*, *Trans. Farad. Soc.*, Vol. 56, pp. 606-612, 1960.
- [7] Bogduk L., Twomey L.T.: *The interbody joints and the intervertebral discs*, in 'Clinical anatomy of the lumbar spine', pp. 11-24, 1985.
- [8] Buchholz F.L.: *Polyacrylamides and Poly(Acrylic Acids)*, *Ullmann's Encyclopedia of Industrial Chemistry*, Vol. A21, VCH Publishers Inc., pp. 143-156, 1992.
- [9] Bourdais J.: *Réactivité de l'acide acrylique dans les copolymerizations*, *Bull. Soc. Chim. Fr.*, pp. 485-489, 1955.
- [10] Brannon-Peppas L., Peppas N.A.: *Equilibrium swelling behavior of pH-sensitive hydrogels*, *Chem. Engng. Sc.*, Vol. 46 (3), pp. 715-722, 1991.
- [11] Buckwalter J.A.: *The fine structure of human intervertebral disc*, in 'Anatomy and ultrastructure of the lumbar spine', pp. 108-143, 1982.

- [12] Cabaness W.R., Yen-Chin Lin T., Parkanyi C.: *Effect of pH on the reactivity ratios in the copolymerization of acrylic acid and acrylamide*, J. Polym. Sc. Part A-1, Vol. 9, pp. 2155-2170, 1971.
- [13] Crank J.: *Mathematics of diffusion*, Oxford Univ. Press, New York, 1975.
- [14] Donnan F.G.: *The theory of membrane equilibria*, Chem. Rev., Vol. 1, pp. 73-90, 1924.
- [15] Drost M.R., Snijders H., Huyghe J.M., Janssen J.D., Huson A.: *Triphasic confined compression of canine anulus fibrosus slices*, Proc. WAM-ASME, Anaheim, California, pp. 167-170, 1992.
- [16] Eyre D.R.: *Biochemistry of the intervertebral disc*, International review of connective tissue research, Ed. Hall D.A. et al., Academic Press, Vol. 8, pp. 227-291, 1979.
- [17] Flory P.J.: *Phase equilibria in polymer systems: Swelling of network structures*, Principles of Polymer Chemistry, Cornell University, Ithaca, New York, 1953.
- [18] Fung Y.C.: *Biorheology of soft tissues*, Biorheology, Vol. 10, pp. 139-155, 1973.
- [19] Gehrke S.H., Cussler E.L.: *Mass transfer in pH-sensitive hydrogels*, Chem. Engng. Sc., Vol. 44 (3), pp. 559-566, 1989.
- [20] Grodzinsky A.J., Roth V., Meyers E., Grossmann W.D., Mow V.C.: *The significance of electromechanical and osmotic forces in the nonequilibrium swelling behaviour of articular cartilage in tension*, J. Biomech. Engng., Vol. 103, pp. 221-231, 1981.
- [21] Gromov V.F., Galperina N.I., Osmanov T.O., Khomikowskii P.M., Abkin A.D.: *Effect of solvent on chain propagation and terminal reaction rates in radical polymerization*, Eur. Pol. J., Vol. 16, pp. 529-535, 1980.
- [22] Gu W.Y., Lai W.M., Mow V.C.: *Transport of fluid and ions through a porous-permeable charged-hydrated tissue, and streaming potential data on normal bovine articular cartilage*, J. Biomech., Vol. 26 (6), pp. 709-723, 1993.
- [23] Guilak F., Zhu W.B., Weidenbaum M., Best B.A., Mow V.C.: *Compressive material properties of human anulus fibrosus*, in 'Abstracts First World Congress Biomechanics Vol. II', San Diego, pp. 41, 1990.
- [24] Haldanker G.S., Spencer H.G.: *Properties of bound water in poly(acrylic acid) and its sodium and potassium salts determined by differential scanning calorimetry*, J. Appl. Pol. Sc., Vol. 37, pp. 3137-3146, 1989.
- [25] Happey F.: *Studies of the structure of the human intervertebral disc in relation to its functional and aging processes*, 'The Joints and Synovial Fluid', Vol. 2, Ed. Sokoloff L., Academic Press, pp. 95-137, 1980.

- [26] Helfferich F.: *Ion-exchange*, McGraw-Hill, New York, 1962.
- [27] De Heus H.J., Huyghe J.M., Oomens C.W., Nelissen L., Janssen J.D.: *Model materials for validation of mathematical models describing intervertebral disc tissue behavior*, Advances in Bioengineering, Proc. ASME-WAM, Vol. 26, New-Orleans, pp. 373-376, November 1993.
- [28] Holmes M.H., Mow V.C.: *The non-linear characteristics of soft gels and hydrated connective tissues in ultrafiltration*, J. Biomech., Vol. 23 (11), pp. 1145-1156, 1990.
- [29] Humzah M.D., Soames R.W.: *Human intervertebral disc: Structure and function*, Anat. Rec., Vol. 220, pp. 337-356, 1988.
- [30] Ikada Y.: *Fundamentals of biomaterials*, Biom. Engng. Applic. Basis Comm., Vol. 6 (1), 1994.
- [31] Kabanov V.A., Topchiev D.A., Karapatadze T.M., J. Pol. Sci. Polym. Symp., Vol. 42, pp. 173-183, 1973.
- [32] Kabanov V.A., Topchiev D.A., Karapatadze T.M., Mkrtchian L.A.: *Kinetics and mechanism of radical polymerization of weak unsaturated acids in aqueous solution*, Eur. Pol. J., Vol. 11, pp. 153-159, 1975.
- [33] Kazanskii K.S., Dubrovskii S.A.: *Chemistry and physics of 'agricultural' hydrogels*, in Advances in Polymer Science, Vol. 104, pp. 97-133, 1992.
- [34] Katchalsky A., Curran P.F.: *Nonequilibrium thermodynamics in biophysics*, Harvard University Press, Cambridge, Massachusetts, 4th printings, 1975.
- [35] Kedem O., Katchalsky A.: *A physical interpretation of the phenomenological coefficients of membrane permeability*, J. Gen. Phys., Vol. 45, pp. 143-179, 1961.
- [36] Klein J., Heitzmann R.: *Preparation and characterization of poly(acrylamide-co-acrylic acid)*, Makromol. Chem., Vol. 179, pp. 1905-1911, 1978.
- [37] Kraemer J., Kolditz D., Gowin R.: *Water and electrolyte content of human intervertebral discs under variable load*, Spine, Vol. 10, pp. 69-71, 1985.
- [38] Kremer M., Pothmann E., Rössler T., Baker J., Yee A., Blanch H., Prausnitz J.M.: *Pore-size distributions of cationic polyacrylamide hydrogels varying in initial monomer concentration and cross-linker / monomer ratio*, Macromolecules, Vol. 27, pp. 2965-2973, 1994.
- [39] Kulicke W.M., Klein L.: *Zur Preparation und Charakterisierung hochmolekularer Polyacrylamide*, Angew. Makromol. Chemie, Vol. 69, pp. 169-188, 1977.
- [40] Lai W.M., Hou J.S., Mow V.C.: *A triphasic theory for the swelling and deformation behaviors of articular cartilage*, J. Biomech. Engng., Vol. 113, pp. 245-258, 1991.

- [41] Lakshminarayanaiah N. : *Equations of membrane biophysics*, Academic Press, Inc. London Ltd., 1984.
- [42] Mansour J.M., Mow V.C.: *The permeability of articular cartilage under compressive strain and at high pressures*, J. Bone Joint Sur., Vol. 58A (4), pp. 509-516, 1976.
- [43] Maroudas A.: *Biophysical chemistry of cartilaginous tissues with special reference to solute and fluid transport*, Biorheology, Vol. 12, pp. 233-248, 1975.
- [44] Maroudas A.: *Physical chemistry of articular cartilage and intervertebral disc*, in 'Joints and Synovial Fluid Vol. 2, Ed. Sokoloff L., Academic Press, New York, pp. 239-291, 1980.
- [45] Meares P.: *Transport in ion-exchange polymers*, in 'Diffusion in polymers', Eds. Crack J. & Park G.S., chapter 10, pp. 373-427, 2nd print, Academic Press, London, 1975.
- [46] Molyneaux P.: *Water-soluble synthetic polymers. Properties and behavior*, Vol. 1, chapt. 3, CRC Press, Inc., Boca Raton, Fla., 1984.
- [47] Mow V.C., Lai S.C., Armstrong C.G.: *Biphasic creep and stress relaxation of articular cartilage: theory and experiments*, ASME, J. Biomech. Engng. Vol. 102, pp. 73-84, 1980.
- [48] Mow V.C., Holmes M.H., Lai W.M.: *Fluid transport and mechanical properties of articular cartilage: A review*, J. Biomech., Vol 17 (5), pp. 377-394, 1984.
- [49] Odian G.: *Principles of Polymerization*, 2nd ed., London, Wiley-Interscience, chapter 3, pp. 199-331, 1981.
- [50] Oomens C.W.J., Campen D.H. van, Grootenboer H.J.: *A mixture approach to the mechanics of skin*, J. Biomech., Vol. 20, pp. 877-885, 1987.
- [51] Park J.B., Lakes R.S.: *Biomaterials, an introduction*, Plenum Press, New York and London, 1992.
- [52] Peppas N.A.: *Hydrogels in Medicine and Pharmacy*, CRC Press, Boca Raton, FL., 1987.
- [53] Potnatram S., Kapur S.L.: *Reactivity ratios of ionizing monomers in aqueous solution*, Makromol. Chem., Vol. 178, pp. 1029-1038, 1977.
- [54] Quinn T.M., Grodzinsky A.J.: *Longitudinal modulus and hydraulic permeability of poly(methacrylic acid) gels: Effects of charge density and solvent content*, Macromolecules, Vol. 26, pp. 4332-4338, 1993.
- [55] Ratingen M.R. van: *Mechanical identification of inhomogeneous solids: a mixed numerical experimental approach*, Ph.D. Thesis, Department of Mechanical Engineering, Eindhoven University of Technology, The Netherlands, 1994.

- [56] Richards E.G. : *An introduction to physical properties of large molecules in solution*, Cambridge University Press, 1980.
- [57] Ricka T. , Tanaka J : *Swelling of ionic gels : Qualitative performance of the Donnan theory*, *Macromolecules*, Vol. 17, pp. 2916-2921, 1984.
- [58] Robinson R.A., Stokes R.H. : *Electrolyte solutions*, Butterworths, London, 1968.
- [59] Sakohara S., Muramoto F., Asaeda M. : *Swelling and shrinking processes of sodium polyacrylate super-absorbent gels in electrolyte solutions*, *J. Chem. Engng. Japan*, Vol. 23 (2), pp. 119-124, 1990.
- [60] Sedowofia K.A., Tomlinson I.W., Weiss J.B., Hilton R.C., Jayson M.I.V.: *Collagenolytic enzyme systems in human intervertebral disc*, *Spine*, Vol. 7 (3), pp. 213-222, 1982.
- [61] Shawski S.M., Hamielec A.E.: *Estimation of reactivity ratios in the copolymerization of acrylic acid and acrylamide from composition-conversion measurements by an improved least-squares method*, *J. Appl. Polym. Sc.*, Vol. 23, pp. 3155-3166, 1979.
- [62] Snijders H., Drost M.R., Willems P., van Dijk P., Huyghe J.M., Janssen J.D.: *Triphasic material parameters of canine annulus fibrosus*, in 'Recent advances in computer methods in biomechanics & biomedical engineering', Ed. by Middleton *et al.*, Books & Journals International LTD, Swansea, pp. 220-229, 1992.
- [63] Snijders J.M.A. : *The triphasic mechanics of the intervertebral disc - A theoretical, numerical and experimental analysis*, Ph.D. Thesis, Department of Movement Sciences, University of Limburg, The Netherlands, 1994.
- [64] Snijders J.M.A., Huyghe J.M., Janssen J.D.: *A theory for the chemo-mechanical behaviour of annulus fibrosus tissue*, submitted for publication *J. Biomech. Engng.*
- [65] Stokes R.H.: *An improved diaphragm-cell for diffusion studies, and some tests of the method*, *J. Am. Chem. Soc.*, Vol. 72, pp. 763-767, 1950.
- [66] Truong N.D., Galin J.C., Francois J.: *Microstructure of acrylamide-acrylic acid copolymers: 2. As obtained by direct copolymerization*, *Polymer*, Vol. 27, pp. 467-475, 1986.
- [67] Urban J.P.G., Maroudas A.: *The measurement of fixed charge density in the intervertebral disc*, *Biochim. Biophys. Acta*, Vol. 586, pp. 166-178, 1979.
- [68] Urban J.P.G., Maroudas A. : *Measurement of swelling pressure and fluid flow in the intervertebral disc with reference to creep*, *Proc. Inst. Mech. Engng.*, C132 (80), pp. 63-69, 1980.

- [69] Urban J.P.G., Maroudas A.: *Swelling of the intervertebral disc in vitro*, Conn. Tissue Res., Vol. 9, pp. 1-10, 1981.
- [70] Urban J.P.G., McMullin J.F.: *Swelling pressure of the intervertebral disc: Influence of proteoglycan and collagen contents*, Biorheology, Vol. 22, pp. 145-157, 1985.
- [71] Urban J.P.G., McMullin J.F.: *Swelling pressure of the intervertebral disc: Influence for age, spinal level, composition and degeneration*, Spine, Vol. 13 (2), pp. 179-187, 1988.
- [72] Vasheghani-Farahani E., Vera J.H., Cooper D.G., Weber M.E. : *Swelling of ionic gels in electrolyte solutions*, Ind. Eng. Chem. Res., Vol. 29, pp. 554-560, 1990.
- [73] The Encyclopedia of Polymer Science and Engineering: *Water Soluble Polymers*, Vol. 17, pp. 731-784, 1989.
- [74] Woo S.L.-Y., Akeson W.H., Jemmott G.: *Measurements of non-homogeneous, directional mechanical properties of articular cartilage in tension*, J. Biomech., Vol 12, pp. 437-446, 1976.
- [75] Yoshio N., Hirohito N., Matsuhiko M. : *Properties of swelling and shrinking of poly-(acrylamide-co-acrylic acid) gels by infinitesimal changes in external conditions*, J. Chem. Engng. Japan, Vol. 19 (4), pp. 274-280, 1986.

Summary

In biomechanics, the validity of mathematical models describing the behaviour of biological materials is generally verified via comparison of computed results with analytical solutions of the same equations (mathematical validation) and with results of experiments performed on the genuine biological material (biological validation). However, the first validation is restricted to limiting cases while, due to the complexity of the experimental conditions, the latter validation is difficult or impossible to perform. As a result, the consequences of the various assumptions, made within the development of the mathematical model, on the computed results are not always clear. The difficulties associated with the biological validation can be circumvented by performing at first experiments on well-controlled synthetic model materials that possess the most important properties of the biological material. Furthermore, model materials can also be used to develop experimental techniques in well-controlled laboratory environments for a possible future use in a biological environment.

In this thesis, the application of synthetic model materials is evaluated for the verification of mathematical models describing the behaviour of soft charged hydrated tissues (Lai *et al.* [40], Snijders [63]). As a case-study intervertebral disc tissue is chosen.

Intervertebral disc tissue is considered as a collagen fibre network embedded in a soft charged hydrated proteoglycan gel containing small nutrients and ions (Eyre *et al.* [16], Happey [25], Humzah *et al.* [29]). Due to the presence of both aligned and randomly orientated fibre networks the structure of the tissue is anisotropic. The tissue exhibits swelling and shrinking behaviour under both mechanical and chemical loading. In the mathematical description of the behaviour of the tissue three different constituents are distinguished: the collagen and proteoglycan matrix are represented by a solid phase, the interstitial water by a fluid phase and the small nutrients and ions by a monovalent NaCl ion phase.

The synthetic model materials are developed on the basis of the above triphasic division and the incorporation of characteristic physical properties of the genuine tissue such as permeability, diffusivity, elasticity and fixed charge density. In first instance, the anisotropy of the tissue, the specific microstructure of the biopolymers and their mutual interaction are not taken into account.

The synthetic model materials are made of a open cell microporous polyurethane (PUR)-foam embedded in a hydrophylic copolymer gel. The gel consists of a water phase containing atactic acrylic acid - acrylamide copolymers. The materials are obtained via free-radical copolymerization of acrylic acid and acrylamide *in-situ* in the pores of the PUR-foams. By using sodium hydroxide and N,N'-methylenebisacrylamide, charged crosslinked copolymer gels are obtained. The copolymer gels possess carboxylate $-C(O)O^-$ -groups as confirmed by infrared analysis. Various materials are prepared via adjustment of the initial acrylic acid - acrylamide monomer feed ratio, the neutralization degree of the acrylic acid, the concentration of the crosslinking agent and the properties of the PUR-foams. Copolymerizations in the absence of the PUR-foams and the crosslinking agent are performed to almost full conversion as verified by High Performance Liquid Chromatography measurements.

Several experiments are performed in order to determine the material parameters essential for the triphasic formulation and to study the behaviour of the material under both mechanical and chemical loading. In all experiments, the material specimen are cylindrically confined. This ensures that flow, diffusion and deformation phenomena are all approximately one-dimensional. In the experiments sodium chloride (NaCl) solutions are used as bathing solutions.

The ability of the materials to swell is studied by measurement of the swelling pressure of material slices. During the experiments, the specimen are kept at fixed height and subjected to NaCl bathing solutions of varying ionic strength. The pressure responses of the materials due to step changes in ionic strength of the NaCl bathing solution are shown to be in good agreement with Donnan theory. This theory is used to estimate the concentration of the fixed charges and the osmotic coefficient of the materials using equilibrium pressure responses. The fixed charge densities are in accordance with those encountered in intervertebral disc tissue. The osmotic coefficients are almost equivalent to the osmotic coefficient of the NaCl bathing solutions. The transient pressure curves are used to estimate the diffusion coefficient. The diffusion coefficient of approximately $3 \cdot 10^{-10} \text{ m}^2/\text{s}$ is about four times lower than the one measured in aqueous solution and is in agreement with diffusivities found for other soft charged hydrated materials.

The hydraulic permeability is determined from fluid permeation rate measurements through material slices. The solutions are forced through the material via application of a constant fluid pressure difference across the specimen. In the experiments the materials are either kept at a fixed deformed state and subjected to NaCl solutions of varying ionic strength, or subjected to various strain conditions and bathed in NaCl solutions of equal molarity. The hydraulic permeability is found to be dependent on both the deformation state of the material and the ionic strength of the surrounding NaCl bathing solution. Only small differences are observed between the permeabilities of the various materials which are of $\mathcal{O}(10^{-16}) \text{ m}^4/\text{Ns}$.

Uni-axial confined swelling and compression experiments are performed in order to determine the behaviour of the materials in a combination of changing mechanical and chemical loading conditions. The behaviour observed is similar to that of intervertebral disc tissue. A decreasing swelling degree of the materials is found with increasing acrylamide content and increasing crosslink density. The influence of the PUR-foams used is limited.

A typical result of the experiments is used to verify whether the triphasic theory is able to describe the transient finite deformation. For the numerical calculations, the material parameters determined for the porosity, the fixed charge density, the osmotic coefficient, the hydraulic permeability and the diffusion coefficient are used. With these values, only the finite equilibrium conditions and the transient consolidation behaviour are described satisfactorily. When an unrealistically high value for the diffusion coefficient is chosen, the complete transient behaviour is described correctly. This result points to an incomplete description by the triphasic theory of the transport phenomena taking place in soft charged hydrated materials. The evaluation of the triphasic material parameters confirms that the swelling behaviour of the materials is caused by Donnan osmosis. Within the deformation range studied, the majority of the mechanical load is transferred by the fluid osmotic pressure. No indication of deformation dependence of the aggregate modulus of the materials is found. Their permeability behaviour should be modeled non-linearly dependent on the deformation for swelling strains exceeding 20%.

In conclusion, it is found that the application of synthetic model materials for the verification of mathematical models, describing the behaviour of soft charged hydrated materials, is significant and feasible. The materials are a useful tool to remove the limitations associated with *in-vitro* experiments on the biological material itself and enable the study of separate physical phenomena contributing to the overall behaviour. Future research should be focused on the investigation and modeling of the electrical effects associated with the movement of fluid and ions in the materials. Furthermore, the multi-axial behaviour of the materials should be studied as well as the application of the experimental techniques developed in a biological environment.

Samenvatting

In de biomechanica wordt de geldigheid van wiskundige modellen, die het gedrag proberen te beschrijven van biologische materialen, in het algemeen geverifieerd door vergelijking van numerieke resultaten met analytische oplossingen (wiskundige validatie) en met resultaten verkregen van experimenten aan het biologische materiaal zelf (biologische validatie). De eerste validatie kan slechts in (eenvoudige) limietgevallen plaatsvinden, terwijl de laatste validatie moeilijk is uit te voeren door de veelal complexe experimentele condities. Hierdoor zijn de consequenties van de verschillende veronderstellingen, die gemaakt zijn bij de ontwikkeling van het wiskundige model, op de berekende resultaten niet altijd even duidelijk. De moeilijkheden die zich voordoen bij de biologische validatie kunnen worden omzeild door allereerst experimenten uit te voeren met goed gedefiniëerde synthetische model-materialen die karakteristieke eigenschappen bezitten van de biologische realiteit. Tevens kunnen deze materialen worden gebruikt voor de ontwikkeling van experimentele technieken onder goed gedefiniëerde laboratorium-omstandigheden voor een mogelijk toekomstig gebruik in biologische omgevingen.

In dit proefschrift worden synthetische model materialen toegepast voor de verificatie van wiskundige modellen die het gedrag beschrijven van zachte, geladen, gehydrateerde weefsels (Lai *et al.* [40], Snijders [63]). Als test probleem is tussenwervelschijf-weefsel gekozen.

Tussenwervelschijf-weefsel bestaat uit een netwerk van collageen fibers waartussen zich een zachte, geladen gel van proteoglycanen bevindt. In de gel komen kleine voedingstoffen en ionen voor (Eyre *et al.* [16], Happey [25], Humzah *et al.* [29]). Door de aanwezigheid van zowel parallelle als willekeurig georiënteerde vezelstructuren, heeft het weefsel een anisotroop karakter. Het weefsel vertoont zwel- en krimpgedrag bij zowel mechanische als chemische belasting. In de wiskundige beschrijving van het materiaalgedrag worden drie verschillende componenten onderscheiden: de matrix van collageen en proteoglycanen wordt vertegenwoordigd door een vaste fase, het tussenliggende water door een vloeistof fase en de ionen door een monovalente NaCl ion fase.

De synthetische model-materialen zijn ontwikkeld op basis van bovenstaande driedeling. Karakteristieke fysische eigenschappen van tussenwervelschijf-weefsel zoals permeabiliteit, diffusie, elasticiteit en de hoeveelheid gebonden lading zijn in het ontwerp betrokken. De anisotropie van het weefsel, de specifieke microstructuur van de biopolymeren en hun onderlinge interactie zijn niet meegenomen.

De model-materialen bestaan uit een opencellig, microporeus polyurethaan (PUR) schuim waarin zich een hydrofiële copolymeer gel bevindt. Deze gel bestaat uit een waterfase waarin zich atactische copolymeren bevinden opgebouwd uit monomere eenheden van acrylzuur en acrylamide. De materialen zijn gesynthetiseerd door in water acrylzuur en acrylamide *in situ* radicalair te copolymeriseren in de poriën van het schuim. Door toevoeging van natriumhydroxide en N,N'-methyleenbisacrylamide zijn geladen, vernette copolymeergelen verkregen. Door aanpassing van de initiële acrylzuur - acrylamide monomeer voedingsverhouding, de neutralisatiegraad van het acrylzuur, de concentratie crosslinker en de eigenschappen van de PUR-schuimen, zijn verschillende materialen verkregen. Met behulp van infrarood analyse is vastgesteld dat de copolymeergelen gebonden carboxylaat $-C(O)O^-$ -groepen bezitten. Uit High Performance Liquid Chromatography metingen is gebleken dat de copolymerisaties bij afwezigheid van de schuimen en de crosslinker tot vrijwel 100% conversie verlopen.

Er zijn verschillende experimenten uitgevoerd teneinde de materiaal-parameters te bepalen die van belang zijn voor de driedfasen-beschrijving. Tevens zijn deze experimenten gebruikt om het gedrag van de materialen te bestuderen bij wisselende mechanische en chemische belasting. In alle experimenten zijn proefstukjes van de materialen cilindrisch opgesloten zodat vloeistofstroming, diffusie en deformatie in goede benadering één-dimensionaal zijn. In de experimenten zijn zoutoplossingen (NaCl) gebruikt als omgevingsvloeistof.

Om na te gaan in hoeverre de ontwikkelde materialen kunnen zwellen, zijn zweldruk-experimenten uitgevoerd. In deze experimenten zijn de proefstukjes, gefixeerd op hun beginhoogte, in evenwicht gebracht met NaCl oplossingen van verschillende ionische sterkte. De gemeten drukvariatie ten gevolge van stapvariaties in de ionische sterkte van de NaCl oplossing blijken goed overeen te stemmen met Donnan theorie. Deze theorie is toegepast om uit evenwichtsdrukwaarden de hoeveelheid gebonden lading en de osmotische coëfficiënt van de materialen te bepalen. De ladingsdichtheden zijn van dezelfde orde grootte als die van tussenwervelschijf-weefsel. De osmotische coëfficiënten zijn vergelijkbaar met die van de NaCl oplossingen. Een schatting voor de NaCl diffusie-coëfficiënt is verkregen uit het transiënte verloop van de zweldrukcurves. De geschatte waarde van circa $3 \cdot 10^{-10} \text{ m}^2/\text{s}$ is ongeveer vier keer kleiner dan de waarde van de NaCl diffusie-coëfficiënt in water en in overeenstemming met waarden gevonden voor andere zachte, geladen, gehydrateerde materialen.

De doorlaatbaarheid voor NaCl oplossingen is bepaald via meting van vloeistofsnelheden door proefstukjes. De vloeistofstroming is geïnduceerd door een verschil in vloeistofdruk over het proefstuk aan te brengen. In de experimenten zijn proefstukjes ofwel in evenwicht gebracht met NaCl oplossingen van verschillende molariteit, terwijl ze op een vaste hoogte zijn gehouden, ofwel in evenwicht gebracht met NaCl oplossingen van gelijke molariteit en onderworpen aan verschillende rekken. De permeabiliteit blijkt niet alleen afhankelijk te zijn van de deformatietoestand van het materiaal maar ook van de molariteit van de omringende NaCl oplossing. De verschillen tussen de permeabiliteiten van de materialen

zijn slechts klein. De waarden zijn orde grootte $10^{-16} \text{ m}^4/\text{Ns}$.

Om het gedrag van de materialen te bepalen bij een combinatie van veranderende mechanische en chemische belasting zijn uni-axiale zwel- en compressie-experimenten uitgevoerd. Het geobserveerde materiaalgedrag is vergelijkbaar met het gedrag van tussenwervelschijfweefsel. Uit de metingen blijkt dat de zwelgraad afneemt bij toenemend acrylamidegehalte en toenemende vernettingsgraad. Het materiaalgedrag wordt niet noemenswaardig beïnvloed door de verschillen in eigenschappen van de gebruikte PUR-schuimen.

Een typisch resultaat van de experimenten is gebruikt om te verifiëren in hoeverre de driefasen theorie in staat is de transiënte eindige deformatie te beschrijven. Voor de numerieke berekeningen zijn de materiaal-parameters gebruikt die zijn bepaald voor de porositeit, de hoeveelheid gebonden lading, de osmotische coëfficiënt, de permeabiliteit en de diffusie-coëfficiënt. Met deze waarden worden alleen de evenwichtscondities en het eindige transiënte consolidatie-gedrag goed beschreven. Wanneer een niet realistische waarde voor de diffusie-coëfficiënt wordt gekozen, wordt het gehele eindige transiënte gedrag juist beschreven. Dit resultaat wijst op een niet volledige beschrijving door de driefasen-theorie van de transport-processen die een rol spelen in zachte, geladen, gehydrateerde materialen. De gebruikte materiaalparameters bevestigen dat het zwelgedrag van de materialen wordt veroorzaakt door Donnan osmose. Binnen het bestudeerde deformatie-gebied wordt het merendeel van de mechanische belasting gedragen door de osmotische druk van de vloeistof. Er zijn geen aanwijzingen gevonden dat de aggregatie-modulus van het materiaal deformatie-afhankelijk is. De permeabiliteit van de materialen neemt voor zwelrekken groter dan 20% niet lineair toe met de deformatie.

Al resumerend kan worden gesteld dat de toepassing van synthetische model-materialen voor de verificatie van wiskundige modellen die het gedrag beschrijven van zachte, geladen, gehydrateerde weefsels, niet alleen van grote betekenis is, maar ook goed mogelijk. De materialen zijn een bruikbaar alternatief om de beperkingen op te heffen die zich voordoen bij *in-vitro* experimenten aan het biologische materiaal zelf. Tevens maken de materialen het mogelijk specifieke fysische fenomenen te bestuderen die bijdragen aan het algehele materiaalgedrag. In toekomstig onderzoek zal de aandacht moeten worden gericht op de bestudering van de elektrische effecten die een rol spelen bij het transport van vloeistof en ionen. Tevens is het van belang het multi-axiale gedrag van de materialen te onderzoeken en na te gaan in hoeverre de ontwikkelde meetmethoden ook toepasbaar zijn op biologische materialen.

Acknowledgements

Many people have contributed to the realization of the research presented in this thesis, as the project was multi-disciplinary in nature. I thank those who assisted me during the years. In particular, I wish to thank the following persons:

- *Jan Janssen*, for his unconditional support and guidance throughout the years.
- *Han Meijer*, for pointing me in the direction of hydrogels and for his considerable contribution to the readability of the contents of the thesis.
- *Jacques Huyghe*, *Laurent Nelissen* and *Cees Oomens* with whom I had many stimulating discussions and who inspired me to extend my capabilities.
- *Theo van Duppen*, *Toon van Gils*, *Leo Wouters*, *Albert Wijnja*, *Karel Koekkoek* and *Rob Petterson* for their technical expertise and assistance.
- the students *Raymond van As*, *Caroline Schils*, *Arnoud de Geus*, *Kees van Weert*, *Jack van Hoof*, *Eric Agten* and *Nicole van 't Oost* for their contribution to the project.
- my room-mates and colleagues *Monique van Lankveld*, *Hans Baaijens*, *Danielle Palmén*, *Ivonne Lammerts* and *Jeroen Schoonen* for being such a great team.
- *Frank van der Voet*, for his review of the grammar of the contents of the thesis.
- my *friends* and *parents* for their support and listening ear.
- *Yvonne*, who is the key person in my life and whose love and support is valued tremendously.

Huib de Heus, oktober 1994

Curriculum Vitae

- December 30, 1964 Born in Delft, The Netherlands
- 1977 - 1983 Gymnasium β , Lorentz Lyceum, Eindhoven
- 1983 - 1989 Masters degree at the Faculty of Applied Physics,
Eindhoven University of Technology
- 1990 - 1994 Research assistant at the Faculty of Mechanical Engineering,
Department of Computational and Experimental Mechanics,
Eindhoven University of Technology

Stellingen

behorende bij het proefschrift

Verification of Mathematical Models Describing Soft Charged Hydrated Tissue Behaviour

1. De toepassing van synthetische modelmaterialen als alternatief voor biologische materialen heft beperkingen op die zich voordoen bij *in-vitro* experimenten aan het biologische materiaal zelf en maakt bestudering van specifieke fysische processen die bijdragen aan het algehele materiaalgedrag mogelijk.
 - dit proefschrift
2. De radicaalpolymerisatie van acrylzuur en acrylamide in een waterige oplossing *in-situ* in de poriën van een zacht microporeus polyurethaan schuim leidt tot synthetische modelmaterialen met eigenschappen overeenkomstig met tussenwervelschijf-materiaal.
 - dit proefschrift
3. Voor de beschrijving van het transiënte deformatiegedrag van zachte, geladen, gehydrateerde materialen is de modellering van de elektrische effecten die een rol spelen bij het transport van vloeistof en ionen noodzakelijk.
 - Gu *et al.* (1993) *J. Biomech.*, **26**, 709-723.
 - dit proefschrift, hoofdstukken 4 en 5
4. De in dit proefschrift weergegeven experimentele resultaten geven geen aanleiding te veronderstellen dat andere fysische processen dan Donnan osmose verantwoordelijk zijn voor het zweelgedrag van gematigd geladen, zachte, gehydrateerde materialen (dichtheid gebonden lading orde-grootte $0.3 \cdot 10^3 \text{ mol/m}^3$).
 - Lai *et al.* (1991), *J. Biomech. Engng.*, **113**, 245-258.
 - Sniijders (1994), *proefschrift*, Rijksuniversiteit Limburg.
 - dit proefschrift, hoofdstukken 3 en 5
5. Het wiskundige model, ontwikkeld door Sniijders, is slechts dan in staat het eindige, één-dimensionale, transiënte deformatiegedrag in meerfasen materialen te beschrijven, indien niet-realistische waarden voor de diffusiecoëfficiënt worden meegenomen. Dit duidt op een onvolledige beschrijving door het model van Sniijders van de transportprocessen die een rol spelen in deze materialen.
 - Sniijders (1994) *proefschrift*, Rijksuniversiteit Limburg.
 - dit proefschrift, hoofdstuk 5

6. Het bezoeken van en het spreken op grote internationale congressen is van wezenlijk belang voor de wetenschappelijke vorming van assistenten in opleiding.
7. De invoering van een beurzensysteem voor assistenten in opleiding door de universiteiten leidt niet alleen tot een vermindering van het aantal wachtgelders, maar ook tot een nog grotere onderwaardering voor wetenschappers.
8. Het lage percentage vrouwen in Nederland dat doorstroomt naar topfuncties in vergelijking met de ons omringende landen, is wellicht verklaarbaar door de grotere angst van de Nederlandse man voor vrouwen op concurrerende posities.
 - Afgeleid uit *Vrouwen op hoog niveau*, Intermediair no. 29, juli 1994.
9. Schoeisel is gezichtsbepalend voor karakter.
10. Het zelfstandig laten winkelen van kleine kinderen in de supermarkt op zaterdag is vanuit opvoedkundig oogpunt juist, maar draagt niet bij tot een snelle doorstroming van klanten.
11. Hora Est, en nu de rest!

Houten, november 1994

Huib de Heus